DETERMINATION OF TRACE LEAD AND CADMIUM IN BIOLOGICAL MATERIALS BY AUTOMATED DIFFERENTIAL PULSE ANODIC STRIPPING POLAROGRAPHY

Steve Hon-Ying Seto

A Thesis

in

The Department

of

Chemistry

Presented in Partial Fulfillment of the Requirements

for the degree of Master of Science (Chemistry) at

Concordia University

Montreal, Quebec, Canada

April, 1982

ABSTRACT

DETERMINATION OF TRACE LEAD AND CADMIUM IN BIOLOGICAL MATERIALS BY AUTOMATED DIFFERENTIAL PULSE ANODIC STRIPPING POLAROGRAPHY

Steve Hon-Ying Seto

The application of automation to electrochemical stripping analysis was investigated via the quantitative determinations of two trace heavy metals in two biological samples; namely, lead and cadmium in fish muscle tissue and in bovine liver. Differential pulse anodic stripping polarography (DPASP) was employed for the current-sampling at a hanging mercury drop electrode (HMDE), in an acetate supporting electrolyte. Preliminary analysis of the relationship between the stripping current and the various instrumental parameters demonstrated that responses were in accordance with the theory of DPASP. The results obtained from the analysis of the biological samples indicated that the sensitivity and accuracy of the electrochemical technique were at least comparable to those of the graphite-furnace, atomic absorption spectrophotometry (GF-AAS), and that better reproducibility could be obtained by the former method with the aid of automation. Its reproducibility and accuracy were estimated to be 3% and

98%, respectively. The practical detection limits were found to be 0.05 ppb (ng/ml) for lead and 0.02 ppb (ng/ml) for cadmium.

The experimental work and observations have indicated that, in terms of equipment and labour cost, and of analysis time, the automated DPASP technique has distinct advantages over the GF-AAS technique for the analysis of multi-elemental samples from the different sources.

ACKNOWLEDGEMENT

I would like to express my sincere gratitute to Professor J.G. Dick for his constant support and valuable guidance beyond the interest of academic research.

Thanks are extended to Sybron/Brinkmann Instruments (Canada) Ltd. for its unconditional loan of the automated equipment, to the Limnology Research Group (Lake Memphremagog Project) of the Dept. of Biology, McGill University, for its provision of the whole fish sample, and to the Dept. of Chemistry, Concordia University, for its partial financial support.

Appreciation is also extended to my fellow graduate and undergraduate students for their constant moral support; special thanks are also due to Mr. S. Nadler, with whom I had many valuable discussions on the matter of electrochemistry, to Messers R. Patterson and R. Harris, of the Science and Industrial Research Unit, for their helpful advice on the matter of wet chemistry, and to Messers S. Chiang and P. McNeil, who taught me the technique of flameless atomic absorption spectrophotometry.

Gratitude is also extended to Messers J. Schultz, K. Lee, A. Abdon and I. Quadri, for their help in obtaining the necessary chemicals and equipment for this Thesis work, and

to Misses A. Clements and S. Rodericks, for their help throughout the period of my graduate study.

I am particularly grateful to Misses A. Cekal and F. Lorrain, two esteemed friends, for their constant encouragement, without which this Thesis might never have been completed.

Last, but not the least, I especially thank the typist, Mrs. D. Gordon, for her patience in enduring my very messy hand-written manuscript.

TABLE OF CONTENTS

Description

LIST OF TABLES

LIST OF FIGURES

1.0 INTRODUCTION

The detection of heavy metals in environmental materials has long been of interest to analytical chemists, but emphasis on the health hazards of heavy metals in recent years has shifted the interest from a scientific curiosity to a matter of grave concern. In the past two decades, industries, universities, and governmental agencies have engaged in a vigorous search for sensitive and accurate methods of determining heavy metals, in a variety of matrices, at very low concentrations. Where parts-per-million (ppm) levels of detection once sufficed, parts-per-billion (ppb) and sub-ppb levels are now required almost routinely.

To meet these requirements, a variety of techniques exists. Anodic stripping polarography/voltammetry, colorimetry, neutron activation analysis, atomic absorption, emission and fluorescence spectrophotometries, and the emission spectrograph have been used with varying degrees of success, convenience and cost.

As part of its interdisciplinary programme, the Analytical Chemistry Division of the Department of Chemistry has set up methodologies for the Department of Biological Science, Fish Toxicology Group, associated with the determination of trace heavy metals in fish tissues, fish foods and fish tank waters. These methodologies have involved,

basically, atomic absorption spectrophometric, flame and graphite-furnace (FAAS/GFAAS) techniques.

When the levels of the trace metal analytes approach those where GFAAS methods of analysis are required, and particularly where the levels approach the limits of detection of the graphite furnace technique, the absorbance values obtained tend to become less precise, due to lamp-source intensity variations, the higher proportional influences of the sample matrices, memory effects of the graphite tube of the furnace, etc. Under these circumstances, it becomes necessary to carry out multiplicate determinations for each of the background solutions, the standards and the samples.

In the determination of lead at low levels by the graphite-furnace technique, for example, for a set of solutions consisting of one standard solution background, five standard samples, one fish tissue sample background and one tissue sample, at least quadruplicate determinations would be required. Including three spikes of standard each to the tissue background and the tissue sample, a total of fifty-six sample applications (injections) to the graphite-furnace atomizer would be needed. If four fish tissue samples were to be analyzed for lead alone, this would require a total of 104 injections, which is generally the average life time of a pyrolytic graphite tube. For the determination, therefore, on a per element basis, a period of about four hours of analysis time and a graphite tube,

at a cost of about $15 per tube, would be needed for each run. Under these conditions, both the analysis time and cost factors become excessive for the analyses of multiple elements by the GFAAS techniques.

It is possible, in most cases, to determine many trace heavy metals simultaneously by polarographic means under favourable conditions.

Differential pulse polarography (DPP), one of the most widely used quantitive techniques, has a limit of detection for heavy metals of approximately 2-5 ppb (ng/ml) in the test solution. This detection limit, however, becomes generally inadequate in cases where appreciably lower trace metal contents may be encountered, as in some biological or environmental samples.

Research on increasing the sensitivities of electro-analytical methods has led to development of the technique of stripping polarographic/voltammetric analysis. The anodic variant of stripping polarography (ASP) is a two-step process, in which a metal ion in solution is first deposited and preconcentrated in the form of an amalgam in a HMDE and the stripped current is monitored by the polarographic instrument throughout the anodically-scanned potential range. DPASP is currently the most favoured technique, owing to the capability of DPP of yielding relatively higher signal-to-noise (S/N) ratios for the

stripping-peak current than those for the other polarographic monitoring modes. It is possible to determine up to five elements simultaneously by the DPASP technique, without any interference, at concentrations as low as 0.008 ppb, in a 20-ml solution. In a 2-g. freeze-dried fish-tissue sample, the value represents a detection of 0.08 ppb. (ng/g), which is generally better than competitive with the GF-AAS (1,2).

Introduction of automation to DPASP instrumentation is a fairly recent development, and has given the electroanalytical technique advantages of greater precision, lower cost and time-saving relative to the GF-AAS method.

Considering again the case in which four samples of fish tissue are to be analyzed by GF-AAS, as noted before, in order to determine the contents of Cu, Pb, Cd, and Zn, there will be required a total of four graphite tubes, and approximately 20 man-hours of analysis time, during which period an operator must be present continuously to apply the sample aliquot to the AA spectrophotometer. (Although GF-AAS equipment can generally be supplied on request with automation to the graphite tube, solution spiking operations still require the presence of the operator. One should also not overlook the very considerable cost increase for automated GF-AAS equipment.) With automated DPASP, the four metals can be quantitated simultaneously in the course of 2.5 to 3 hours per sample by using the multi-elemental

standard additions (spiking) analyzing technique. For the same set of sample solutions, it will only require a total of about 1.5 g. of super-pure, triple-distilled mercury at a cost of $120 per 3 kg and a total analysis time of not more than 12 hours during which time, because of the automated process, an operator can attend to other areas of manual analysis and sample preparation, being needed only for a total of 20 min. (5 min. each for every 3 hours, in order to replace and set up the new sample solutions on the DPASP analyzing stations).

It is apparent therefore that, within limitations as to the heavy metals required to be determined, the DPASP technique has advantages over the GF-AAS method in terms of:-

(a) Cost of materials consumed in determination

(b) Cost of labour based on direct attention time required

(c) Total elapsed time to carry out a series of determinations

The capital cost layout for equipment is another factor which must not be ignored, and which provides an advantage for DPASP over GF-AAS. With automated injection equipment for multiple sample handling, GF-AAS units would require capital expenditures approximating $60,000 to $70,000. Even the best of DPASP equipment, including a unit for prepurification of the supporting electrolyte, would not

cost in excess of $30,000. While it can be argued that GF-AAS equipment has metal determination capabilities which may be superior to those of DPASP, particularly with respect to the number of metallic elements determinable, it must also be remembered that the polarographic/voltammetric units have inorganic anion and organic compound determination capabilities not available at all with AAS or GF-AAS equipment.

2.0 THEORETICAL PRINCIPLES

2.1 General Theory

2.1.1 Classical DC polarography

The term voltammetry deals with the current-potential (i-E) behaviour of an electrochemical system. The i-E curve arises as a result of electron-transfer processes that occur at the surface of a micro-electrode when diffusion is the rate-determining step in an electrochemical reaction. Polarography is a particular case of voltammetry in which the measurements of the i-E curves are carried out at a dropping mercury electrode (DME) or a hanging mercury drop electrode (HMDE).

The development of polarography began in 1922 with the work of Heyrovsky (3,4), and marked a significant advance in electrochemical analytical methodologies since it

introduced the element of selectivity through control of electrode potential, an element which was largely lacking in the older electrochemical analytical methods of potentiometry and conductometry.

The fundamental DC, or classical, polarographic techniques were acceptable for analysis to the approximate level of 10^{-5} M, but suffered from lack of sensitivity when compared to atomic absorption spectrophotometry (AAS) and other micro-analytical techniques which were later developed. In addition to the lack of sensitivity, it also suffered from a number of "defects" which made it less than ideal for routine analytical purposes, and made the results obtained somewhat difficult to interpret. The electronic difficulties hindering the classical DC polarographic technique were overcome in the early 1960's with the introduction of low-cost, fast response and more stable operational amplifiers, a wider knowledge of electrode reactions, improved investigation and measuring methods, and the introduction of more efficient electrodes. As a result, the last two decades has witnessed sophisticated techniques such as alternating-current (A.C.) polarography, square-wave and pulses-wave forms of polarography, and stripping analysis. Investigations of such techniques have demonstrated the utility and desirability of the "new" polarographic methods for "fingerprinting" purposes and for trace analytical applications. In addition to the extensive scale on which polarographic/voltammetric methods are now

used, their significance is reflected by the volume of literature devoted to them. Some 2500 papers on the subject are being published yearly, and since Heyrovsky's original paper (4) was published in 1922, more than 50,000 articles and monograms have appeared.

In polarography/voltammetry, a linearly-varying potential is applied across the electrodes of the measuring cell. The quantity which is actually measured and recorded on the polarogramme is the diffusion current, i_d. The data required for the qualitative and quantitative determination of the dissolved substance (the depolarizer or analyte) can be extracted from the i-E curve.

The half-cell reaction occurring at the working micro-electrode is:

$$Ox + ne^- \rightleftharpoons Red \qquad (1)$$

where: Ox and Red are the oxidized and reduced states of an electro-active species, respectively.

The relationship between the potential applied to a working electrode and the activities of Ox and Red in the transition zone between the electrolyte and the electrode surface is given by Nernst's equation:

$$E = E^0 + \frac{RT}{nF} \ln \frac{a_{ox}}{a_{red}} \qquad (2)$$

where: E = cell potential;

E^0 = standard reduction potential;

a = activity;

T = absolute temperature in ^0K;

R = the gas constant;

n = no. of electrons involved in the transfer process;

F = Faraday's constant;

Assuming that the ratio of the activities generally equals to the ratio of the molar concentrations, we have, at 25°C, Equation (2)

$$E = E^{o} + \frac{0.059}{n} \log C_{ox}/C_{red} \qquad (3)$$

Equation (3) shows that, if the potential to the working electrode is altered, the ratio between the concentrations of Ox and Red is also altered. This change inevitably involves a migration of electrons, which is measured as a current, i. When the applied potential is sufficient to ensure that all depolarizers arriving at the electrode are electrolyzed at once, than a maximum concentration gradient is set up between the electrode surface and the surrounding solution. This establishes the diffusion rate for the depolarizer, and hence the value of the diffusion current, i_d. From Ilkovic's equation for i_d (5), and according to Heyrovsky also, the instantaneous current is given as follows:

$$i_d = 706nm^{2/3}t^{1/6}D^{1/2}C_{ox} \quad (25^{o}C) \qquad (4)$$

where:-

i_d = diffusion current (uA)

n = electron transfer for $Ox + ne^{-} \rightleftharpoons Red$

m = rate of flow of mercury in capillary ($mg.s^{-1}$)

t = life-time of mercury drop (s.)

D = diffusion coefficient for the depolarizer Ox ($cm^2/s.$)

C_{ox} = concentration of depolarizer (mM/L).

706 = constant based on the Faraday, Hg density, and etc.

The important feature involved in this interpretation of the diffusion current at the DME are those related to the linear relationship between i_d and C_{ox}.

At an applied cathodic potential permitting immediate reduction of Ox upon arrival at the electrode surface, and in the very early stages of drop life of a mercury drop, the relative rate of increase of the electrode surface area is very high and the movement of the surface into the solution is rapid enough to prevent any worthwhile concentration gradient zone from being established at the electrode surface. The current increases rapidly here, at the early stages, because of these conditions. As the drop grows larger, the relative rate of surface area increase and movement into the solution decreases and, during a short but appreciable period before drop dislodgement, a well-defined concentration zone is established where C_{ox} $(x=o)$ C_{ox} and is approximately equal to zero. This establishes a value of current which is the diffusion, and depends only on the value of C_{ox}. ($C_{ox}(x=o)$ is the concentration of Ox at the electrode surface, and C_{ox} is its concentration in the bulk of solution). This i_d now persists virtually unchanged

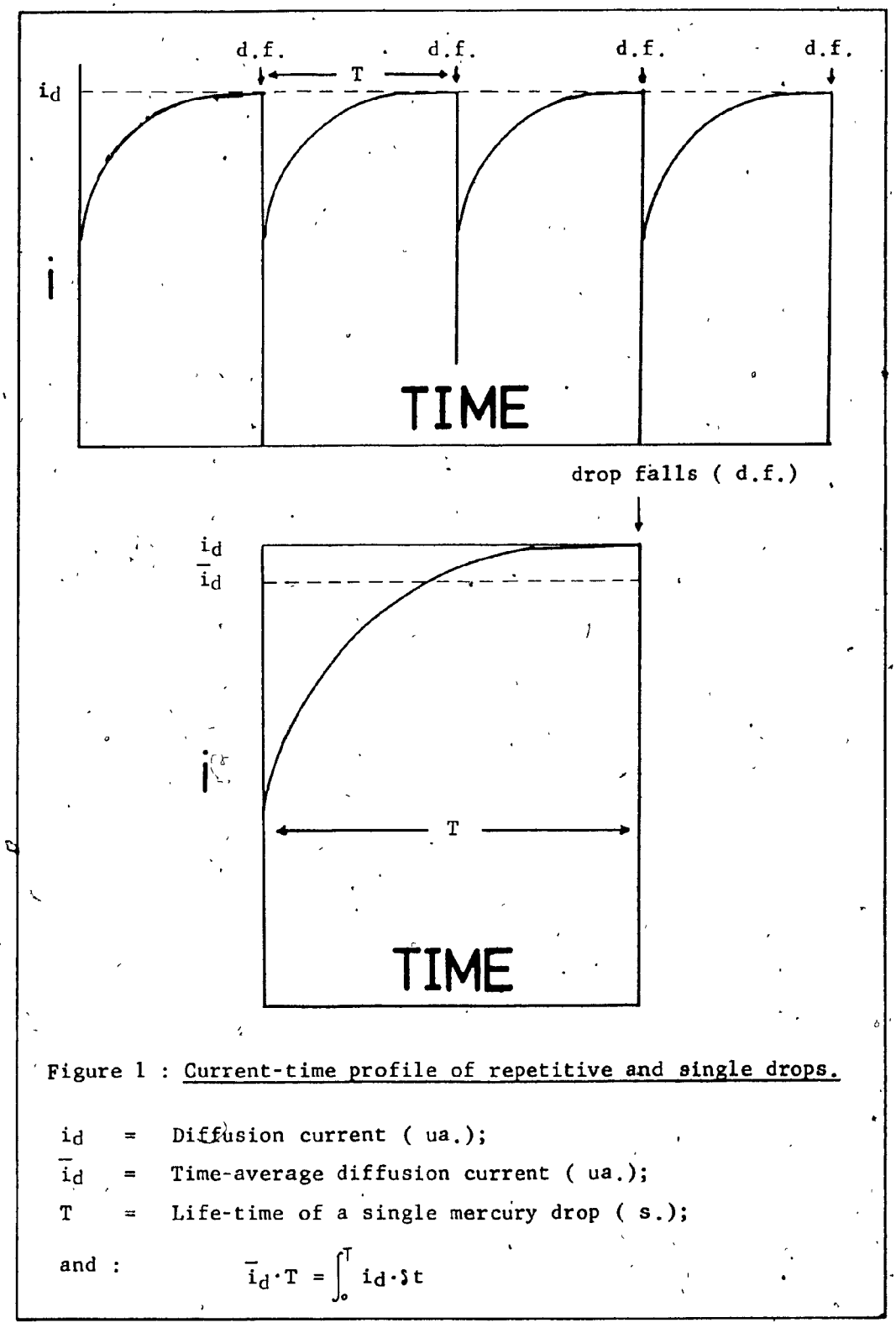

Figure 1 : Current-time profile of repetitive and single drops.

i_d = Diffusion current (ua.);

$\bar{i}_d$ = Time-average diffusion current (ua.);

T = Life-time of a single mercury drop (s.);

and : $$\bar{i}_d \cdot T = \int_0^T i_d \cdot \$t$$

until drop dislodgement. Subsequent to dislodgement, the concentration gradient zone formed around the drop is destroyed by the inrushing solution and the forming of a successive drop. Repetitive drops provide identical i_d values at drop dislodgements, since the amount of depolarizer reduced per drop is negligible and the stirring effect due to drop fall is insignificant. The theoretical repetitive pattern is shown in Figure 1. The current, as shown in Figure 1, grows in the early stages of drop life. The plateau section of current represents the i_d value which is concentration-dependent.

2.1.2 The charging, condenser, or capacitive current

If a DME disconnected from the external circuit is immersed in a pure supporting electrolyte such as KCl, for example, chloride ions will be preferentially absorbed on the surface of a drop and, as a result, the mercury in the reservoir will acquire a negative charge. This in turn will be imparted to the succeeding drops, which will hence absorb fewer and fewer chloride ions until equilibrium is attained. The negative charge accumulated by the mercury will then be just great enough to counterbalance the tendency for the adsorption of excess chloride ion to occur on the drop surface. The electrostatic potential of the mercury under this equilibrium condition is known as the potential of the electro-capillary maximum, Eecm.

The Eecm varies with the nature of the supporting electrolyte and is, for example, -0.46 V vs SCE for a 0.1 M KCl. At applied potential either more or less cathodic than this, adsorption of cations or anions, respectively, occurs on the surface of each mercury drop. In order to polarize or charge the electrode to a desired potential in the presence of depolarizers, a quantity of current is required to charge the capacitance of the electrical double layer created as a result of adsorption of the non-electroactive supporting electrolyte ions at the drop surface. The magnitude of the average charging current, i_c, during drop life is large enough to be recorded, and is the limiting factor determining the lowest concentration that can be detected by the normal DC polarography. That is to say, i_c constitutes the detection limit of the classical technique, and its values correspond to concentrations of about 10^{-5} to 10^{-6}M of the depolarizer, depending on its electrode reactivity. In addition to its influence on the detection limit of the classical technique, i_c distorts the i-E curve of an analyte (depolarizer) at low concentration. The differential capacity of the electrical double layer varies markedly with potential, and the capacity current varies accordingly. As a result, the i-E curves are distorted and the measured peak current is smaller than the actual peak current (AB and ab, respectively, in Figure 2).

It is, however, possible to compensate for the charging

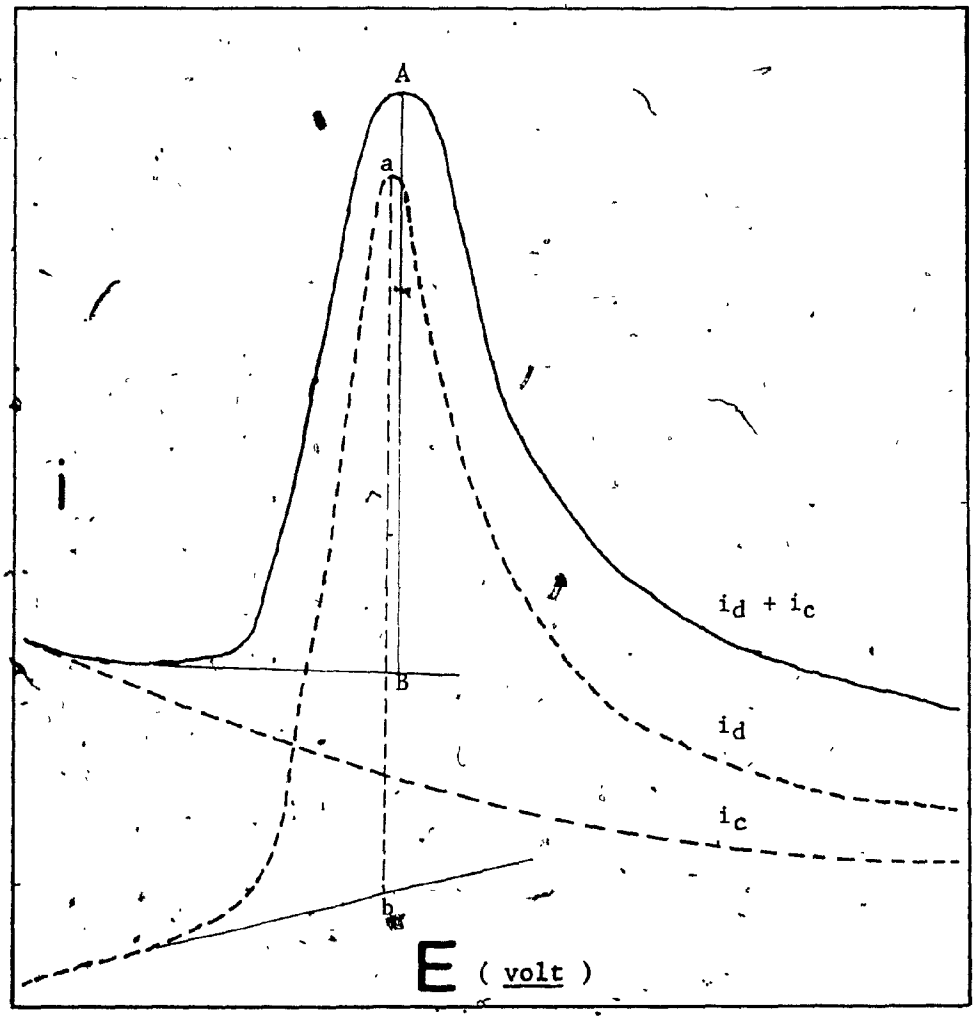

Figure 2 : Distortion of the current-potential (i-E) curve by the charging current, i_c (6).

i_d = Diffusion current (ua.);

i_c = Charging current (ua.);

a-b = actual peak-current due to i_d only;

A-B' = measured peak-current ($i_d + i_c$).

current by proper design of the recording device. Attempts to overcome the influence of i_c in the 50's led to the use and development of wave forms different from and usually more complex than the simply varying DC potential normally used in the classical polarography.

2.2 Stroke (Tast) Polarography (7,8,9)

In classical polarography, the average current, i, is measured throughout the whole drop life-time, during which i_d increases proportionally to $t^{1/6}$ while i_c decreases by a rate proportionally to $T^{-1/3}$ (Figure 3, Ref. 9). This means that when the drop starts to grow the ratio i_d/i_c is considerably smaller than it is toward the end of the drop life-time, when the increase in surface area of the drop and the magnitude of i_c are both small. It is apparent that the current should be measured only during a small fraction of the drop-life toward the end rather than throughout almost the whole drop-life. This theory formed the foundation of strobe or tast polarography, and led to the development of square-wave polarography by Barker and Jenkins (10).

The advantages of tast polarography over the conventional are as follows:

(a) Current oscillations due to drop falls are minimized and, as a result, less instrumental damping is needed. Polarogrammes with well-formed

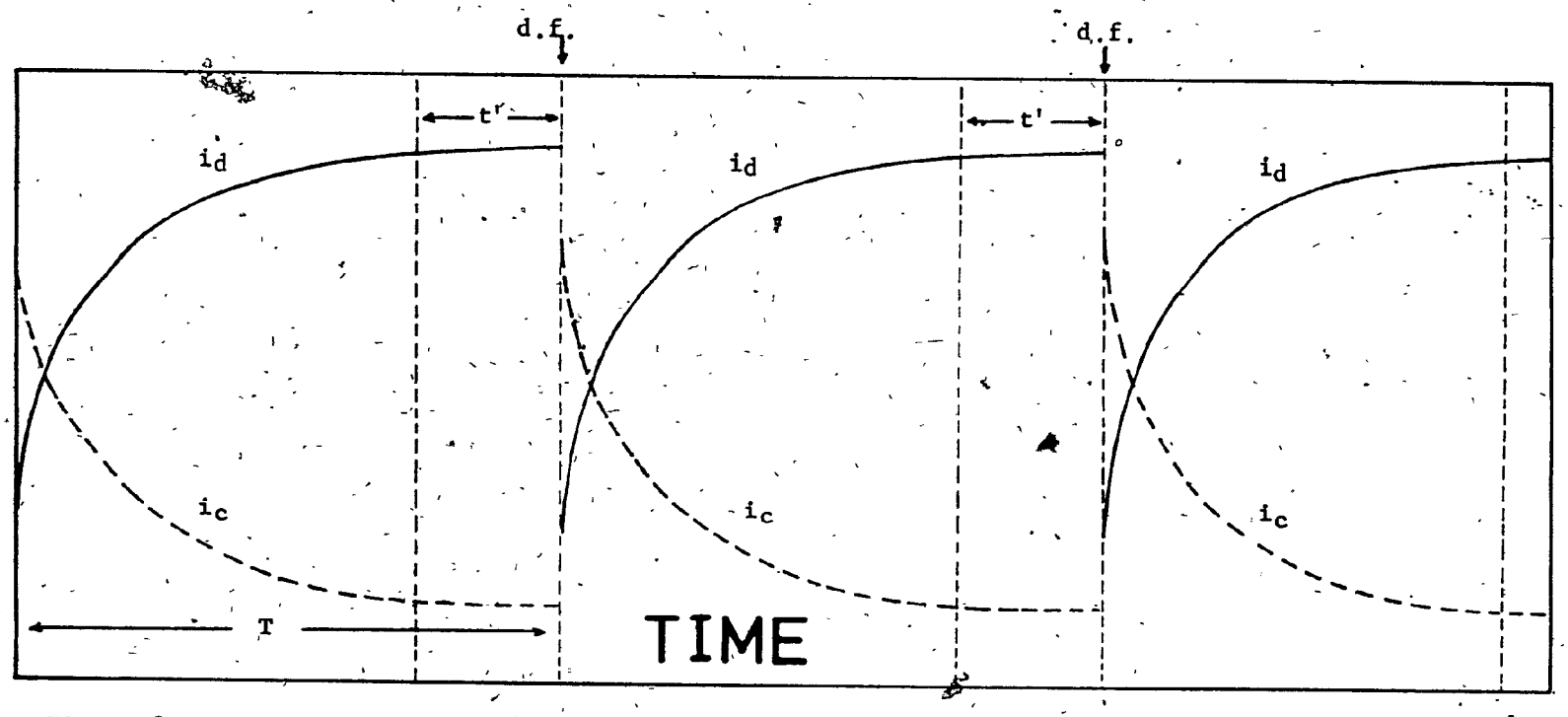

Figure 3 : Current-time (i-t) profile of repetitive mercury drops (9).

T = Life-time of a single drop (s.);

t' = Period of current-sampling (s.).

i-E curves are obtained for better evaluation;

(b) Because i_c varies almost linearly with potential in the measuring zone, the use of linear i_c compensation (as contrasted to the non-linear i_c compensation employed in the conventional method) is much more suitable, and consequently the utilizable data are increased somewhat.

The overall sensitivity of tast polarography is increased by about 1/2 order of magnitude over that of the conventional DC polarography. This increase, however, relates only to the minimization of i_c. The other factors contributing to the residual current, such as faradaic current resulting from impurities or traces of oxygen, are not compensated. The elemental resolvability and separation are not improved.

2.3 Alternating-Current (A.C.) Polarography

The first experiments in A.C. polarography were performed by Muller et al (11). In this technique, a small, low-frequency a.c. voltage is superimposed upon the slow, linearly-varying d.c. potential ramp, and the alternating current is plotted against the d.c. potential. This leads to a current peak in the region of the d.c. polarography step, with the current values both before and after the step being much lower.

The theoretical principle of A.C. polarography may be explained as follows At the foot of the ordinary d.c. polarographic wave the a.c. is entirely due to the charging and discharging of the electrical double layer and is relatively small. On the plateau of the wave, analyte is consumed as fast as it reaches the electrode surface at any time during a.c. voltage cycle, and the a.c. is again due mainly to variations in the double layer potential. On the rising part of the wave, the a.c. depends on the reversibility of an analyte's half-reaction. If the electron-transfer step is instantaneous, a certain equilibrium is attained at the drop surface at an instant when the a.c. voltage is zero. As it becomes more negative, the rate of reduction increases rapidly and, at the same time, the oxidation rate decreases rapidly. A large increase of the net cathodic current is therefore obtained. The changes become reversed as the instantaneous value of the a.c. voltage becomes more positive and the current becomes more anodic. The greatest variations in the composition of the layer of solution around the drop occur at the half-wave potential, and consequently the maximum a.c. is observed at this potential (Figure 4).

Since the magnitude of the a.c. peak is dependent also on the reversibility of the half-reaction of the analyte, it is much smaller for semi-reversible or irreversible systems than for the reversible ones.

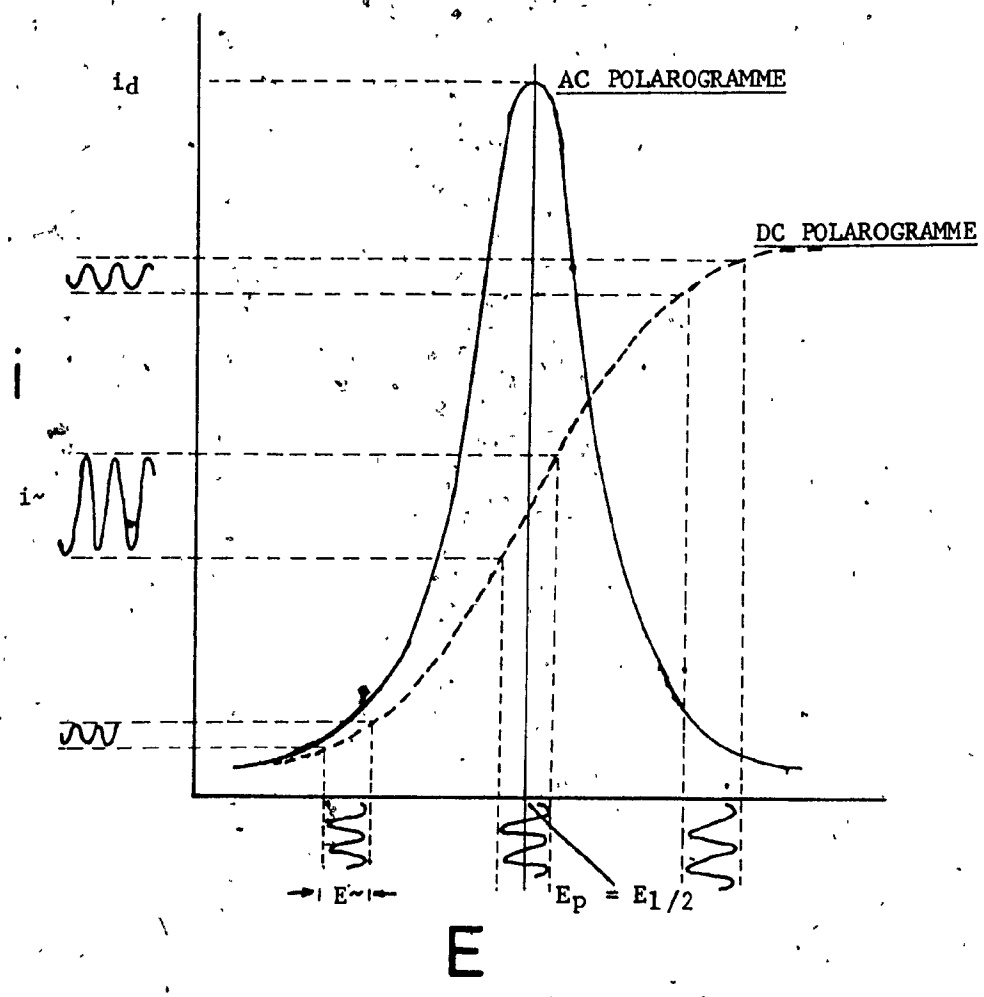

Figure 4 : The relationship between the DC and AC polarogrammes.

i	=	DC current (ua.);
E	=	DC voltage (v.);
i~	=	AC current (ua.);
E~	=	AC voltage (v.);
E_p	=	AC peak-potential (v.);
$E_{1/2}$	=	Half-wave potential (v.)

In the technique, the d.c. component of the total current is blocked out, and only the rectified a.c. component is displayed as a function of the d.c. potential, and the current can also be sampled during part of the drop-life. As a result, the faradaic and charging currents are separated because of the phase difference between them. By employing a phase-sensitive lock-in amplifier, one can measure the faradaic current alone, rejecting the condenser current.

A.C. polarography gives a better resolution of closely-spaced i-E waves and is quantitatively more sensitive than d.c. polarography (with the detection limit at about 10^{-7}M). However, since the technique responds mainly to reversible electrode reactions, this limits its applicability in quantitative analysis.

2.4 Square-Wave Polarography

Square-wave polarography was developed by Barker and Jankins (10) with the object of establishing a method having the advantages of A.C. polarography, but with an increase of sensitivity. In order to increase the sensitivity in polarographic/voltammetric quantitative analysis, i_c must somewhat be minimized relative to the current being measured. In the A.C. polarography, there is a condenser current produced by the periodic changes in the charge of the double layer, in addition to the main charging current resulting from the drop growth. The minimization of these

two components hence constitutes the basis of the square-wave polarography.

The principle of this method is essentially the same as the A.C. polarography but with a rectangular superimposing a.c. voltage. The minimization of i_c may be explained by reference to Figure 5. The reaction faradaic current, i_f, and i_c are shown on the same time scale, in the figure, as the applied potential. Both currents rise vertically at the instant the periodically changing voltage switches from one polarity to another, and start to decay exponentially right after the a.c. voltage reaches its maximum magnitude. I_c decreases much faster than i_f, because the time constant of the network measuring circuit, the double layer capacity is always so small so that i_c is virtually equal to zero long before the voltage reversals. The i_f, on the other hand, decays at a much lower rate because of the diffusion process involved. By current-sampling, as in tast polarography, at the end of the drop-life and just before the switch-over of the applied a.c. voltage, i_c of the a.c. component can be rendered ineffectual. With the aid of phase-shift circuitry, the total i_c from both the a.c. and d.c. components can be effectively reduced. This consequently provides for better sensitivity and detection limits (5×10^{-8}M) than those obtainable from (sinusoidal) A.C. polarography.

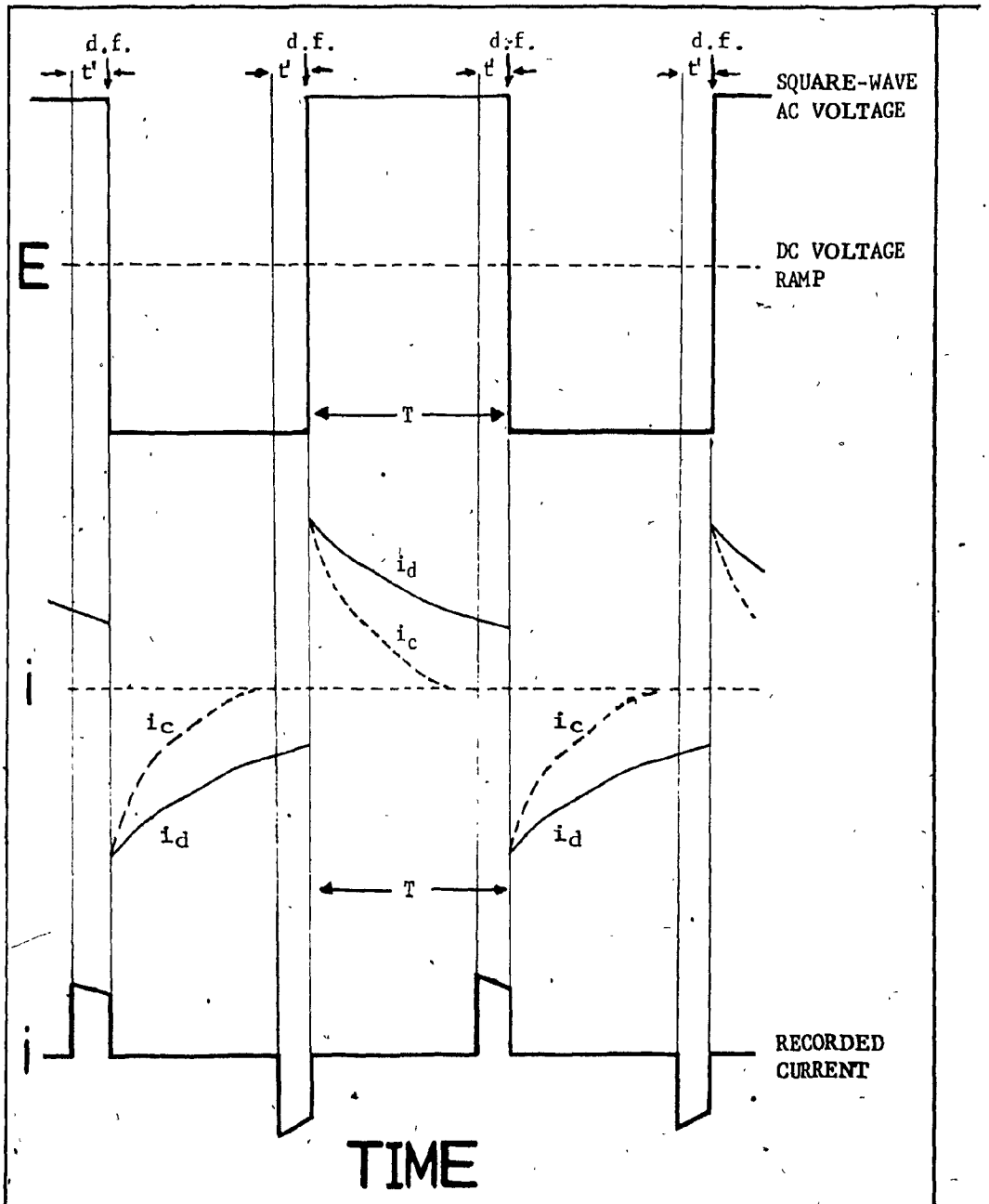

Figure 5 : Schematic presentation of the periodicity of the superimposing square-wave voltage (14).

T = Drop life-time (s.);

t' = Current-sampling period (s.)

2.5 Pulse Polarography

The concept of pulse polarography was originally developed by Barker and Gardner (15) as an outgrowth of their work on square-wave polarography. In all the pulse techniques, a single rectangular voltage pulse of short duration is superimposed on the linearly changing d.c. potential. The pulse is repeated at regular intervals and is synchronized with the maximum growth of each drop. Pulse polarography utilizes the principle of the square-wave polarography of minimizing the charging current and the fact that the i_f/i_c ratio becomes more favourable with increased duration of the square-wave pulse. The current which is measured depends on the position and duration of the time interval over which the measurement is made, and better results can be obtained with longer pulse duration, or, lower pulse frequency - at one pulse per drop-life. This forms the fundamental basis of pulse polarographic techniques.

Various kinds of pulse polarography may be distinguished according to the applied voltage function and the method of current measurement. The two most important ones are the normal pulse and differential pulse techniques.

2.5.1 Normal pulse polarography (NPP)

In normal pulse polarography, voltage pulses of successively increasing amplitude are applied to the DME at

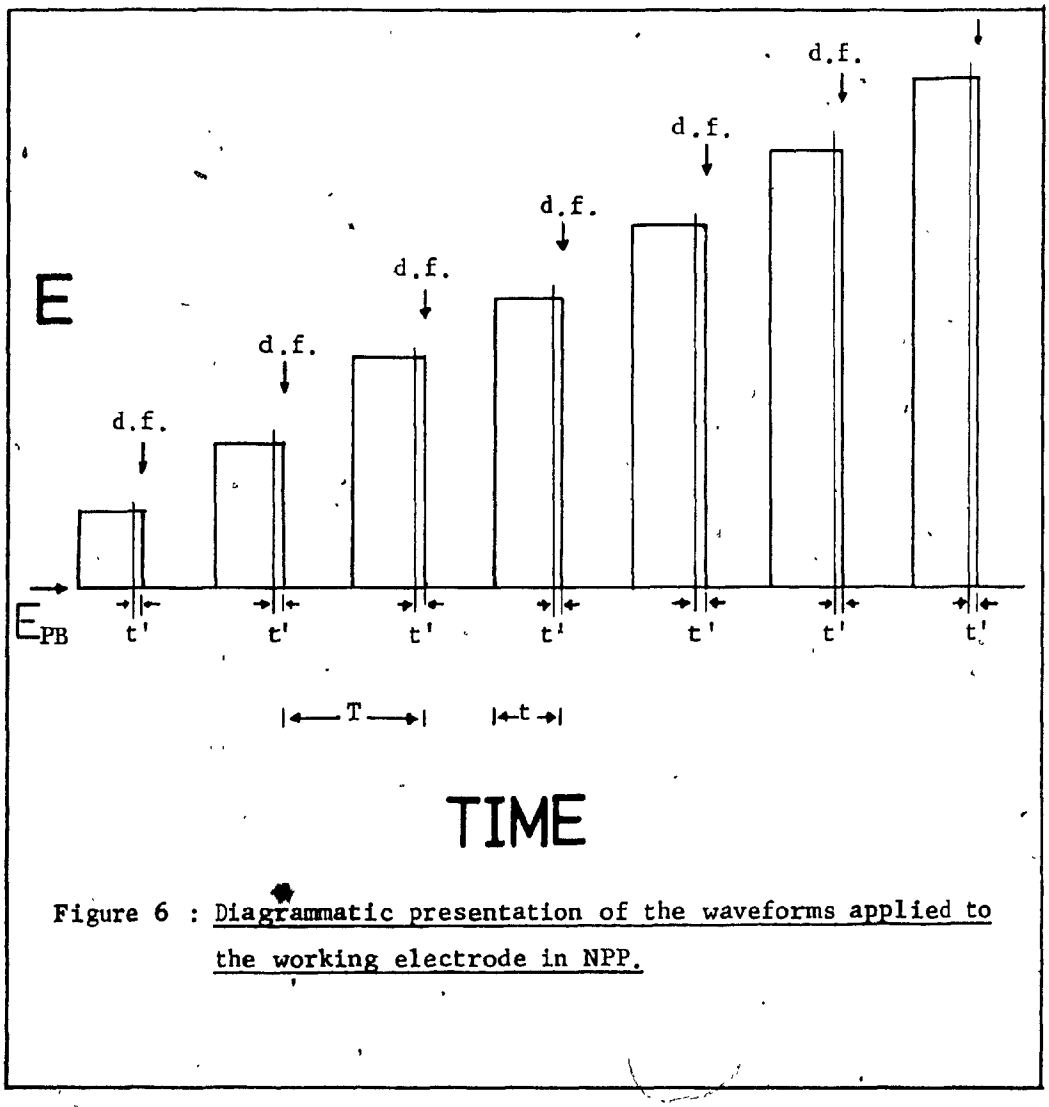

Figure 6 : Diagrammatic presentation of the waveforms applied to the working electrode in NPP.

Typical parameters on the Metrohm E 506 Polarecord :

T = Drop life-time (at DME) or modulating pulse cycle (at HMDE), lowest T = 0.4 s.;

t = Pulse duration = 200 ms. (constant);

t' = Current-sampling period = 20 ms. (constant);

E_{PB} = Pulse-base potential in volt (adjustable).

one pulse per drop. Starting from a constant, adjustable pulse base voltage, the amplitudes of individually rising voltage pulses determine the linearly rising d.c. potential pulse ramp (Figure 6). Owing to the fact that, in the intervals between pulses, the polarographic voltage returns to the pulse base voltage, which may be either anodic or cathodic to the half-wave potential of an analyte, no depletion of material from the solution in the vicinity of the drop takes place since the electrode reaction does not occur during these intervals.

Current sampling takes place only once during each drop life, and occurs over the last few milliseconds of the drop life and pulse application. The resultant i-E curve resembles a conventional D.C. polarogramme. The measured current signal is the faradaic current that flows at the pulse potential (i_{f1}), minus any faradaic current flow due to the fixed d.c. potential (i_{f2}).

Sensitivity of NPP attains a 10^{-9}M level and is independent of the degree of reversibility of a reaction. The gain in sensitivity is achieved through the virtual elimination of the charging current.

2.5.2 Differential pulse polarography (DPP)

This pulse technique , which differs from NPP, consists of superimposing a single, fixed amplitude voltage pulse at regular intervals on the slowly varying d.c.

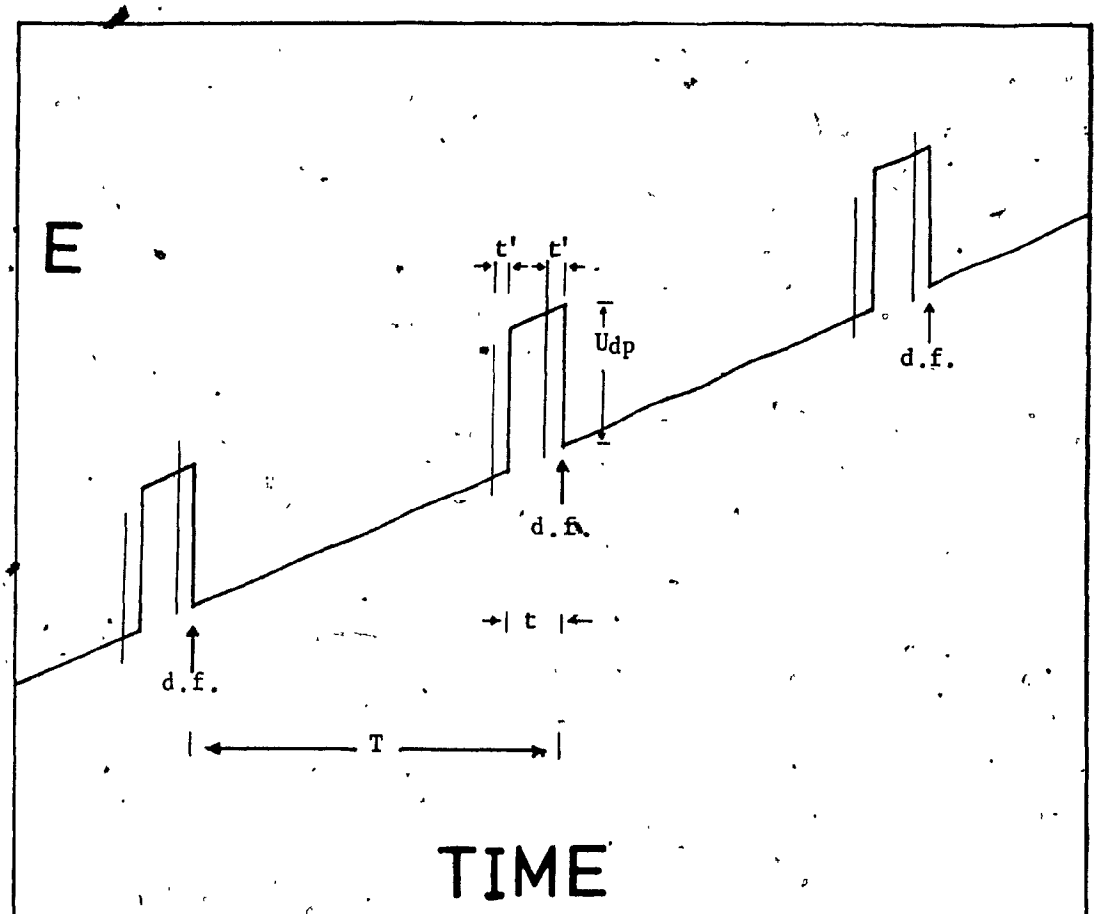

Figure 7 : Diagrammatic presentation of the waveforms applied to the working electrode in DPP.

Typical parameters on the Metrohm E 506 Polarecord :

T = Drop life-time (at DME) or differential-pulse cycle (at HMDE), lowest T = 0.4 s.;

t = Pulse duration = 60 ms. (constant);

t' = Current-sampling period = 20 ms. (constant);

U_{dp} = Differential-pulse amplitude = (adjustable : +100 mv. ------ -100 mv.)

potential ramp. The pulse is repeated and synchronized with the maximum growth of each drop. Current-sampling is carried out twice per pulse, each for an equal duration, one immediately before the application of the pulse, and the other at the end of the pulse during the life of the same drop (Figure 7). The first current-sampling is essentially equivalent to what would be obtained in normal D.C. polarography, that is, i_f due the d.c. potential ramp. The second current sample is the total i_f due to the d.c. ramp and the voltage pulse. These two currents are largely unaffected by perturbing influences such as i_c from the d.c. and/or the a.c. sources. The difference between them, developed by applying two stored signals in the memories to a differential amplifier, is finally presented after amplification to the output of the recording system.

As in all other caseswhere a superimposed voltage is applied to the linearly-changing d.c. potential ramp, the voltage pulse may cause an additional faradaic current flow, if the applied voltage has suddenly induced a change to the equilibrium potential of an electroactive species whereby the equilibrium between Ox and Red is shifted. When both the potentials involved lie either before or after the rising portion of the polarographic wave, little or no change in i_f due to the pulse will be observed in the second sampling and, consequently, zero current-difference will be presented and recorded as a horizontal line parallel to the

potential axis in the polarogramme. However, when either one or both the potential, of the d.c. ramp and the pulse, are on the rising portion of the polarographic wave, a significant change in i_f flow takes place. Therefore, a gradual increase in the current-difference will be recorded. The current-difference reaches its maximum value at the half-wave potential, $E_{\frac{1}{2}}$, of the analyte, and gradually declines to a lower value at the plateau portion of the normal i-E curve. The differential pulse (DP) polarogramme hence gives an i-E curve with peaks appearing at the $E_{\frac{1}{2}}$ (s), corresponding to the analyte(s) present in the solution. The magnitude of the current peak is proportional to the analyte concentration and the applied pulse amplitude.

The DPP technique provides solutions to most of the problems which plague polarographers. The influence of the i_c is minimized by the pulsing and sampling processes, and peaks are obtained rather than steps, so that resolution is improved. Such problems as polarographic maxima, poorly defined waves and severely-sloping background baselines are at least partially resolved by the technique. Subject to limitations relative to the duration of the applied pulse, the technique is applicable to both reversible and irreversible reactions, and yields peak shapes which closely approximate the theoretically-predict derivative of the d.c. waveform in most cases. It thus permits one to obtain the maximum possible resolution between closely-spaced

waves, while permitting examination of large and small signals in the same scan.

In principle the DP mode is less sensitive than the NP mode, but the resolution is better. It is capable of detecting concentrations at 10^{-8}M, a 100- to 500- fold increase over the classical D.C. polarography, and is by far the most sensitive polarographic technique for direct quantitation without sample preconcentration.

2.6 Electrochemical Stripping Analysis

2.6.1 General

To increase the sensitivity and accuracy of electrolytic methods by several orders of concentration, it is necessary to preconcentrate the very dilute analyte solution. In order to avoid the tedious and time-consuming process of continuous extraction and separation (and the danger of loosing part of the sample and of contaminating the analyte(s)), it is far more advantageous to carry out the preconcentration procedure directly in the system on which the measurement itself will be performed. This is the principle of electrochemical stripping methods, in which the analyte is concentrated electrolytically on the working electrode (in the form of an amalgam or mercury-compound layer with mercury working electrodes), and is then transferred back into the solution by reversing the electrolytic

process. This stripping process is monitored by a suitable polarographic instrument. Since there is now a substantially higher concentration of analyte at the electrode-solution interface than that originally present in the solution, the sensitivity and accuracy of the determination is increased many times.

Electrolytic concentration of an analyte from a dilute solution is mostly performed at a constant potential, which is chosen in such a way that the required electrode reaction proceeds at a reasonable rate. The solution is stirred during electrolysis to ensure a constant supply of analyte from the bulk of solution. After a predetermined set time, the stirring is stopped and the solution is left to become quiescent and equilibrated. During this period, the concentration of the analyte at the electrode surface decreases, and consequently the magnitude of the electrolytic current drops rapidly to the value of the stationary diffusion current over the concentration polarized zone.

After the "rest period", the stripping of the deposit at the electrode is carried out.

Generally the stripping current is monitored as a function of the electrode potential changing linearly with time. Current peaks are obtained on the resulting polarization curve, the positions of which ($E_{p/2}$) are characteristic of the given analytes (in analogy to $E_{1/2}$ in classical

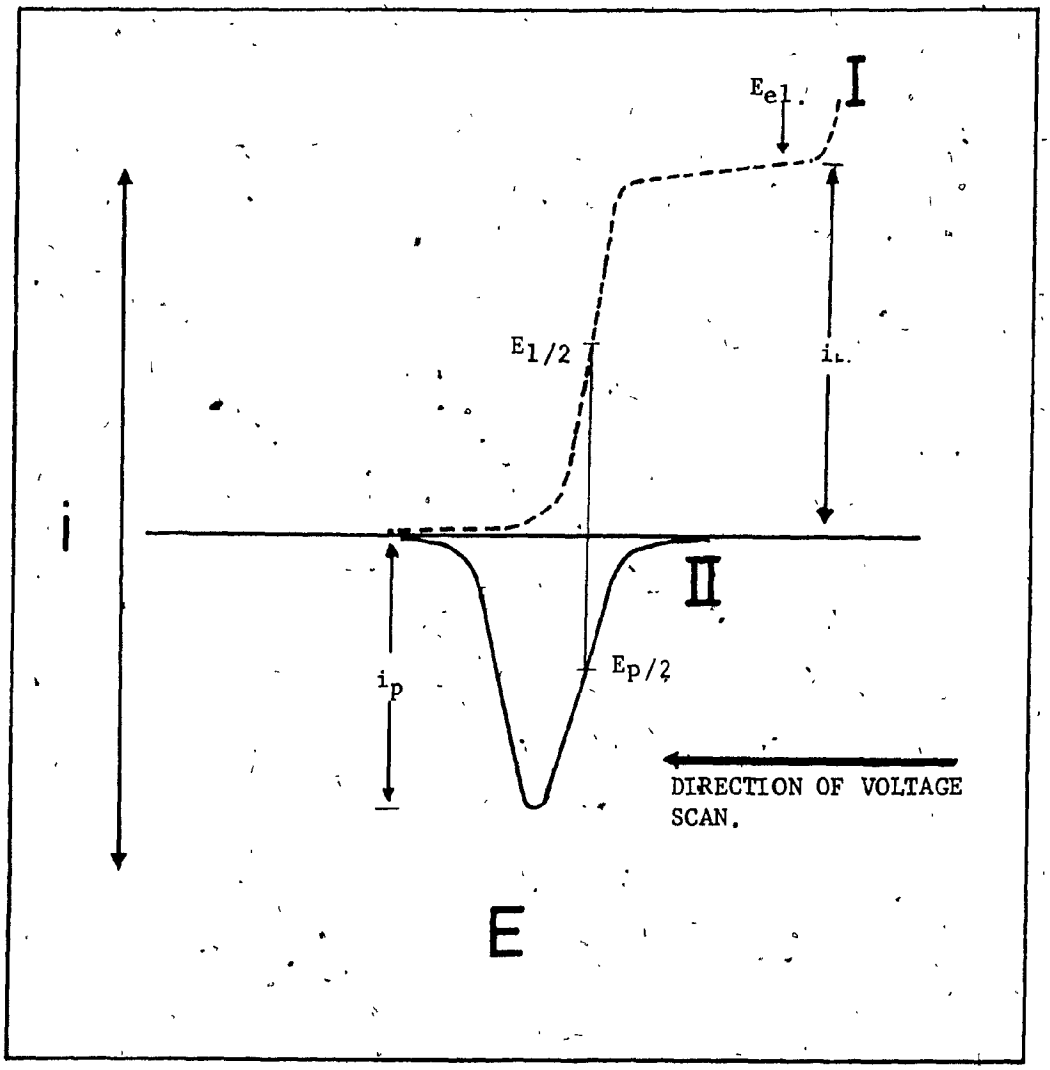

Figure 8 : Schematic presentation of the principles of electrochemical stripping analysis (16).

I = The electro-deposition step;
II = The stripping step;
$E_{el.}$ = Controlled electrolytic (deposition) potential (v.);
$E_{1/2}$ = Half-wave potential (v.);
$E_{p/2}$ = Half-peak potential (v.);
i_L = Limiting (effective electrolytic) current (ua.);
i_p = Stripping-peak current (ua.)

polarography), and their height (or area) is proportional to the concentrations in the solution, when constant pre-electrolysis conditions are employed (16). The stripping analytical process is shown schematically in Figure 8.

Polarographic (or voltammetric) stripping techniques are termed either anodic or cathodic, according to the character of the stripping process (oxidation or reduction, respectively).

Generally two approaches can be employed in stripping analysis:

(a) this approach involves the complete electrolysis of analyte(s) from the solution and monitoring of the stripping current during the time period necessary for the complete dissolution of the deposit;

(b) this approach, which is at present far more frequently employed, involves pre-electrolysis carried out under reproducible conditions for a certain time period, so that the amount of analyte(s) deposited at the electrode is a reproducible fraction of the total initial amount of analyte(s) in the solution.

The first approach secures very accurate and precise results under favourable conditions but suffers from the drawback of being time-consuming, especially with large

solution volumes.

The second approach requires maintaining a constant mass-transport velocity towards the electrode, and it is suitable to choose the pre-electrolysis conditions so that the fraction deposited is only a very low percentage of the total amount present. Because of the rigid requirement of constant electrolytic conditions, automation becomes favourable in the second approach.

2.6.2 Theory of anodic stripping (A.S.) analysis

In anodic stripping analysis, the preconcentration step is a cathodic or reductive deposition process, and the stripping step is an anodic or oxidative re-dissolution process. Anodic stripping polarography/voltammetry is the most widely applied version, mainly because of its usefulness in trace metal analysis in the fields of environmental control and toxicology.

For any electrode material employed in the anodic stripping polarographic (ASP) system, the same general electrolysis or plating theory applies. An elementary evaluation of the theory governing the plating process affords an indication of the parameters which can be adjusted to maximize the plating efficiency, and hence the stripping current measured.

Consideration will first be given to the preconcent-

ration step. It is assumed, for this treatment, that a constant current is maintained during the cathodic deposition. This will be the case if the concentration in the bulk solution is not appreciably altered during the course of electrodeposition (17) and if the solution is stirred at a constant rate. For a hanging mercury drop electrode, HMDE, the concentration of the reduced metal in the mercury, in the amalgam form is given by the Faraday's law:

$$Ca = {}^{it}/_{nFv} = {}^{3it}/_{4n\pi r^3F} \qquad (6)$$

where:

Ca = the concentration of analyte-amalgam ($^{moles}/_{l}$);

i = the reduction current (amp.);

t = the preconcentration time (sec.);

V = volume of the HMDE (mm^3),

The reduction current, i, is analogus to the limiting current in a diffusion - controlled process:

$$i = nFDC_bA/\delta \qquad (7)$$

where:

D = the diffusion coefficient ($^{cm^2}/_{sec}$);

C_b = the analyte concentration in the solution bulk (M);

A = the surface area of the working electrode (mm^2);

δ = the thickness of the diffusion layer (mm).

Since the solution is stirred, δ will be affected by the

stirring rate, cell geometry and the electrode design. To take this into account, Eq'n (7) becomes:

$$i = nmFDC_bA \qquad (8)$$

where m is the mass transport coefficient, which is approximately proportional to the square root of stirring rate (17, 18). By substituting Eq'n (8) into Eq'n (6), Ca can be expressed, after simplification, as follows:

$$Ca = 3mDC_bt/r \qquad (9)$$

where r is the radius of the HMDE.

In the electrodeposition step the analyte-amalgam is re-oxidized and stripped out of the HMDE. Several different potential-time waveforms may be used to strip the deposited analyte and obtain the quantitation parameter, the stripping peak current (i_p). By far the most common choice is the linear ramp of the potential. The behaviour at a HMDE may be considered as analogous to that of potential sweep chronoamperometry in the case of a reversible reaction (19). Thus, for a HMDE, i_p is expressed by the Randals-Sevcik equation:

$$i_p = 2.72 \times 10^5 \, n^{3/2} \, AD^{1/2} \, \nu^{1/2} \, C_a \qquad (10)$$

where

ν = the rate of potential scan (mv/s)

By substituting Eq'n (9) into Eq'n (10), i_p may be rewritten, after simplification, as follows:

$$i_p = kmn^{3/2} \, D^{3/2} \, {}^{1/2}\nu rtC_b \qquad (11)$$

where:

$$k = 3.264 \times 10^{6}$$

Equation (11) delineates the nature of the current signal, but in an ASP system there is "noise" as well, due to the instrumental electronics, and the nature of a electrolyzed solution. The total current flowing through the system is:

$$i_t = i_p + i_c + i_b \qquad (12)$$

where i_b is the background residual current due to the oxidation of impurities or decomposition of electrolyte. Together, i_c and i_b make up the residual current or electrochemical noise in the system. I_c is given, theoretically, by the following equation:

$$i_c = A\nu \left(\delta q / \delta E\right) \qquad (13)$$

where

$\delta q / \delta E$ = the differential capacity of the double layer.

Equations (11) to (13) demonstrate the fact that, while the absolute signal can be enhanced by increasing A and ν, i_c in the system is also increased. In the case of the HMDE, the signal, i_p, increases with $\nu^{1/2}$ and r, whereas i_c increases with ν and r^2.

In the search to increase the sensitivity of ASP, a variety of approaches have been employed. Although the sensitivity can be increased by lengthening the deposition time, this approach has only limited merit. In addition to

the undesirability of long analysis times from a workload standpoint, long deposition times present problems due to the diffusion of analyte up the mercury capillary column of the HMDE, increasing the memory effect. System and electronic instabilities can also create problems over long deposition times.

Several monitoring techniques have been used to enhance the sensitivity of ASP analysis by minimizing the effect of i_c signal. The differential pulse (DP) method has in recent years become the most popular technique applied to ASP, simply because of its advantages over the other polarographic techniques (see previous sections). In addition, the DP mode allows the use of very dilute supporting electrolytes, such as 0.05M HCl. This feature is very important in stripping analysis, where trace impurities in the supporting electrolyte complicate the quantitation process. DPASP has been performed on waste water and sea water samples without any additional supporting electrolyte beyond a very low HNO_3 or HCl concentration.

It is found that, when the DP mode is used, i_p is influenced by the amplitude of the modulating pulse, Udp, and a modification is needed for Equation (11) to give the more appropriate expression:

$$i_p = k'mn^{3/2}D^{3/2}r\,\nu^{1/2}tC_b\,Udp \qquad (14)$$

3.0 AUTOMATION IN STRIPPING ANALYSIS

3.1 General

Automatic methods of chemical analysis were virtually unknown a quarter of a century ago, but are now sufficiently commonplace to be applied to a greater or lesser extent in most analytical laboratories. Although many factors have contributed to the overall stimulus to develop automated methods, two of these have proved to be particularly significant. First, where the volume of analytical information required is large the requirement of producing it as economically as possible becomes important. Secondly, there are many instances, notably analytical services to industrial processes, where the value of such information is greatly enhanced when it can be produced and evaluated rapidly.

The term "automation", according to the Commission on Analytical Nomenclature of the Analytical Chemical Division of the International Union of Pure and Applied Chemistry, IUPAC (20), is defined as 'the use of combinations of mechanical and instrumental devices to replace, refine, extend or supplement human effort and facilities in the performance of a given process, in which at least one major operation is controlled, with human intervention, by a feed-back system.' In these terms there are, as yet, relatively few completely automatic methods in laboratory use.

In control analysis, generally, chemical constituents have been determined on grab samples which are subsequently analyzed by conventional manual techniques with obvious shortcomings in time, economy, and human-error possibilities. More and more industrial processes, however, require constant surveillance and control at each step in the process. Instruments and methods are needed to provide a dynamic rather than historical analysis. This requires either continuous, or at least repetitive analyses of starting materials, intermediate products, and end products for the desired component(s). Often monitored also are possible contaminants that could be damaging at various stages in the process. Only through analyses of these types can production facilities reduce off-specification materials to a minimum. Remedial action can be taken within a short time with automated analyzers.

Although automated instrumentation costs are generally high, they still represent a small fraction of plant or laboratory costs. Because the limits of accuracy of both process and laboratory work can be no better than the reliability of instruments used in making measurements, high costs are easily justified. Other advantages to be gained include greater safety of operation, greater time-savings and operating economy. Applicability of a method that initially appears to be borderline may be actually proven to be acceptable in service because the continuous sampling process tends to improve precision.

The field of electrochemical analysis embraces a wide range of techniques including potentiometry, coulometry, polarography/voltammetry and ion-specific electrodes. By a suitable choice of technique and experimental conditions, a high degree of analytical sensitivity and specificity can be achieved. It is therefore not surprising that electrochemical techniques have found considerable favour in the design of continuous and automatic methods, especially where trace components of a sample are to be determined and where their selectivity can reduce or eliminate the need for pretreatment stages , thereby simplifying the design of the automated system. The range of electrochemical methods which are amenable to automation is extremely diverse, incorporating the determination of organic and inorganic materials in aqueous, non-aqueous, gaseous and molten salt media. One particular advantage of electrochemical methods is their independence of sample colour. In many instances the response of the sensing electrodes is a linear function of the analyte concentration.

3.2 Automated Anodic Stripping Polarography

3.2.1 Principles

Automated laboratory methods enhance the ease of carrying out analyses that would be impossibly tedious by manually controlled methods, and consequently increase the

precision of results through precisely controlled procedure.

The determination of heavy metal at the parts-per-billion (ppb) and sub-ppb levels by use of DPASP requires that experimental parameters such as deposition time, drop size of the HMDE, the system temperature, deposition voltage, stirring rate, and the size of "spike", when the multiple spiking technique of quantitation is used, be carefully controlled to achieve reproducible results. Some, but usually not all of these parameters, can be controlled by devices connected with the electroanalytical instrument, or by a microprocessor-controlled instrument.

In practice, if the multiple spiking technique is employed, a complete anodic stripping analysis consists of the following stages in sequence:

1. The deaeration of the test solution. Inert gas, such as nitrogen or argon, is bubbled into the solution to remove the dissolved oxygen.
2. The feed of a new HMDE of pre-set size. The cell potential of the system during this stage is held at a value (U pause) which is more anodic than that of the analyte having the highest anodic, or the lowest cathodic, potential.
3. The electrodeposition process. The potential of the HMDE is controlled at a predetermined cathodic value, Udep., throughout the stirring and the quiescent periods.

4. The anodic stripping step. The desired potential range is scanned at a preset rate of potential application.

5. The stoppage of the stripping process, the dislodgement of the used HMDE, and the start of the pause period. Throughout the pause period, the cell potential is controlled at a value equal to U pause, the solution is stirred and purged once again, and standard(s) may be added into the system, if needed, upon the completion of the necessary number of replications for the same solution. After the pause period, the sequence of analysis is repeated until all necessary data are collected.

In principle, hence, a controller for automated ASP should possess the following basic functions:

1. Control of gas valves for proper directional purge-gas flow through the system at different stages of analysis.

2. Triggering the feed and dislodgement of the automated HMDE at the proper moments.

3. Switching on and off a magnetic stirrer.

4. Control of the times of deposition, potential scan, and pause, and the corresponding cell potentials at the different stages.

5. Triggering the proper device to deliver necessary amounts of standard(s) (spiking solution(s)) into the analyte solution at the predetermined moments between the analyzing cycles.

6. Termination of analysis upon the completion of the analysis programme.

The Metrohm E608 VA-Controller is one such micro-processor-control device. It is designed to be used in conjunction with an automated polarographic stand consisting of two operating stations, a polarographic analyzer/recorder, two automatic burettes, and a volume preselector.

3.2.2 Functional descriptions

N.B. This section is intended to give a brief description on the operational functions of each of the components that composed the instrumentation for automated stripping analysis. Emphasis is given to the VA-Controller, the central unit of the automated set-up.

3.2.2.1 General

To conduct stripping analyses, the most basic, simple equipment required consists of an electrochemical cell for a three-electrode system, a timer, and a polarographic analyzer/recorder. To quantitate an analysis by the use of the standard additions (spiking) method, an automated burette is usually employed for accurate and precise delivery of the standard solutions. Finally, to automate a stripping analyzing system, a volume preselecting device and a central command and control unit need to be added to the

above basic assembly. These provide the basic instrumentation for automated stripping analysis. Figures 9-11 show the Metrohm devices involved.

3.2.2.2. E506 Polarecord (Metrohm Herisau)

The polarographic analyzer/recorder comprises four main functions: voltage generation, potentiostat, current evaluation and current recording.

The polarographic voltage ramp is generated in digital form by means of synchronized pulse generators, and then converted to analog form with the aid of digital/analog convertors. This gives it a "staircase" characteristic, and consequently presents great advantages relative to polarography/voltammetry (21,22).

The potentiostat is used to stabilize and maintain the potential differences between the working and reference electrodes.

Current evaluation is much simpler when working with the HMDE than with the DME. Synchronization of the drop falls with the voltage steps of the staircase ramp is of utmost importance in the latter form. With the HMDE, the sampled current signal obtained during each pulse cycle (in the case of pulse techniques), which is synchronized with each voltage step, is integrated and fed to the recorder input after suitable amplification.

The current recording is obtained with a built-in strip-chart recorder which is driven by a stepping motor synchronized with the voltage steps. The Metrohm E626 Polarecord can also be used for DPASP.

3.2.2.3 E542 Dosifix* (Metrohm Herisau)

The unit is a volume preselector intended for use as an auxiliary component to the E535 Dosimat, an automatic burette equipped with an auto-changeover three-way valve. Its enables any desired volume to be fed out from two separate burettes conveniently, accurately, and reproducibly. The pre-set volumes may be selected on the Dosifix by means of two 4-figure selector switches, corresponding to the burette capacity. By connecting to the VA-Controller, the Dosifix is remotely controlled for use in automated feeding processes.

3.2.2.4 E535 Dosimat* (Metrohm Herisau)

This automatic burette, when connected to the Dosifix, can be triggered to deliver accurately and reproducibly a minimum volume of 20.0 µl, and to refill automatically when the limit-switch is actuated.

3.2.2.5 E607 Double Stand (Metrohm Herisau)

This polarography stand is designed to be used

*See Appendix II - Footnote (1)

specifically in conjunction with the VA-Controller for automated stripping analysis. It consists of two operation positions, each of which functions independently, and consecutively, with an identical programme set on the controller.

3.2.2.6 E608 VA-Controller (Metrohm Herisau)

This instrument functions as the central command unit for the automated assembly. In addition to the basic principal functions necessary for multiple standard additions quantitative analysis, it possesses also the functions of switching over from one operation station to another upon the completion of an analysis programme, allowing the deaeration of a new sample solution while analysis is being carried out on another sample, and, therefore, permits continuity of the analytical process and savings in analysis time.

On the VA-Controller, all the times of deaeration, electrodeposition (with and without stirring), stripping, and pause are preselectable by means of numeral switches, each from zero to 990 sec. Potential settings for periods of deposition and pause are selected by means of two ten-turn potentiometers. The potential value, Udep., set for deposition is added by the E506 or E626 Polarecord to its own value set as the starting potential, Ustart, of the voltage range to be scanned through in the actual determination. The potential value set for the pause period,

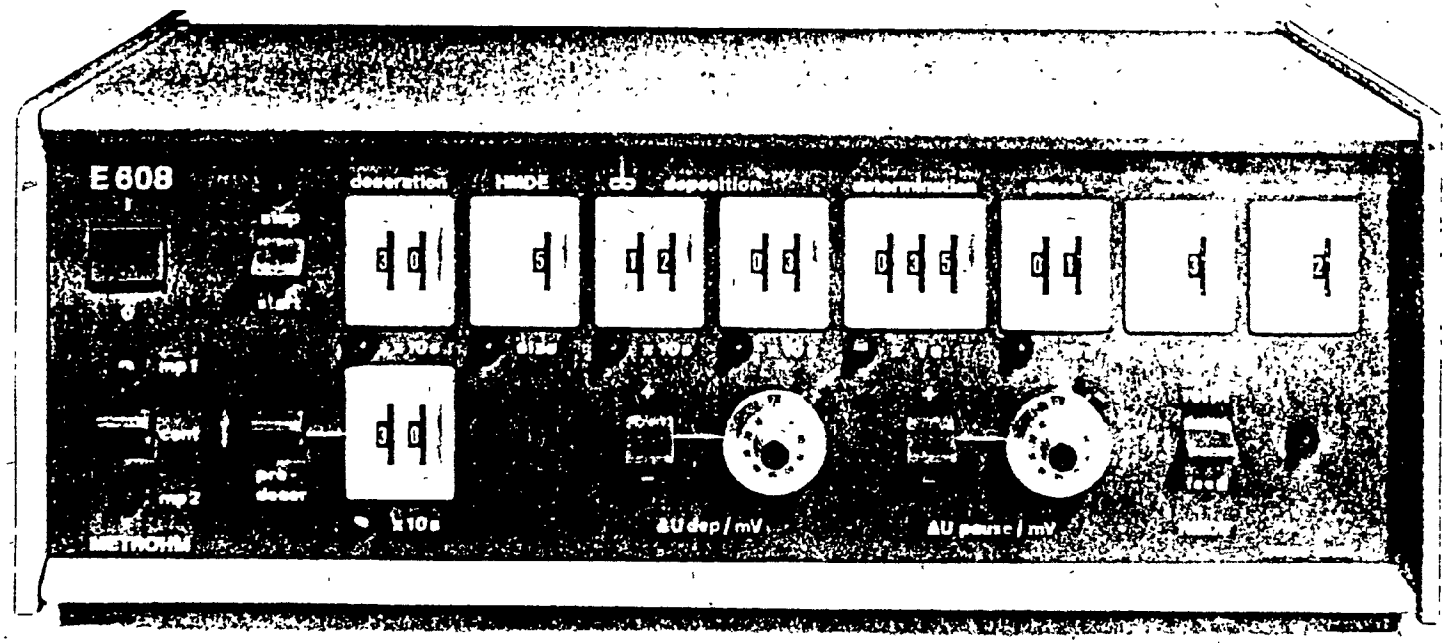

FIGURE 9 : THE E608 VA-CONTROLLER

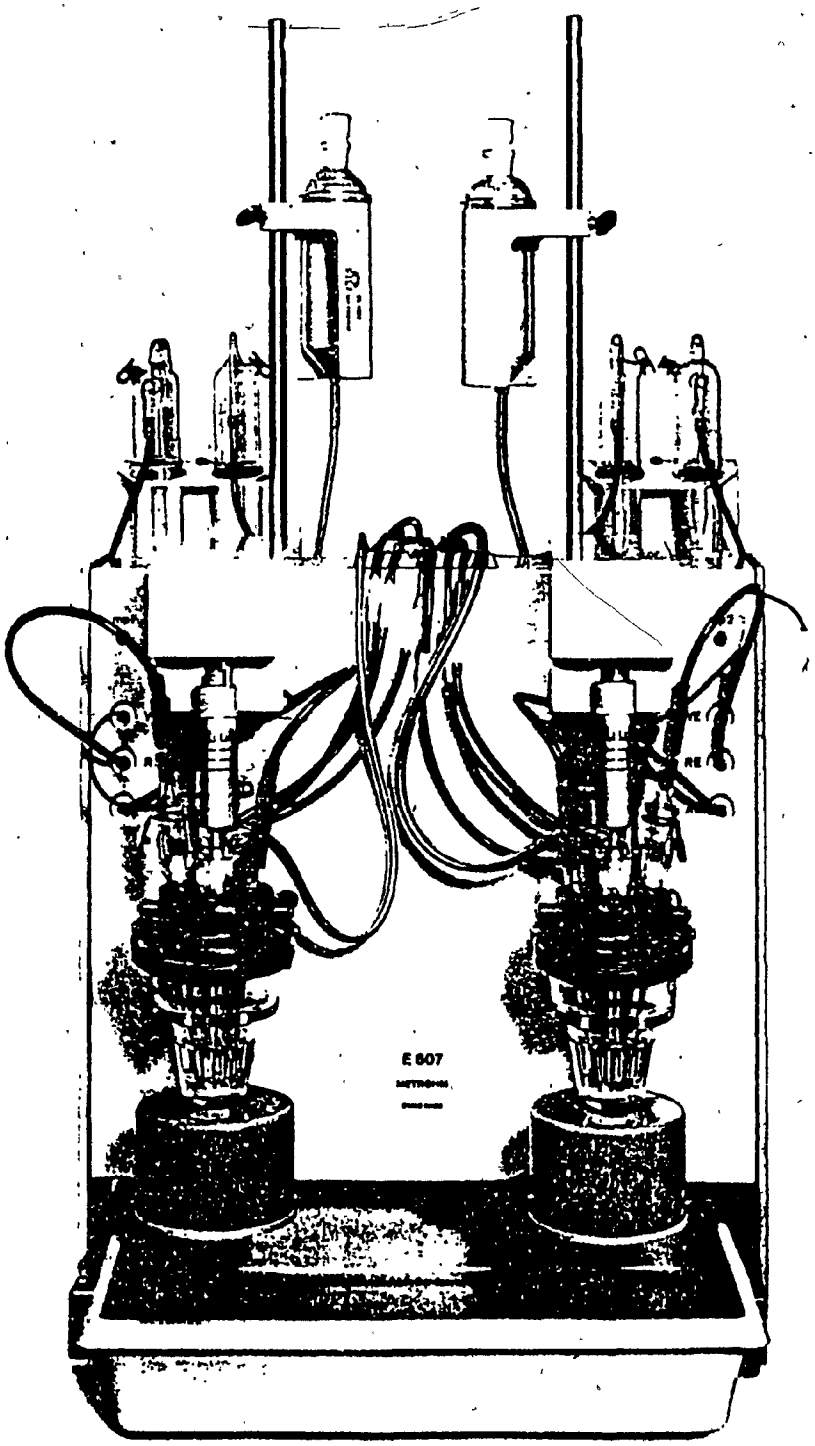

Figure 10 : The E607 VA-Double Stand

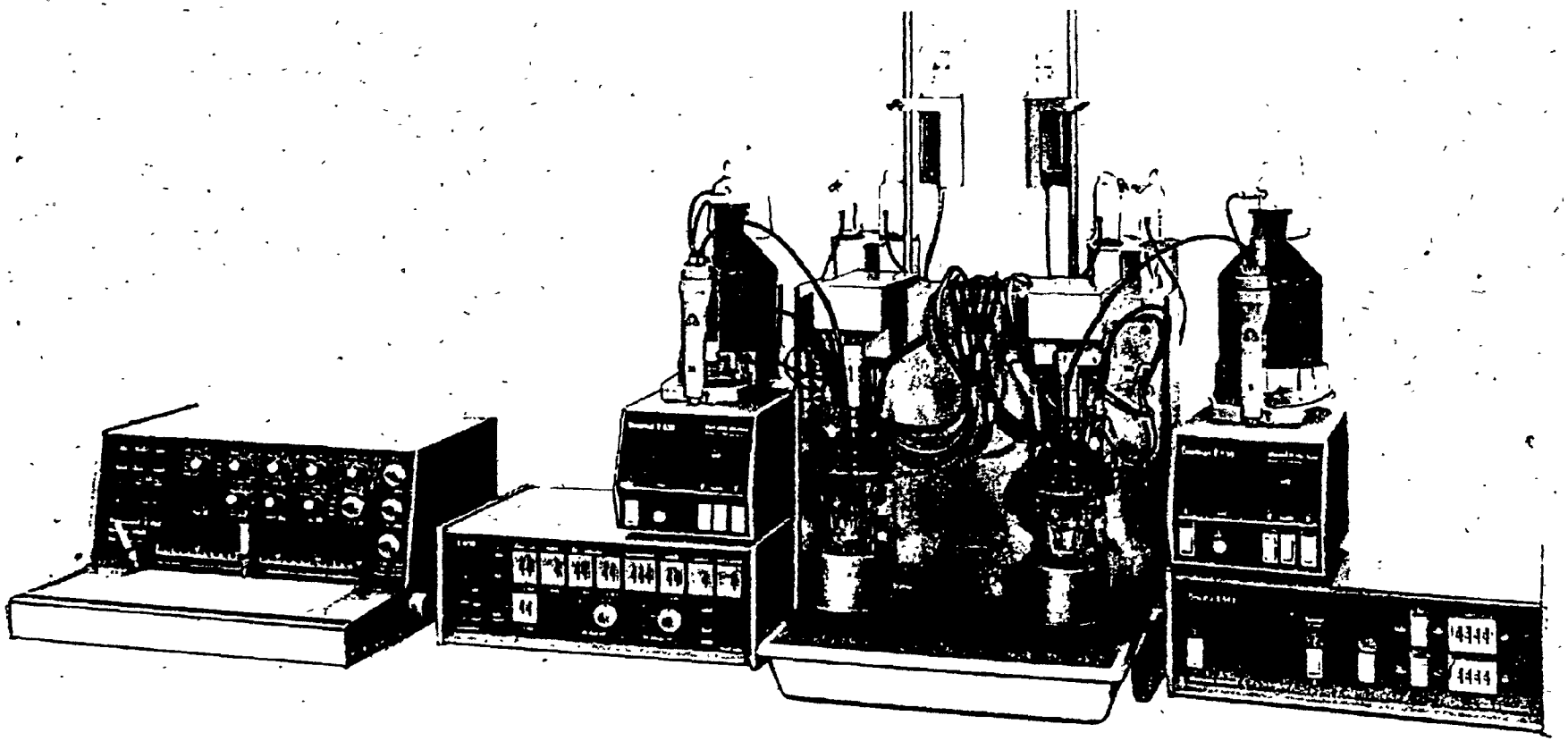

Figure 11 : A complete assembly for the automated electrochemical stripping analysis

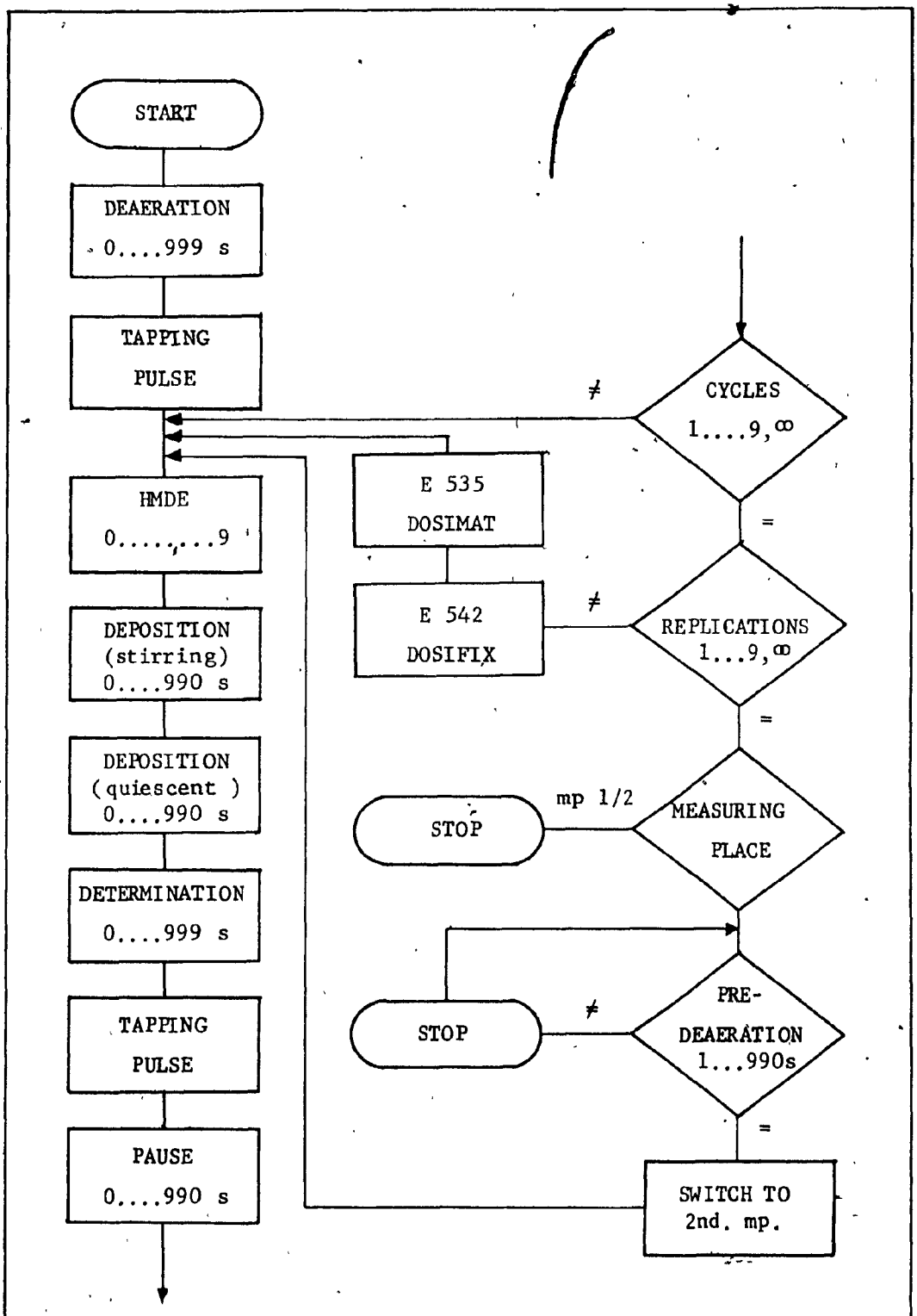

Figure 12 : Flow-chart of the E 608 VA-Controller functions (23).

U_{pause}, on the other hand, is added to the potential value at which the scan stops. The potential settings, however, are independent of the parameter set on the Polarecord(s) for the actual determination. The pause potential value is usually selected in such a manner that the pause period fulfills the following functions: to purify the mercury in the HMDE capillary by extending the anodic stripping process; to prevent the deposition of analyte and homogenize the sample solution once again, hence to ensure reproducible electrolysis in the proper state; and, finally, to allow any added standard solution to mix thoroughly with the sample solution. The VA-Controller starts the voltage scan at U_{start} and stops it when the pre-set "Determination" time has elapsed.

The sequence of the programmed functions of the controller can be summarized and presented by Figure 12 (23).

4.0 EXPERIMENTAL APPROACHES

This chapter is divided into three main sections as follows:

1. Sample preparations:-

   This includes the preliminary preparation of homogenized, freeze-dried fish muscle tissue as the stock samples; the preparations of sample solutions via wet and dry-ash procedures; and the preparation of the standard spiking

solutions.

2. Instrumental parameters:-

The AAS and DPASP instrumental parameters used are listed in these sections.

3. Experimental procedures:-

This section includes brief descriptions of procedures used in the AAS and DPASP applications.

4.1 Sample Preparations

4.1.1 Preparation of the fish sample stock

4.1.1.1 Description of the whole fish specimen *

*See Appendix II - Footnote (2)

4.1.1.2 Homogenizing and Freeze-drying of fish muscle tissue

Approximately 20 kg of whole fish were filleted to yield a quantity of fresh muscle tissue, weighing 6,297 g. The amount of non-muscular tissues (e.g. bone and skin) adhering to the muscle tissue was kept to a minimum.

The fresh muscle tissue was first homogenized with adequate amount of de-ionized, glass-distilled water (hereinafter referred to as H_2O), in a 450 ml Nalgene beaker, in 200-250 g lots, by means of a homogenizer (Polytron*, P.T. 10-35, kinematica GmbH, Switzerland). The homogenized tissue was frozen on large watch-glasses (15-cm diam.) before

*See Appendix II - Footnote (3)

being freeze-dried. The freeze-drying process was carried out in a lyophilizer (Varian 801, Vir Tis Co., Ltd., N.Y.), at temperature of -60^{0}C and reduced pressure of 100 mm Hg, for approximately 36 hours per batch. The total freeze-dried tissue powder was weighed and mixed thoroughly, by the inquartation method, on the rotation unit of a ball mill (Stoneware, Ohio). A total amount of freeze-dried weight of 1,173 g - equal to 18.64% of the wet weight - was obtained. Finally, the dried sample was stored in a freezer under anhydrous conditions.

4.1.2 Sample treatment by the dry-ashing method

To quantitate the heavy metal content of biological materials by electrochemical or spectrochemical means, a sample must be completely decomposed. This can be achieved through oxidative digestion by dry or wet methods. The merits of both methods have been published (24-26). Experimental trials had shown that, in the case of fish tissue, dry ashing was more advantageous than wet digestion (26a).

A methodology developed by De Luca (27) in preparing fish tissue sample solution was employed as a guideline. Modifications were made during the course of the experimental work to suit the particular ashing characteristics of the fish tissue material. The following is the modified procedure:-

1. 2.000 g samples were weighed out in 50-ml Pyrex beakers, covered and placed in a muffle furnace (Lindberg, Temperature programmable) at 100°C for one hour. A sample blank was provided and treated in the same manner as the sample.

2. After the initial hour, the furnace temperature was raised gradually by adjusting the temperature control according to the following programme:

200°C	60 min.
300°C	120 min.
50°C/30 min. to 475°C	
475°C	overnight (ca. 12-14 hours)

3. After ashing, the blank and samples were removed from the furnace and allowed to cool to room temperature.

4. Nitric acid (concentrated, 5 ml) was added for the redissolution of the ashed samples at a temperature just under boiling, without splattering, for about 30 min., or until any carbon residue was completely oxidized. (Where necessary, 3-5 ml of 72% $HClO_4$ were added 10 min. after the reaction began to aid the digestion process).

5. After digestion, the acid solution was evaporated to near-dryness, without any baking.

6. The dried contents were allowed to cool before making up the final test solutions with the addition of appropriate solvents (for AAS analysis, 1% HNO_3 in H_2O

was used. The supporting electrolyte, 2M HOAc/2M NH_4OAc, was used for DPASP analysis).

4.1.3 Preparations of the standard stock solutions and the supporting electrolyte

Standard stock solutions of Pb and Cd at concentrations of 1000 ppm were prepared by dissolving 1.000 g of each metal (Fisher, 99.9%), separately, in 10 ml of conc'd HNO_3, boiling, and then diluting volumetrically to 1 liter with deionized/glass distilled water.

The supporting electrolyte (2M each, HOAc and NH_4OAc) was prepared by diluting a prepurified solution, containing 5M each of HOAc and NH_4OAc, with deionized/glass distilled water. (see Appendix 1 for details of the electrolytic purification of the supporting electrolyte).

4.2 Instrumental parameters

4.2.1 Atomic absorption spectrophotometric analysis

4.2.1.1 Instrumental descriptions

Atomic absorption spectrophotometer Perkin-Elmer 503
Graphite-furnace temperature programmer Perkin-Elmer HGA 260

Recorder	Perkin-Elmer 56
Excitation sources	
1. Hollow cathode lamp (h.c.l.) (Cd)	Perkin-Elmer
2. Electrodeless discharge lamp (e.d.l.) (Pb)	Perkin-Elmer
Background-correction source	
D_2 continuum	Perkin-Elmer

4.2.1.2 Analysis for Pb

Wavelength (λmax)	283.3 nm
Slit width	0.7 nm
Excitation source	Electrodeless discharge lamp
Source energy	5 watts
Purge-gas flow rate	30 units, continuous
Recorder : range	5 mv
chart speed	10 mm/min.

HGA 2100 temperature programme

	temperature (^{o}C)	time(s)	ramp time (s)
Drying	120^{o}	10	10
Charring	700^{o}	20	0
Atomizing	2300^{o}	8	0

4.2.1.3 Analysis for Cd

Wavelength (λ max)	228.8 nm
Slit width	0.7 nm

Excitation source	hollow cathode lamp
Source energy	2 ma.
Purge-gas flow rate	30 units, continuous
Recorder : range	5 mv
. chart speed	10 mm/min.

HGA 2100 temperature programme

	temperature (^{o}C)	time(s)	ramp time(s)
Drying	120^{o}	10	10
Charring	250^{o}	20	0
Atomizing	2100^{o}	8	0

4.2.2 Automated DPASP analysis

The following are the principal instrumental settings used in the determination of the polarographic responses for the biological samples.

Electrochemical cell - three-electrode system

Working electrode	automated HMDE (Metrohm EA 290)
Reference electrode	Ag/AgCl, sat'd KCl with diaphram junction (Metrohm EA 407)
Auxilary electrode	micro-Pt (Metrohm EA 285)

E506 Polarecord

Mode	DP
Start potential (Ustart)	-0.100 V
*Potential range (ΔU)	+1.50 V

*Drop life-time (t_{drop})	0.6s and 1.2s
*Chart speed (mm/t_{drop})	1
Sensitivity	0.25 - 1.00 nA/mm
Pulse amplitude (U_{dp})	+30mv and +50mv
Damping	1-2 units

*The three settings combine to determine the potential scan rate according to the general formula given in the "E506 Operation Manual".

$$\text{Scan rate } (^{mv}/s) = \frac{\Delta U \times {}^{mm}/t_{drop}}{250 \times t_{drop}} \times 10^3$$

E608 VA-Controller

Deaeration	900s (N_2)
Drop size (HMDE)	3-9 units
Deposition (stirring)	60-300s
(quiescent)	30s
Pause	30s
ΔU_{dep}	-0.1ov
ΔU_{pause}	0

E542 Dosifix

Volume (per addition)	0.020 ml

E535 Dosimat

Burette size	5.000 ml

E607 Double Stand

Rotational speed of magnetic stirrer	600 rpm

4.3 Experimental Procedure

4.3.1 AAS analysis

Only the fish muscle tissue samples were analyzed by AAS. The contents of Pb and Cd were determined, separately, in solutions of different dilution factors, those being a 10.00 ml volume for Pb, and 50.00 ml for Cd. In both cases, the metal contents were quantitated by means of the multiple spiking method, due to the failure of the water-based standard solutions to account for matrix interferences. Quadruplicate determinations were carried out for each original sample and spiked sample , using an injection volume of 50 µl for each determination. A micropipette (Eppendorf, W. Germany) with disposable tips was employed for sample application.

4.3.2 Automated DPASP analysis

4.3.2.1 Preliminary analysis for instrumental optimization

The preliminary analysis involved the determination of the dimensional properties of the automated HMDE, the instrumental responses due to analyte concentrations, amplitude, deposition times, and the radii of the HMDE.

The dimensional properties, i.e., radius, surface area, and volume, were established from the average weight

of a single mercury drop. The procedure was as follows: Ten drops of mercury of each predetermined size setting were extracted automatically from the HMDE and weighed. This was repeated four times for each drop size. The corresponding dimensions were calculated using the density of mercury at the ambient temperature for the procedures.

The instrumental responses were recorded by using only one variable parameter at a time.

4.3.2.2 Analysis of the biological samples

In addition to the fish tissue material, a reference sample, Bovine Liver (N.B.S. Material No. 1577), obtained from the National Bureau of Standards, was also used, in order to substantiate the validity of the quantitative method and evaluate the performance of the automated electroanalytical instrument. In the case of the NBS sample, it was found, after many trials, that dry-ashing induced a significant loss of material, and that the wet-digestion of 1.000 g samples with a 5.00 ml solution mixture of HNO_3-$HClO_4$ (1:1) yielded better and more consistant results.

In any case, the following procedure was carried out after material decomposition: 50.00 ml of the supporting electrolyte was added to dissolve each sample, and 25.00 ml aliquots were transferred from each sample solution to separate electroanalytical vessels each of which had a water-jacket that allowed the circulation of water of

constant temperature. Thermostatically controlled conditions were preferable in the lengthy multiple spiking analysis in order to avoid any error caused by temperature fluctuation (the i_d can vary by 1-2% per ^{o}C between 15^{o} and $50^{o}C$). The two samples were mounted on the measuring stations on the E607 polarographic stand, and were ready to be analyzed according to the programme set on the VA-Controller. The analysis of the sample by the programme sequence was then initiated by one single tapping on the "start" button.

5.0 RESULTS AND DISCUSSIONS

5.1 Preliminary Experimental Data

5.1.1 Dimensional properties of the automated HMDE

The dimensions of the HMDE at the different E608 size settings were calculated from the weight data of the mercury drops obtained at $23^{o}C$, using the density of mercury, and the dimensional formulations for a sphere (Appendix VII). These are listed in Table 1 and diagrammatically presented in Figure 13.

These data demonstrated the important fact that the weight, and consequently the volume, of the average mercury drop changed linearly with the control settings (HMDE) on the Controller. Because of the existence of the exponential relations in the dimensional formulae for a sphere, the

Table 1 : The dimensional properties of the HMDE* (at 23°C)

HMDE Setting	Av.Wt./Drop (mg)	Av. Radium (r, mm)	Av. Surf. Area (A, mm^2)	Av. Volume (V, mm^3)
2	1.06 ± 0.03	0.265 ± 0.008	0.88^5 ± 0.02^5	0.078 ± 0.002
3	1.55 ± 0.00	0.301 ± 0.000	1.14 ± 0.00	0.114^5 ± 0.000
4	2.09 ± 0.00	0.333 ± 0.000	1.39 ± 0.00	0.154 ± 0.000
5	2.65 ± 0.01	0.360 ± 0.001	1.63 ± 0.00^6	0.196 ± 0.001
6	3.20^5 ± 0.02	0.384 ± 0.003	1.85 ± 0.01	0.236 ± 0.002
7	3.72 ± 0.00	0.404 ± 0.000	2.05 ± 0.00	0.276 ± 0.000
8	4.29 ± 0.03	0.423 ± 0.003	2.25 ± 0.02	0.317 ± 0.002
9	4.92 ± 0.00	0.443 ± 0.000	2.46 ± 0.00	0.363 ± 0.000
Correlation coefficient	0.9997	0.9925	0.9987	0.9997
Av. Rel. Std. Dev.	0.59%	0.60%	0.58%	0.55%

*See Fig. 13

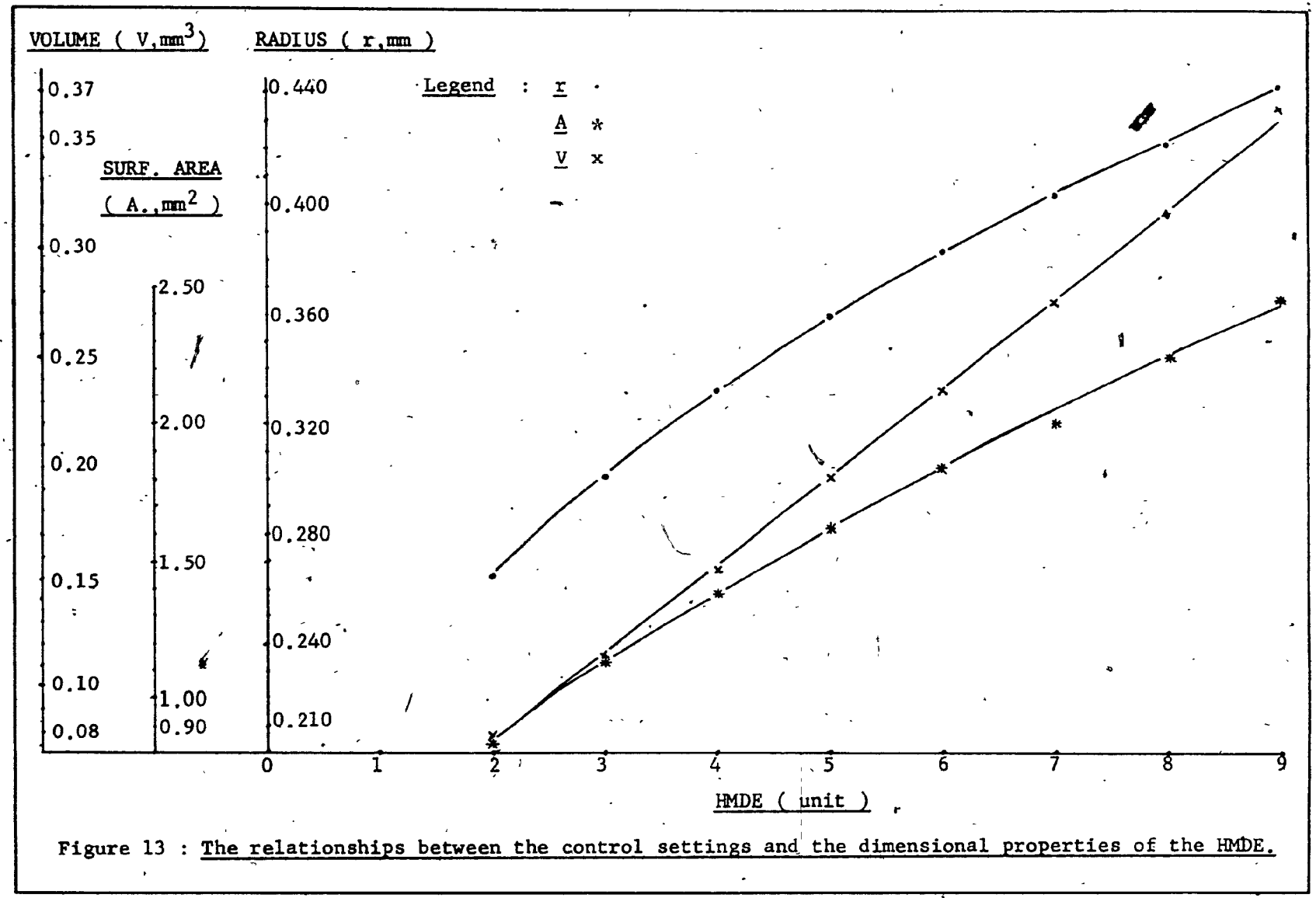

Figure 13 : The relationships between the control settings and the dimensional properties of the HMDE.

changes in drop radius and surface area were not linear with reference to the weight, even though the correlation coefficients resulting from linear regression analysis of the data indicated otherwise.

The conclusions drawn from the statistical analysis may be considered only partially valid, however, since changes in all dimensions become linear only when the mercury drop becomes larger. This may be explained by considering all the dimensional changes in relation to the change in the weight of mercury drops. At the stages where the drop weight is small, the dimension increases, in drop radius and surface area, per unit weight of mercury are relatively higher, in comparison with those for larger drop volumes, where change is relatively constant. As the mercury drop expands at a constant pace, the rates of increase in the two dimensions decline, subsequently reaching a point where the changes in the rates become so insignificant that all the dimensional increase rate may be regarded as constant.

It is of interest to note that a radius of 0.17 mm, and surface area of 0.1 mm^2, were estimated graphically at the zero position, of the HMDE, through extrapolation of Figure 12, and that these values approximated the cross-sectional dimensions of the capillary of the HMDE.

It is also important to note that the calculated values, shown in Table 1, for the dimensions of the mercury

drops, did not take into consideration any retraction of the mercury into the capillary, nor were those for the surface area corrected for the part of the area that was attached to the capillary and not in any way in contact with the solution. The retraction of the mercury column always occurs upon the dislodgement of a drop, due, it is believed, mainly to the surface tension of mercury (provided that EA290 automated HMDE is set up properly). Since the degree of retraction is constant and undeterminable, its effect becomes proportionally greater the smaller the drop formed. Consequently, a drop of reasonably large size is generally used in order to minimize the effect of this constant error.

The accuracy of the experimental data acquired using the average weights of mercury drops was a confirmation of the measurements secured optically by the instrument manufacturer (28). Comparison between the two sets of data yielded an overall deviation of 0.6%, with respect to the manufacturer's values.

The overall relative standard deviation of 0.6%, shown in Table 1, on the other hand, represented the reproducibility of the sizes of mercury drops produced by the EA290 automated HMDE.

5.1.2 Polarographic responses due to pulse amplitude (Udp)

Table 2 and Figure 14 contain the experimental data obtained in tabular and in graphic form.

Table 2 : The effect of pulse amplitude (Udp) on the DPASP response*

Udp (+mv)	Av. Peak Current ± Std. Dev.'n (ip, nA) Pb	Cd
10	1.60 ± 0.06	1.44 ± 0.00
20	3.82 ± 0.12	2.94 ± 0.12
30	4.46 ± 0.62	4.70 ± 0.34
40	6.31 ± 0.13	6.75 ± 0.16
50	7.99 ± 0.07	8.84 ± 0.02
60	11.32 ± 0.11	12.25 ± 0.06
70	12.77 ± 0.18	13.76 ± 0.09
80	15.90 ± 0.30	17.51 ± 0.77
90	17.43 ± 0.38	19.83 ± 0.17
Conc'n (ppb)	3.40 ± 0.04	2.11 ± 0.05

* Specific parametric settings:

HMDE : 5 units;

t_{dep} (stirring) : 180 sec.;

(quiescent) : 30 sec.;

Scan rate : 5 mv/sec.;

Damping : 1 unit.

** See Figure 14

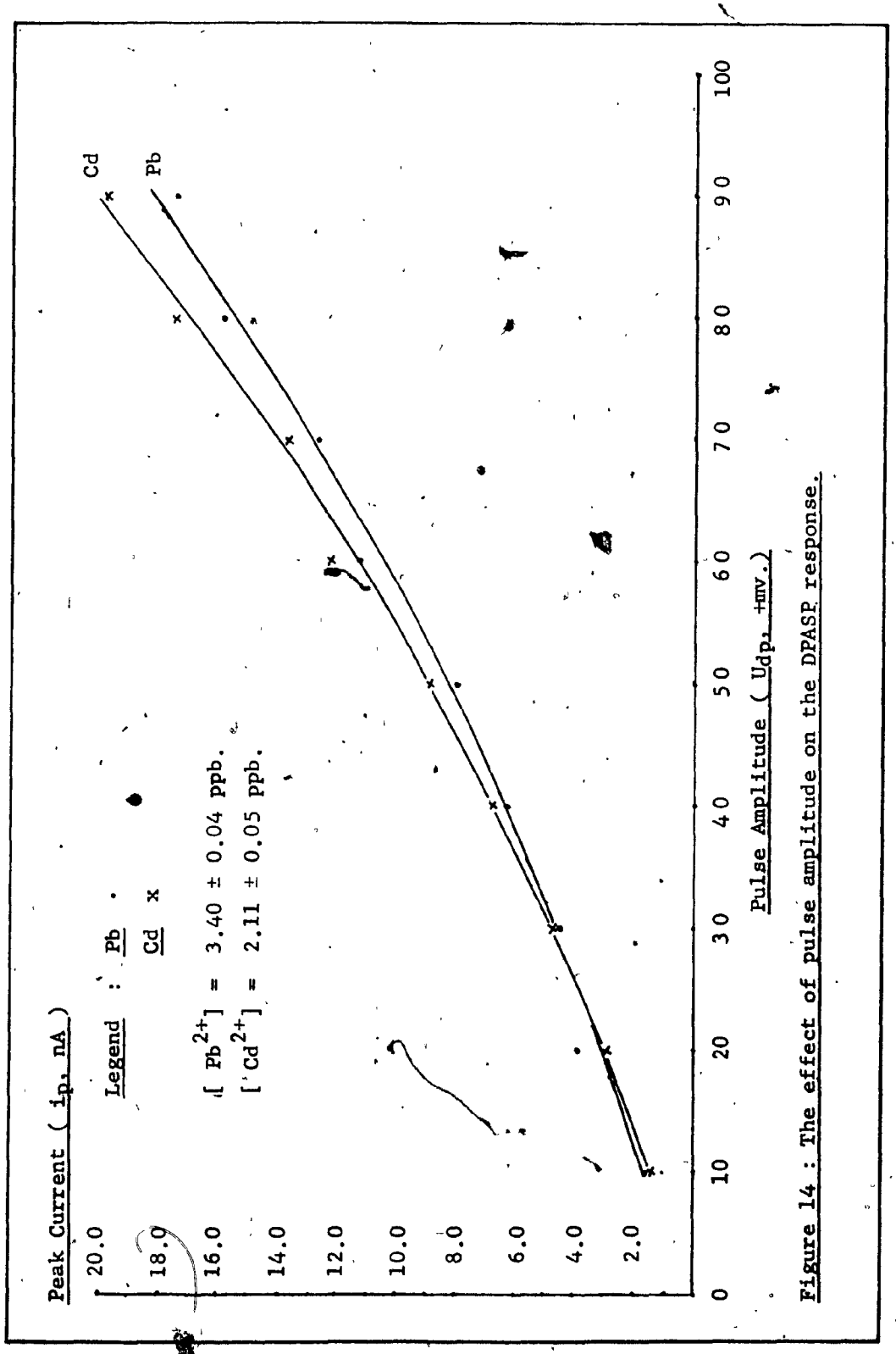

Figure 14 : The effect of pulse amplitude on the DPASP response.

It has been theoretically predicted that, in general, the polarographic response increases proportionally with the applied pulse amplitude (29,30). Consequently, the instrumental sensitivity may be increased theoretically to a level limited only by the electronic capacity of the instrument to provide pulse amplitude values. However, the instrumental capacity is not the only limiting factor.

In the derivative mode, polarographic response is presented in terms of the size of a peak, which is the product of its height and its half-width. By convention, the peak height is expressed in terms of the quantity of current in amperes, whereas the peak half-width may be given either in terms of potential (in volts) or time (in seconds). In any case, any increase in response means the increase of a peak in both dimensions. In reversible systems, such as Pb and Cd, for example, the increase in peak height is usually much greater than that in the half-width. Therefore, it is sufficient to express the peak height as the response signal for reversible systems. Nevertheless, the peak half-width does increase along with its height, and this increase is more significant in irreversible systems. This results in a reduction in resolution between two polarographic signals (31) and this is undesirable when there are two closely-located peaks to be considered.

The modulating pulse has, in general, the effect of amplifying the polarographic response as a whole. This means

that background noises from both chemical and electronic media are also amplified in the same proportion as the polarographic signal due to the analyte. This consequently reduces the snesitivity and leads to the steepening of the baseline of the polarogramme, making it difficult to quantitate it.

For practical reasons, it is thus desirable to apply pulses of low amplitudes in order to yield the most easily analyzed polarogrammes. In fact, the improved model of the Polarecord (E626), designed for industrial use, offers a choice of only two pulses amplitudes, one of 10 mv and the other of 50 mv.

5.1.3. Polarographic responses due to analyte concentrations

The DPASP responses for Pb and Cd in the acetate supporting electrolyte were secured in terms of families of concentration-calibration curves at various electrode sizes (with constant U_{dp} and t_{dep}) and deposition times (with constant U_{dp} and HMDE), and are presented in Figures 15-18 and Tables 3-6. A linear linear relationship between the stripping-peak current, i_p, and the analyte concentration was established within the concentration range chosen for the analyses. It had been found that this linear working limit could be extended to a considerably higher concentration level for most heavy metals. For example, in the case of Cd, this could be up to a concentration of approximately 600 ppb, a level which may

be quantitated accurately and simply by direct pulsed polarographic techniques. Since the DPASP method is mainly used for trace quantitations, it was thus logical and practical to put more emphasis on the lower concentration levels.

Close examination of the calibration curves revealed that all their least-square lines intercepted the current axis at negative values. If, theorectically, all the background-corrected calibration curves should rise from the origin, this might mean that they curved off at the low concentration region, starting at approximately 0.5 ppb. It seemed that each curve was composed of two different parts, with the lower part having a parabolic slope function and the upper part a linear one. (This condition persisted throughout the course of the investigation, but the cause is not known. Unfortunately this was not fully realized until recently, when the equipment used for this thesis work had been returned to its owner, and was no longer accessible).

Possible explanations have been postulated for this occurrence.

1. It was known that the concentration of analyte-amalgam became homogeneous throughout the HMDE during the quiescent period (32). The density distribution of the amalgam at the end of this period was therefore higher in a mercury drop having a higher concentration of amalgam than in one of lower amalgam concentration. For this reason, it would take a longer time to remove a certain amount of analyte

out of an HMDE containing a low concentration of amalgam than out of the one with a higher amalgam concentration. Conversely, with the same stripping force (i.e., potential-scan rate), the amount of re-oxidized analyte being stripped out would be higher in the case of high amalgam concentration than for that of a lower amalgam concentration, within the same time period. Polarographically, this gives rise to the anodic stripping current, which is actually dependent on the concentration of analyte-amalgam in the HMDE. Experimentally, there seemed to be a threshold amalgam concentration, below which i_p increased parabolically but, above and beyond which, i_p increased linearly at a greater constant rate.

2. The ionic concentration of supporting electrolyte might be part of the cause. In a supporting electrolyte of high ionic concentration, the ionic mobility would be generally low, because the high mass distribution could reduce the degree of freedom for mass transport. There might exist an opposing force which would retard the diffusion of the analyte cations, being stripped out of the HMDE, into the solution bulk. The magnitude of this retardation force might not be high. However, it could significantly reduce the momentum of diffusion of the analyte when the amalgam concentration was low. As the amalgam concentration increased, the divergently diffusing momentum might also increase, and reach a point at which the retardation force exerted by the non-electroactive species in the solution

bulk became negligible. Because of this constant reduction in the momentum of analyte diffusion, the resulting diffusion-limited i_p could assume a parabolic rise below the threshold point, and a linear increase at and beyond it.

The two factors, described above, might exert their influences separately, but the resulting effects could be a combined one since there could be interaction between these factors.

The problem would be simply solved by increasing the amount of analyte amalgam formed in the HMDE, and this could be accomplished in two ways; by employing a larger mercury drop, or a longer deposition time, or a combination of the two parameters. A larger mercury drop has a greater surface area, and thus a higher effective deposition current (Ilkovic's equation). However, the parameter is hampered by the limitations of the automated instrument, and, most of all, by the maximum size of the hanging mercury drop which can maintain a reasonably spherical shape, and still be attached to the mercury capillary column. A longer deposition time increases the amount of deposit, according to Faraday's law, but it also means running the risk of significantly depleting the bulk concentration of analyte in the test solution after only a few measurements, resulting in non-reproducible data. In addition, it lengthens the analysis time, making it too time-consuming and, to an extent, impractical. Apparently, a combination of these

parameters at compromise settings may be the only solution. In the case of supporting electrolyte concentration, it may be intrinsic only to those solutions of high ionic concentrations, and might be simply resolved by using lower concentrations, say, in the 10^{-1}M range.

In spite of the presence of the curvature in the concentration-calibration curves, the technique of DPASP showed a superior sensitivity which was more than adequate for the analysis of biological samples, and other samples containing trace levels of heavy metals. The detection limits, unlike those of most other trace analytical techniques, are normally dictated by the magnitude of the blank value of the background supporting electrolyte in which the samples are analyzed, and not by the instrumental sensitivity (33). The detection limit of DPASP using the HMDE has been theoretically calculated to be, for example, 0.005 ppb for Cd and 0.001 ppb for Pb. These findings were estimated based on three times the values of standard deviation of the blank.

To attain these detection limits, an ultrapure supporting electrolyte containing the minutest possible trace of the analytes, and almost no trace at all of any nonparticipating electroactive species, must be used. In addition, a large HMDE, long t_{dep}, large U_{dp} and a low instrumental sensitivity have to be used in order to secure a set of polarogrammes with smooth baselines and high S/N

ratios. All of these requirements are not reasonable, since it is time-consuming and impractical to secure such levels of impurities in a supporting electrolyte generally prepared from common laboratory reagents (see Appendix I). Of-course, one can use the highly expensive, superpure grade reagents as starting materials. This, however, makes the procedure uneconomical for routine work. In practice, most of the samples from various sources contain the trace metals at concentration levels which can be quantitated quite accurately in supporting electrolytes of reasonably high purities. Throughout the course of this research, electrolytically purified electrolytes containing Cd and Pb at 0.1-0.3 ppb were used, and the practical limits of detection of 0.02 and 0.05 ppb for Cd and Pb, respectively, were then easily attained.

Comparisons between the unit-responses* of Cd and Pb have been made, and are presented graphically in Figures 19 and 20, and Tables 7 and 8. It was found that DPASP responses for Cd were higher than those for Pb. Specifically, the former were generally about one and one-half times those of the latter.

* See Appendix II - Footnote 3 for explaination.

Table 3 : The effects of the various concentrations of Pb and the drop sizes on the peak current (N.B. : All values are background-corrected.)

Concentration (ppb, ng/ml)	Av. Peak Current ± Std. Dev.'n (i_p, nA) HMDE Setting 3	5	7	9
0	0.00 ± 0.04	0.00 ± 0.24	0.00 ± 0.02	0.00 ± 0.34
5	4.35 ± 0.28	5.91 ± 0.39	7.06 ± 0.24	7.61 ± 0.74
10	9.21 ± 0.13	11.63 ± 0.64	14.22 ± 0.28	16.45 ± 0.94
15	13.97 ± 0.64	18.51 ± 0.38	19.97 ± 0.32	25.96 ± 0.48
20	19.40 ± 0.25	25.80 ± 2.18	29.28 ± 0.66	34.78 ± 0.78
25	25.61 ± 0.59	31.93 ± 1.27	38.29 ± 0.72	43.14 ± 0.94
Corr. Coef.	0.9981	0.9992	0.9970	0.9996
Slope (nA/ppb)	1.0169	1.2926	1.5078	1.7527
Mean Rel. Std. Dev.	3.2%	5.3%	2.2%	4.3%

* See Fig. 15

** See Appendix IV - Parameters 1

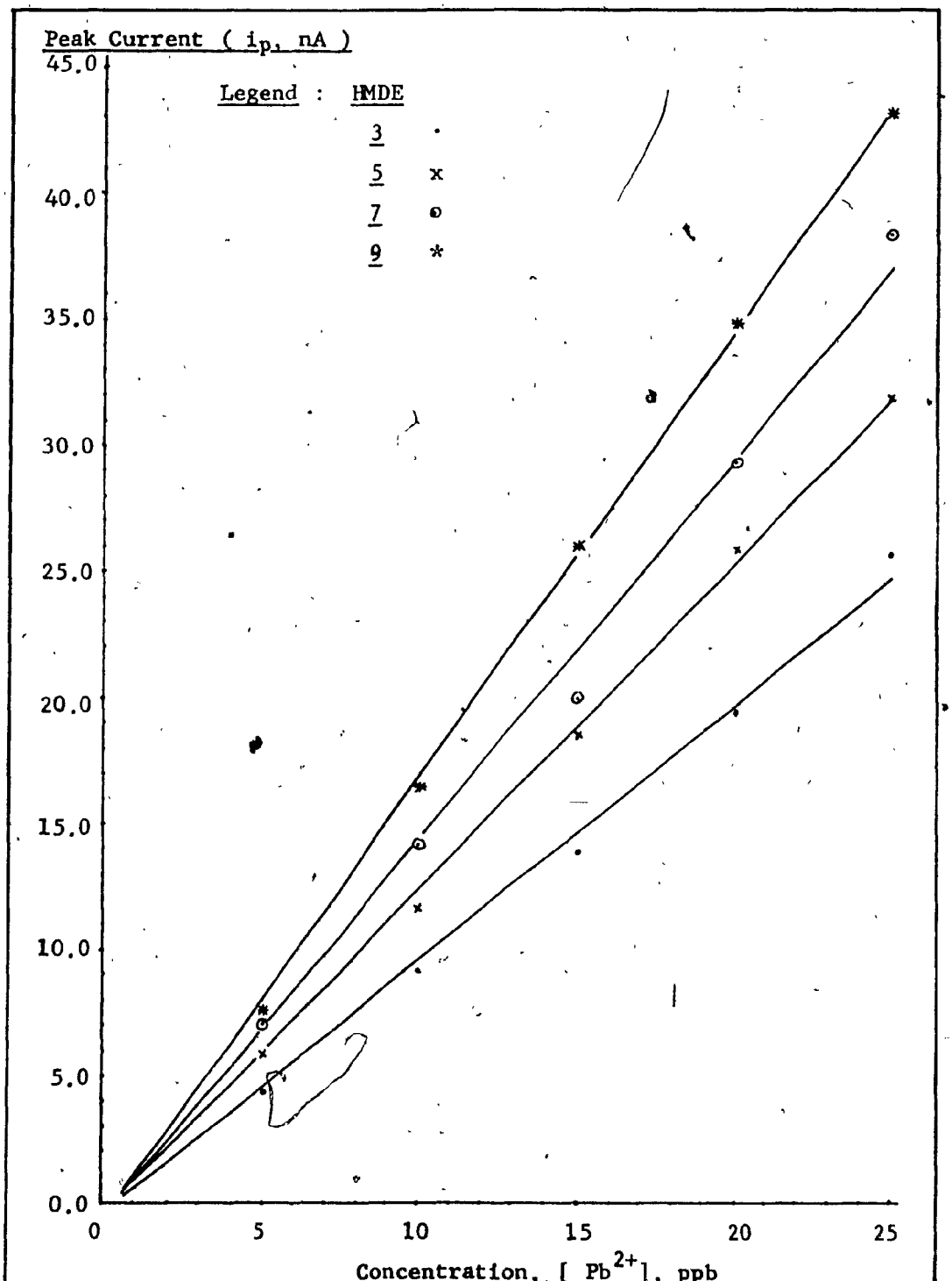

Figure 15 : Concentration-calibration curves of Pb at the various constant mercury-drop sizes.

Table 4 : The effects of the various concentrations of Cd and the drop sizes on the peak current (N.B. : All values are background-corrected)

Concentration (ppb, ng/ml)	Av. Peak Current ± Std. Dev'n (i_p, nA) HMDE Setting 3	5	7	9
0	0.00 ± 0.08	0.00 ± 0.09	0.00 ± 0.13	0.00 ± 0.07
5	5.55 ± 0.09	7.64 ± 0.21	7.97 ± 0.38	10.91 ± 0.43
10	11.85 ± 0.18	15.34 ± 0.21	17.67 ± 0.13	22.69 ± 1.17
15	18.41 ± 0.98	23.82 ± 0.14	25.66 ± 0.59	35.07 ± 0.42
20	24.94 ± 0.28	33.40 ± 2.45	38.25 ± 0.77	47.51 ± 0.76
25	31.94 ± 1.11	40.26 ± 0.78	49.11 ± 0.65	58.39 ± 0.59
Corr. Coef.	0.9994	0.9992	0.9970	0.9998
Slope (nA/ppb)	1.2824^{6}	1.6403	1.9679	2.3664^{6}
Mean Rel. Std. Dev.	2.6%	2.8%	2.2%	2.6%

* See Appendix IV - Parameters 1

** See Fig. 16

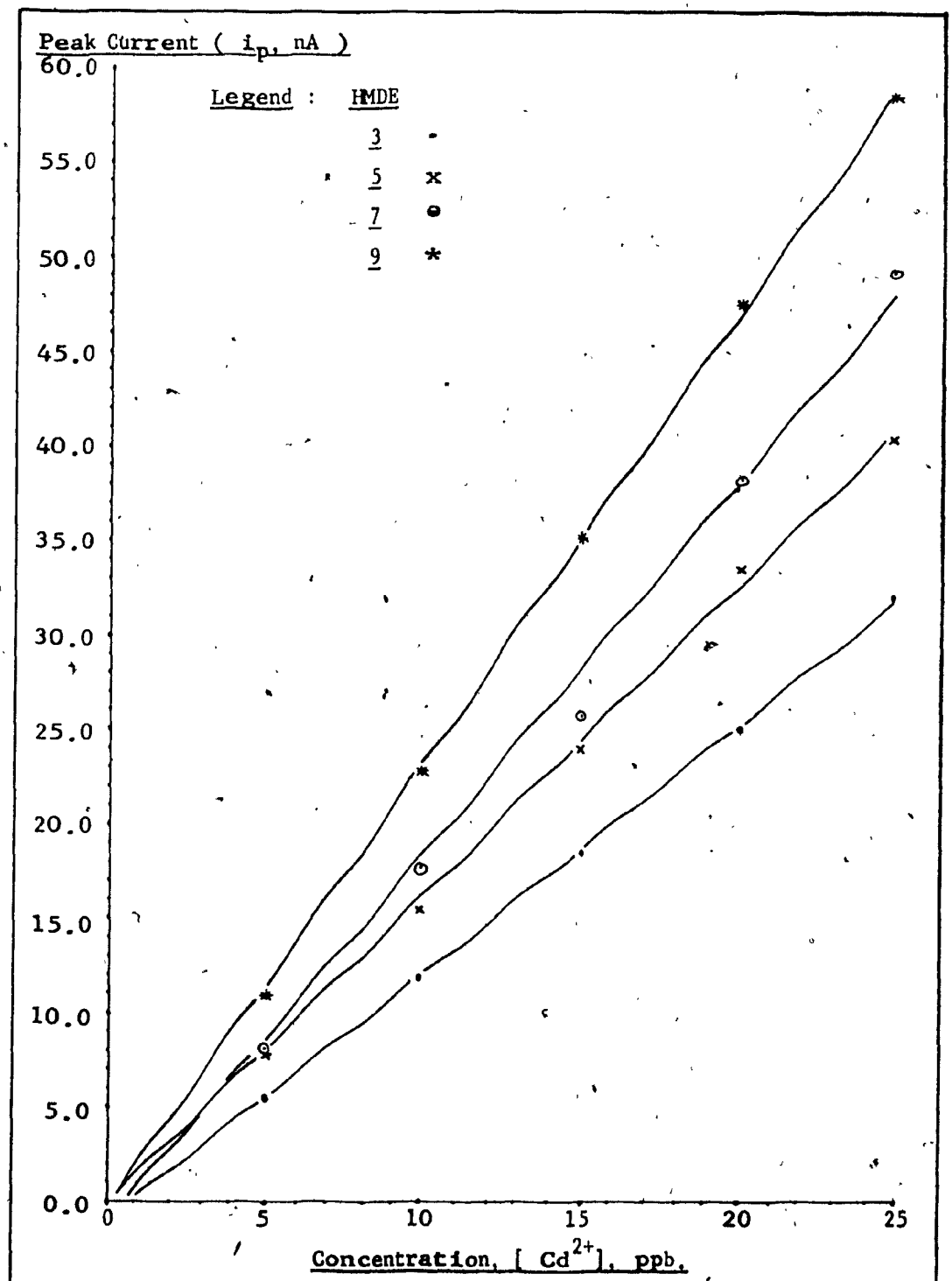

Figure 16 : Concentration-calibration curves of Cd at the various constant mercury-drop sizes.

Table 5 : The effects of the various concentrations of Pb and the deposition times on the peak current (N.B. : All values are background-corrected)

Concentration (ppb, ng/ml)	Av. Peak Current ± Std. Dev'n (i_p, nA) Deposition Time (t_{dep}, min.) 1	2	3	4	5
0	0.00 ± 0.12	0.00 ± 0.06	0.00 ± 0.01	0.00 ± 0.10	0.00 ± 0.46
5	4.16 ± 0.34	7.21 ± 0.23	9.49 ± 0.15	12.72 ± 0.32	15.86 ± 0.95
10	8.75 ± 0.37	14.90 ± 0.28	21.09 ± 0.35	29.10 ± 0.97	31.67 ± 1.19
15	13.68 ± 0.17	22.80 ± 0.12	31.13 ± 0.09	41.96 ± 0.76	48.33 ± 2.85
20	18.08 ± 0.29	31.36 ± 0.84	42.86 ± 1.47	56.11 ± 0.34	66.97 ± 0.96
25	23.41 ± 0.70	38.56 ± 0.39	51.61 ± 0.88	72.37 ± 0.25	84.52 ± 0.81
Corr. Coef.	0.9994	0.9997	0.9994	0.9994	0.9995
Slope (nA/ppb)	0.9356	1.5609	2.1040	2.8850	3.3873
Mean Rel. Std. Dev.	3.6%	1.9%	1.7%	1.7%	3.6%

* See Fig. 17

** See Appendix IV - Parameters 2.

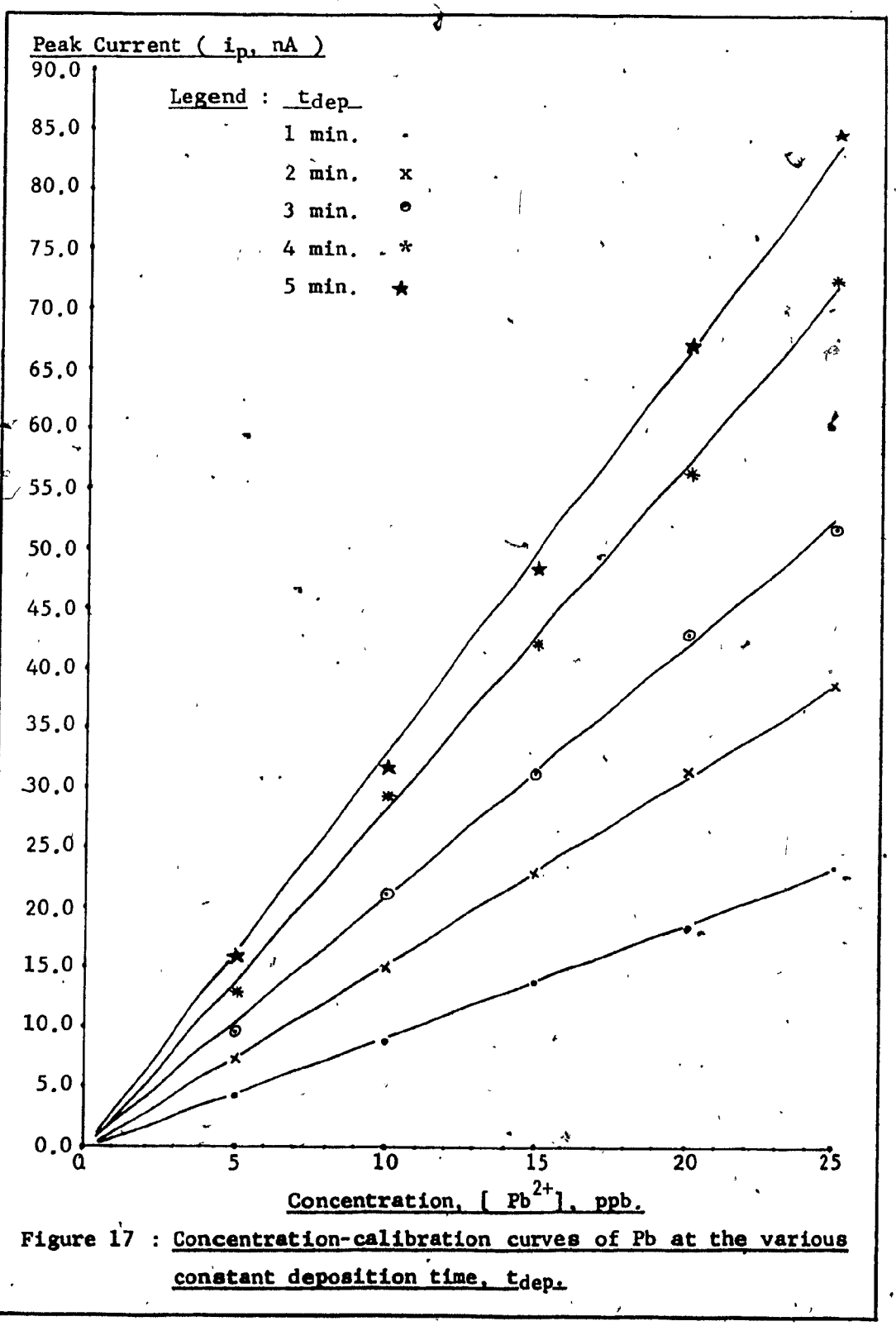

Figure 17 : Concentration-calibration curves of Pb at the various constant deposition time, t_{dep}.

Table 6 : The effects of the various concentrations of Cd and the deposition times on the peak current (N.B.: All values are background-corrected).

Concentration (ppb, ng/ml)	Av. Peak Current ± Std. Dev'n (i_p, nA) Deposition Time (t_{dep}, min.)				
	1	2	3	4	5
0	0.00 ± 0.02	0.00 ± 0.08	0.00 ± 0.33	0.00 ± 0.00	0.00 ± 0.24
5	6.72 ± 0.21	10.92 ± 0.45	15.12 ± 0.92	19.88 ± 0.29	24.29 ± 0.72
10	13.85 ± 0.12	21.85 ± 0.54	32.45 ± 0.53	44.83 ± 0.26	47.62 ± 1.22
15	21.40 ± 0.12	34.55 ± 0.50	47.85 ± 0.49	63.46 ± 0.78	72.75 ± 1.24
20	27.45 ± 0.32	48.22 ± 1.72	66.33 ± 2.91	84.81 ± 0.06	98.65 ± 0.84
25	35.85 ± 1.17	58.50 ± 1.24	77.47 ± 0.75	110.70 ± 0.70	124.78 ± 2.68
Corr. Coef.	0.9994	0.9992	0.9986	0.9991	0.9998
Slope (nA/ppb)	1.4228	2.3834	3.1793	4.3824	4.9835
Mean Rel. Std. Dev'n	1.8%	2.7%	2.8%	1.2%	2.0%

* See Fig. 18

** See Appendix IV - Parameters 2

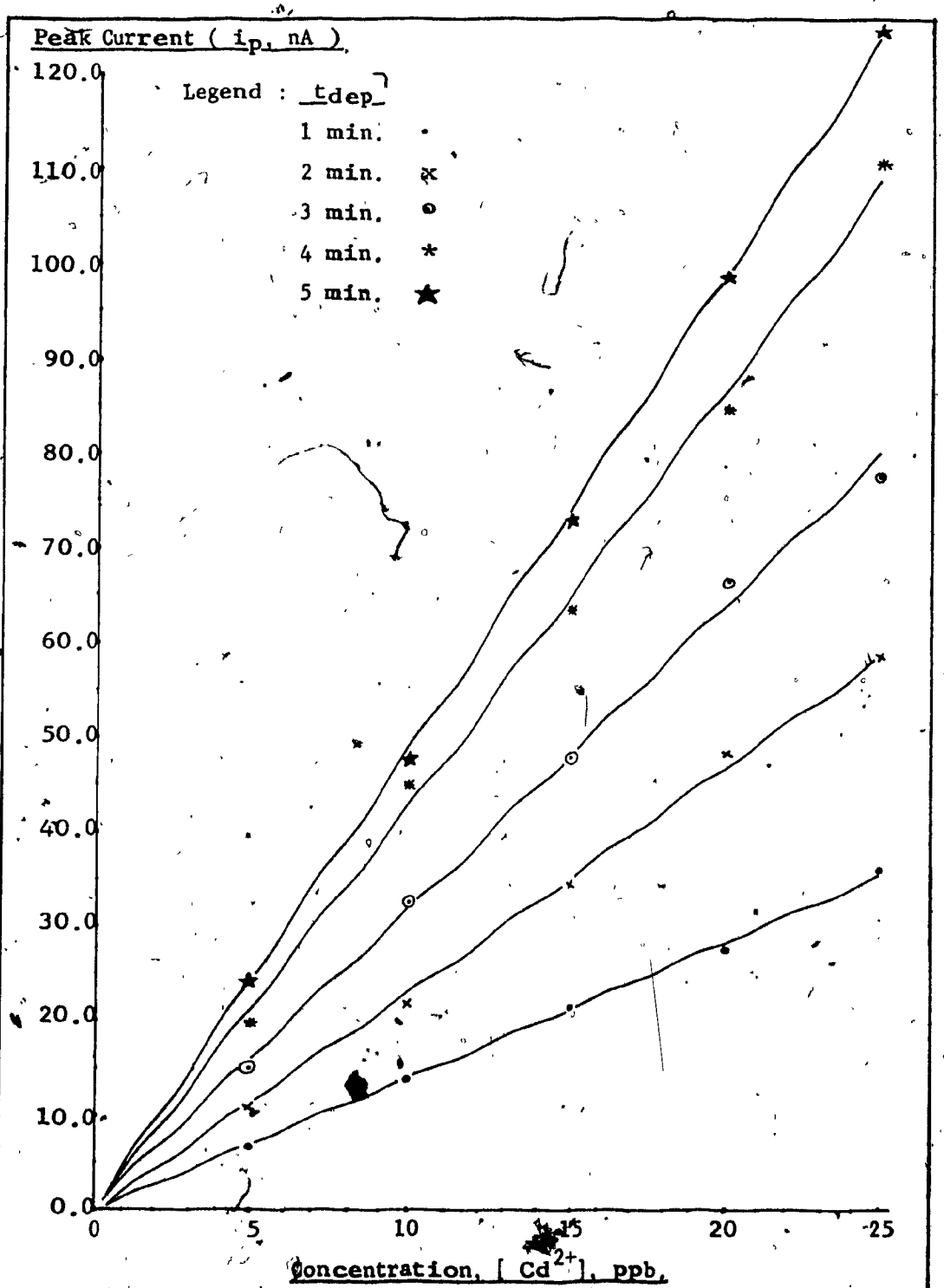

Figure 18 : Concentration-calibration curves of Cd at the various constant deposition time, t_{dep}.

Table 7 : The effect of the analyte concentrations on the unit-radius response***

Analyte Concentration (ppb)	Unit-Radius Response (nA/mm)	
	Pb	Cd
5	23.4807	34.4698
10	51.2978	73.0162
15	78.5794	108.0730
20	105.2054	153.1513
25	124.8341	185.5924
Corr. Coefficient	0.9981	0.9990
Slope (nA/mm-ppb)	5.1323	7.6476

* See Fig. 19

** See Appendix IV - Parameters 1.

*** See Appendix I-I - Footnotes 3.

N.B. : All data points above are the slope values of the peak-current vs. radius plots, i.e., Tables 9 and 10, and Figures 21 and 22.

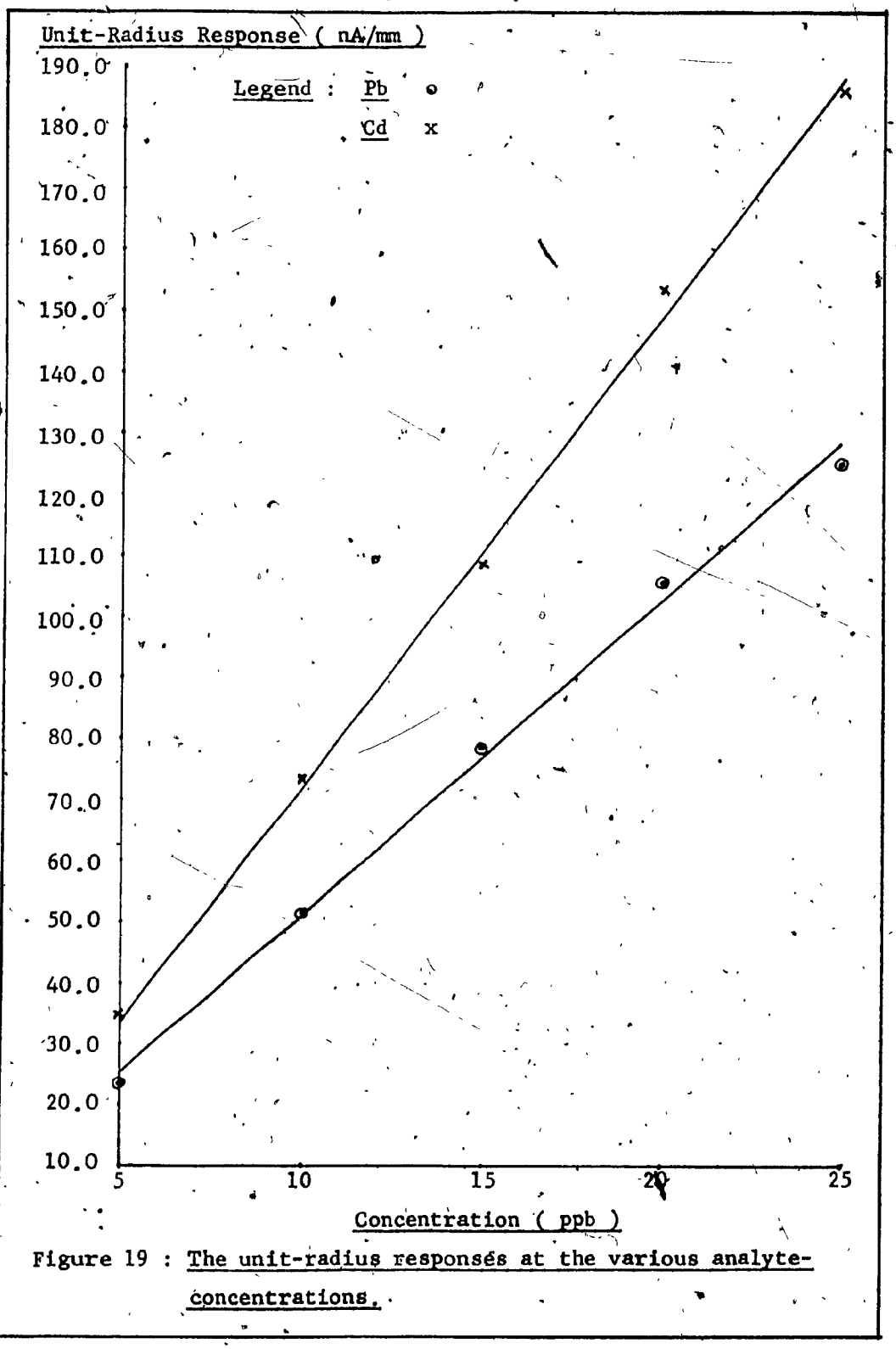

Figure 19 : The unit-radius responses at the various analyte-concentrations.

Table 8 : The effect of the analyte concentrations on the unit-time responses***.

Analyte Concentration (ppb)	Unit-Time Response (nA/min) Pb	Cd
5	2.8910	4.4100
10	6.0540	9.0520
15	8.8460	13.1610
20	12.2530	17.8990
25	15.6030	23.0060
Corr. Coefficient	0.9994	0.9993
Slope (nA/min-ppb)	0.6324^{6}	0.9208

* See Fig. 20.

** See Appendix IV - Parameters 2.

*** See Appendix II - Footnotes 3.

N.B. : All data points above are the slope values of the peak-current vs. deposition-time plots, i.e., Tables 11 and 12, and Figures 23 and 24.

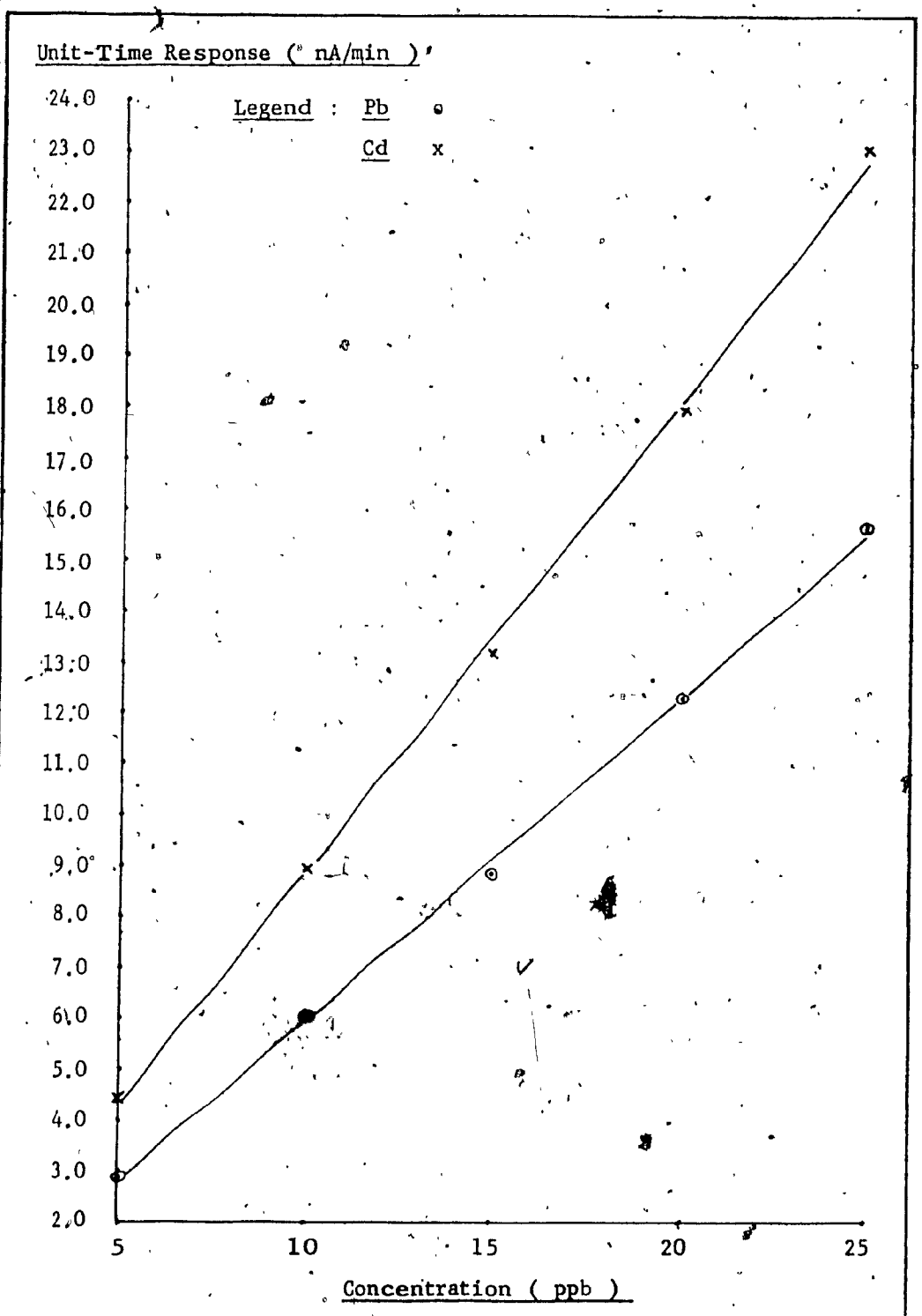

Figure 20 : The unit-(deposition-) time responses at the various analyte-concentrations.

5.1.4 DPASP responses due to the electrode radius and the deposition time:-

The dependence of the DPASP responses on the dimensions of the HMDE and the electrodeposition time can be illustrated by considering the analyte-amalgan concentration in the HMDE. This concentration is the actual factor that dictates i_p, the anodic stripping current response.

According to Faraday's law of electroplating, the amount of amalgam formed in the mercury drop electrode is completely dependent on the number of coulombs that are used during the electrolytic process. Since the coulomb, Q, is a product of the effective electrolytic current, i, and the deposition time, t_{dep}:

$$Q = i \cdot t_{dep} \qquad (15)$$

where i is the reduction current described by Equation (8), from which one may say that i_p is indirectly proportional to the size of HMDE.

The experimental findings confirmed the theoretical prediction that i_p was linearly proportional to the HMDE radius, r, and to t_{dep}. These relationships are presented in Figures 21-24 and Tables 9-12 for Pb and Cd, in the acetate supporting electrolyte system, at different analyte concentrations. The comparisons with the unit-concentration responses* of Pb and Cd at various drop radii and deposition times are also shown in Figures 25 and 26, and Tables 13

Table 9 : The polarographic response at the various radii and the concentrations of Pb.

Drop Radius (r, mm)	Av. Peak Current ± Std. Dev'n. (ip, nA) Concentration, $[Pb^{2+}]$, (ng/ml)				
	5	10	15	20	25
0.301 ± 0.000	4.35 ± 0.28	9.21 ± 0.13	13.97 ± 0.64	19.40 ± 0.25	25.61 ± 0.59
0.360 ± 0.001	5.91 ± 0.39	11.63 ± 0.64	18.51 ± 0.38	25.80 ± 2.18	31.93 ± 1.27
0.404 ± 0.000	7.06 ± 0.24	14.22 ± 0.28	19.97 ± 0.32	29.28 ± 0.66	38.29 ± 0.72
0.443 ± 0.000	7.61 ± 0.74	16.45 ± 0.48	25.96 ± 0.48	34.78 ± 0.78	43.14 ± 0.94
Corr. Coefficient	0.9933	0.9961	0.9680	0.9955	0.9981
Slope (nA/mm)	23.4807	51.2978	78.5794	105.2054	124.8341

* See Fig. 21.

** See Appendix IV - Parameters.

N.B. : Data obtained from Table 3.

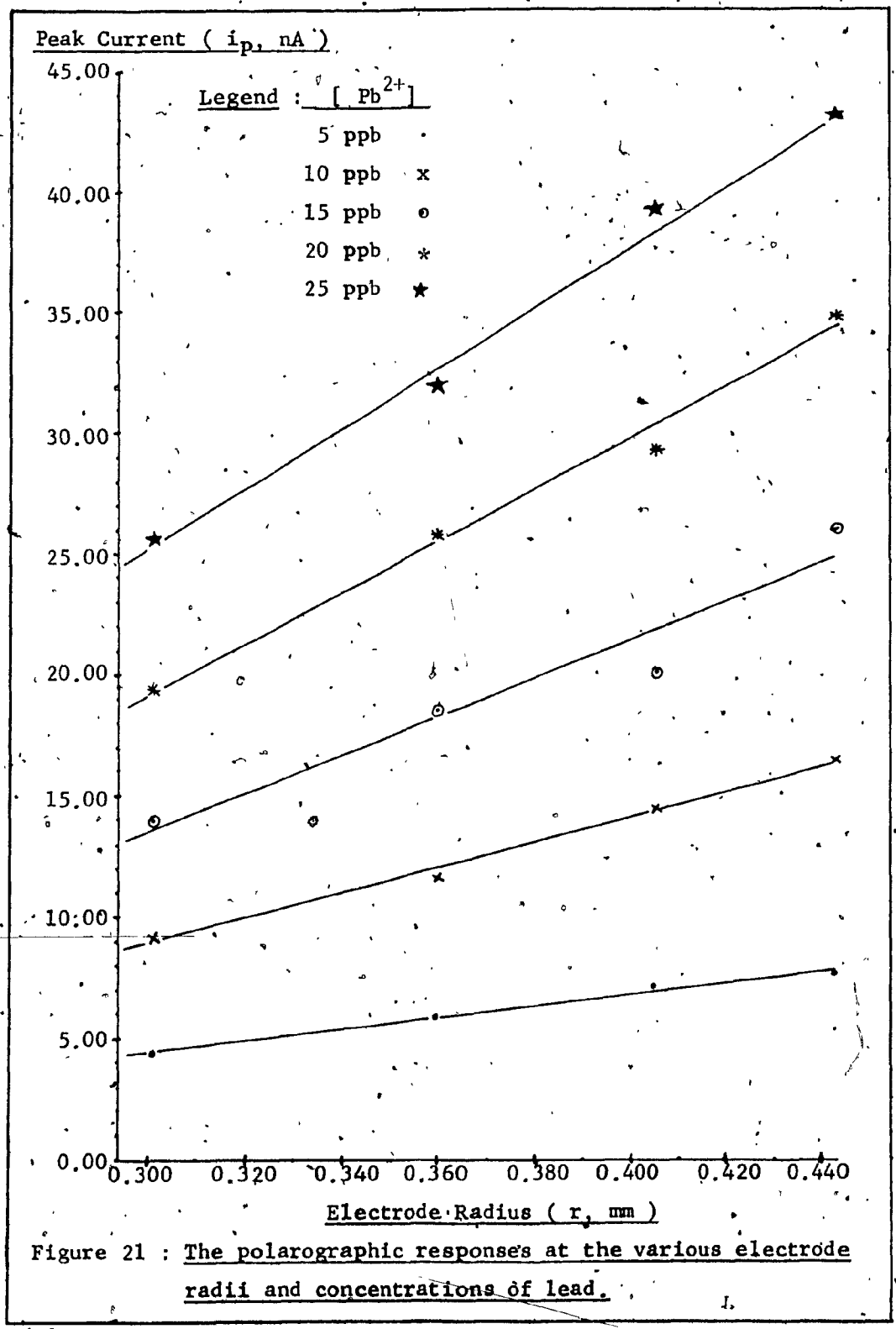

Figure 21 : The polarographic responses at the various electrode radii and concentrations of lead.

Table 10 : The polarographic responses at the various radii and the concentrations of Cd.,

Drop Radius (r, mm)	Av. Peak Current ± Std. Dev'n. (ip, nA) Concentration, $[Cd^{2+}]$, (ng/ml)				
	5	10	15	20	25
0.301 ± 0.000	5.55 ± 0.09	11.85 ± 0.18	18.41 ± 0.98	24.94 ± 0.28	31.94 ± 1.11
0.360 ± 0.001	7.64 ± 0.21	15.34 ± 0.21	23.82 ± 0.14	33.40 ± 2.45	40.26 ± 0.78
0.404 ± 0.000	7.97 ± 0.38	17.67 ± 0.13	25.66 ± 0.59	38.25 ± 0.77	49.11 ± 0.65
0.443 ± 0.000	10.91 ± 0.43	22.69 ± 1.17	35.07 ± 0.42	47.51 ± 0.76	58.39 ± 0.59
Corr. Coefficient	0.9511	0.9773	0.9480	0.9889	0.9919
Slope (nA/mm)	34.4698	73.0162	108.0730	153.1513	185.5924

*. See Fig. 22.

** See Appendix IV - Parameters 1.

N.B. : Data obtained from Table 4.

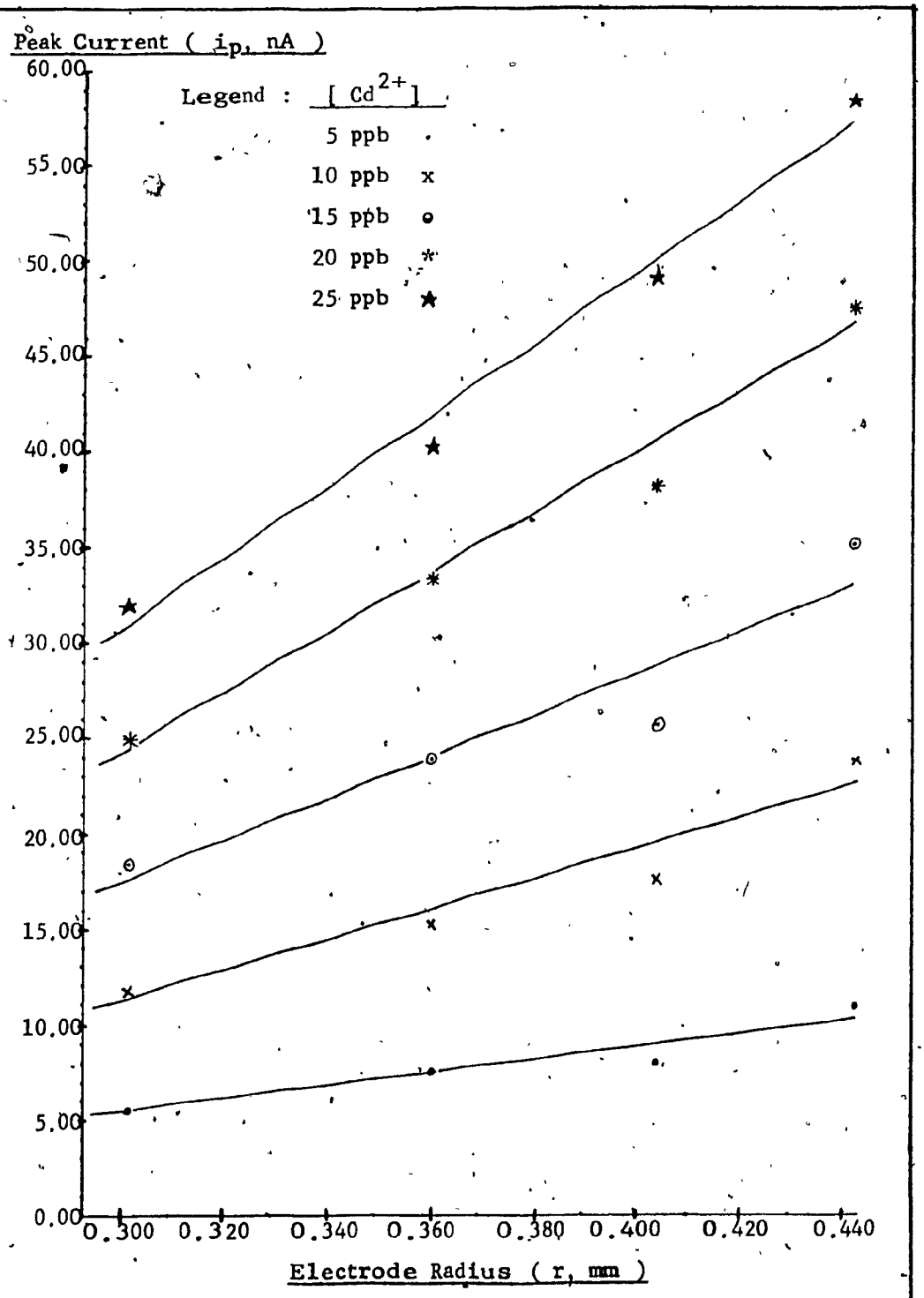

Figure 22 : The polarographic responses at the varios electrode radii and concentrations of cadmium.

Table 11 : The polarographic responses at the various deposition times and the concentrations of Pb.

Deposition Time (t_{dep}, min)	Av. Peak Current ± Std. Dev'n. (ip, nA) Concentration, $[Pb^{2+}]$, (ng/ml)				
	5	10	15	20	25
1	4.16 ± 0.34	8.75 ± 0.34	13.68 ± 0.17	18.08 ± 0.29	23.41 ± 0.70
2	7.21 ± 0.23	14.90 ± 0.28	22.80 ± 0.12	31.36 ± 0.84	38.56 ± 0.39
3	9.49 ± 0.15	21.09 ± 0.35	31.13 ± 0.09	42.86 ± 1.47	51.61 ± 0.88
4	12.72 ± 0.32	29.10 ± 0.97	41.96 ± 0.76	56.11 ± 0.34	72.37 ± 0.25
5	15.86 ± 0.95	31.67 ± 1.19	48.33 ± 2.85	66.97 ± 0.96	84.52 ± 0.81
Corr. Coefficient	0.9985	0.9914	0.9978	0.9995	0.9971
Slope (nA/min)	2.8910	6.0504	8.8460	12.2530	15.6030

* See Fig. 23.

** See Appendix IV - Parameters 2.

N.B. : Data obtained from Table 5.

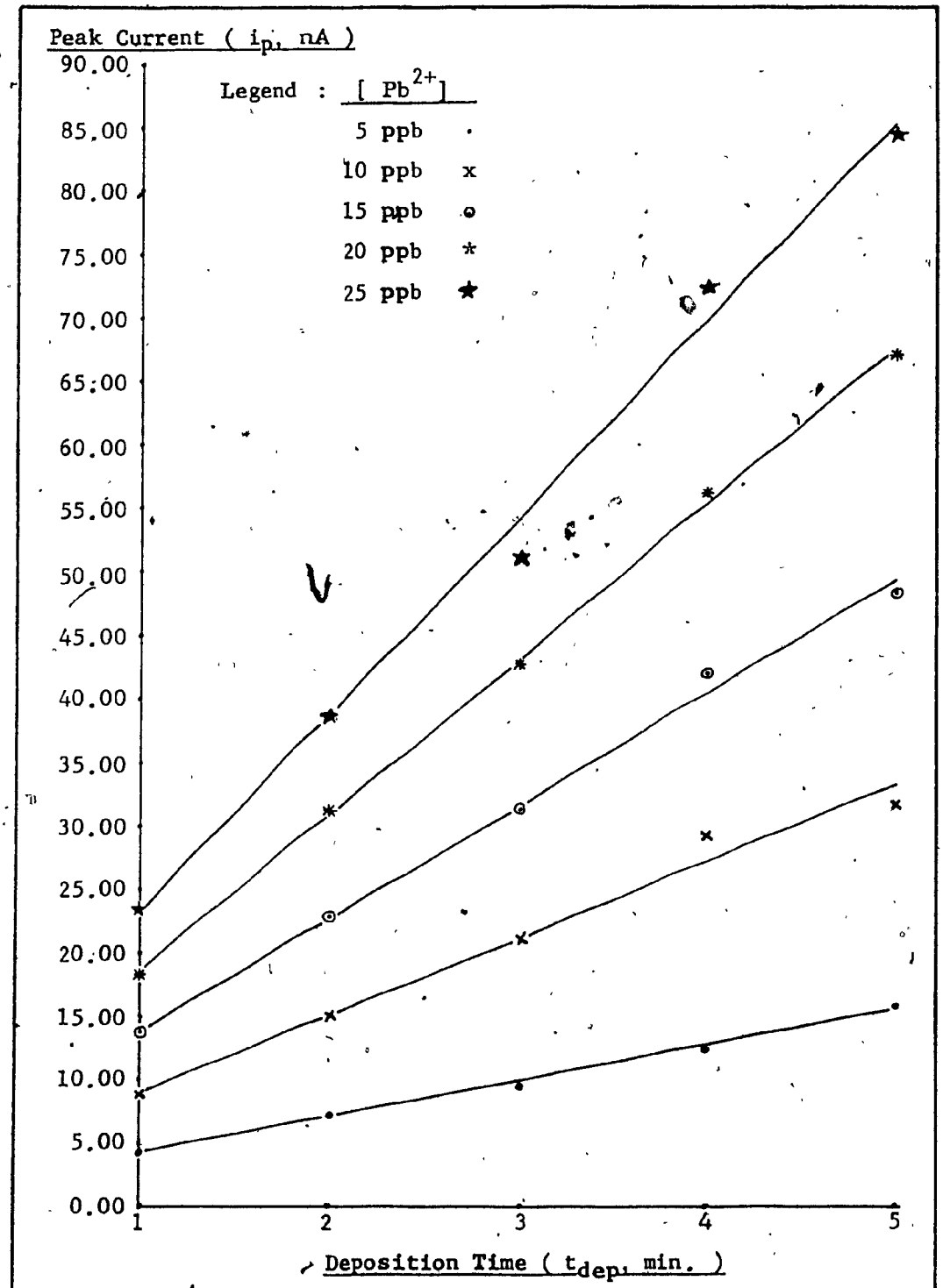

Figure 23 : The polarographic responses at the various deposition times and concentrations of lead.

Table 12 : The polarographic responses at the various deposition times and the concentrations of Cd.

Deposition Time (t_{dep}, min)	Av. Peak Current ± Std. Dev'n. (ip, nA) Concentration, $[Cd^{2+}]$, (ng/ml)				
	5	10	15	20	25
1	6.72 ± 0.21	13.86 ± 0.12	21.40 ± 0.12	27.45 ± 0.32	35.85 ± 1.17
2	10.92 ± 0.45	21.85 ± 0.54	34.55 ± 0.50	48.22 ± 1.72	58.50 ± 1.24
3	15.12 ± 0.92	32.45 ± 0.53	47.85 ± 0.49	66.33 ± 2.91	77.47 ± 0.75
4	19.88 ± 0.29	44.83 ± 1.26	63.46 ± 0.78	84.81 ± 0.06	110.70 ± 0.70
5	24.29 ± 0.72	47.62 ± 1.22	72.75 ± 1.24	98.65 ± 0.84	124.78 ± 2.68
Corr. Coefficient	0.9997	0.9870	0.9977	0.9978	0.9942
Slope (nA/min)	4.4100	9.0520	13.1610	17.8990	23.0060

* See Fig. 24

** See Appendix IV - Parameters 2

N.B. : Data obtained from Table 6

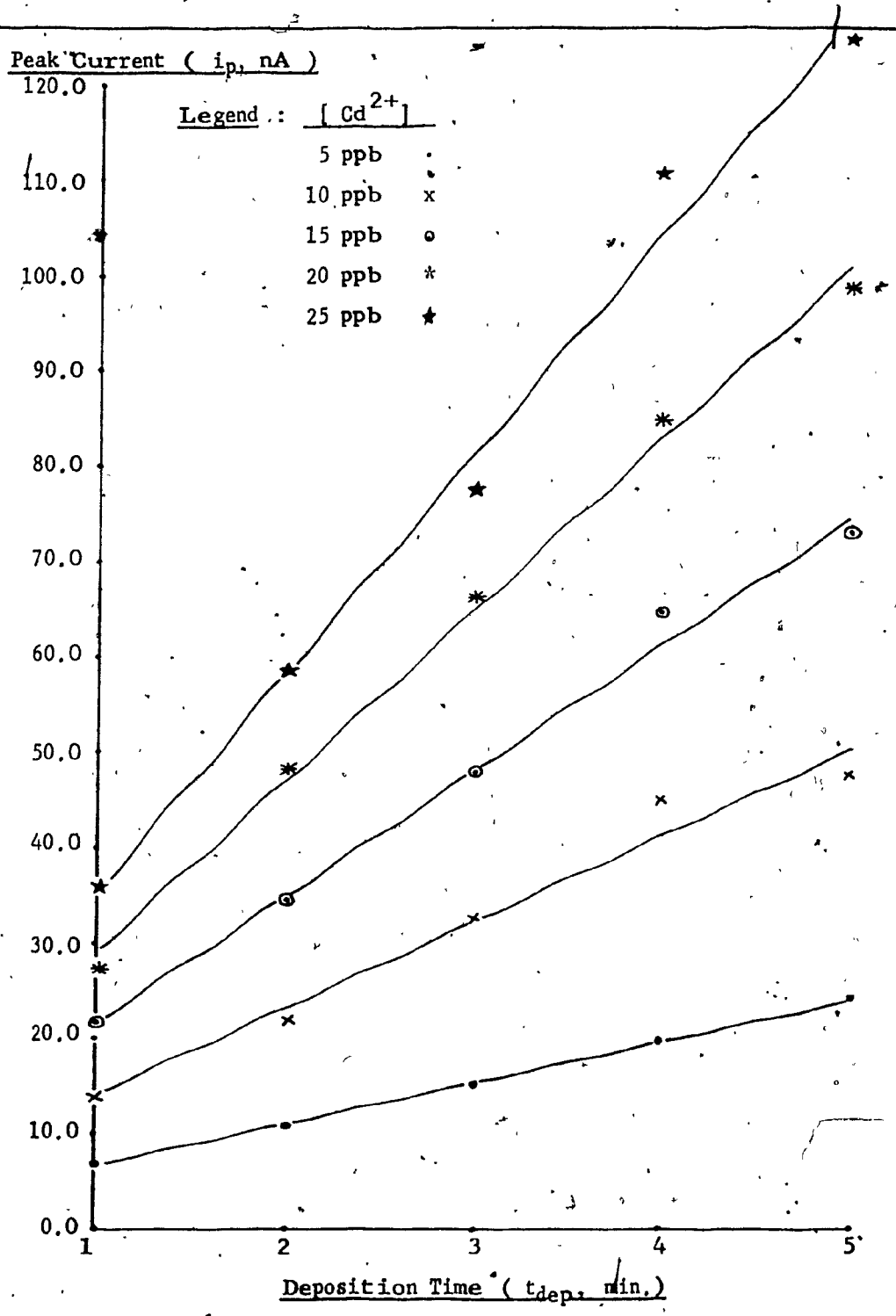

Figure 24 : The polarographic responses at the various deposition times and concentrations of cadmium.

Table 13 : The effect of the electrode radii on the unit-concentration responses***.

HMDE Radius (r, mm)	Unit-Concentration Response (nA/ppb)	
	Pb	Cd
0.301 ± 0.000	1.0169	1.2825
0.360 ± 0.001	1.2926	1.6403
0.404 ± 0.000	1.5078	1.9679
0.443 ± 0.000	1.7527	2.3665
Corr. Coefficient	0.9977	0.9927
Slope (nA/ppb-mm)	5.1238	7.5307

* See Fig. 25.

** See Appendix IV - Parameters b.

*** See Appendix II - Footnotes 3.

N.B. : All data points above are the slope values of the peak-current vs concentration plots, i.e. Tables 3 and 4, and Figures 15 and 16.

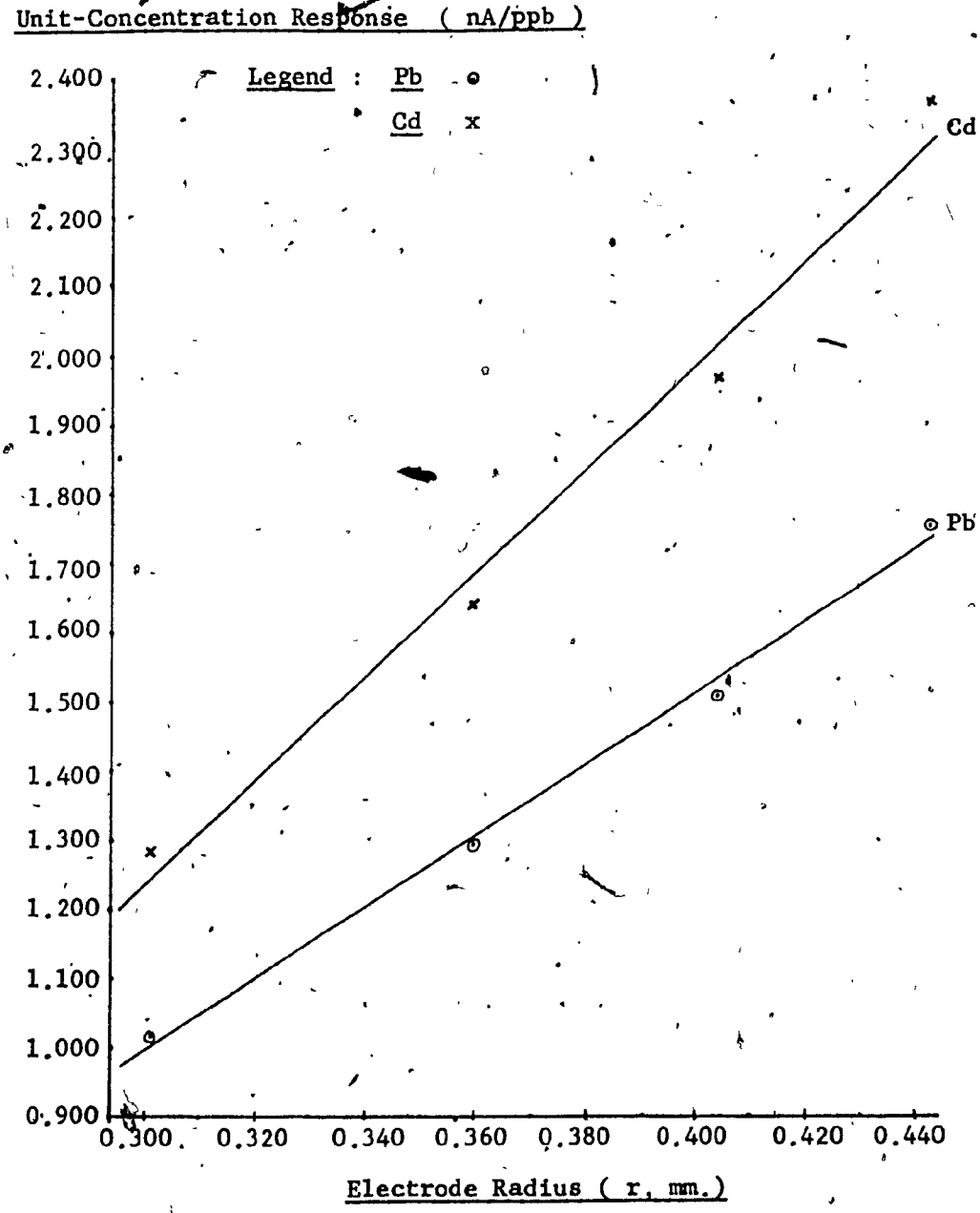

Figure 25 : The unit-concentration responses at the various electrode radii.

Table 14 : The effect of the deposition times on the unit-concentration responses***.

Deposition Time (t_{dep}, min.)	Unit-Concentration Response (na/ppb)	
	Pb	Cd
1	0.9356	1.4228
2	1.5609	2.3834
3	2.1040	3.1793
4	2.8850	4.3924
5	3.3873	4.9835
Corr. Coefficient	0.9982	0.9963
Slope (nA.ppb min.)	0.6228	0.9120

* See Fig. 26.

** See Appendix IV - Parameters 2.

*** See Appendix II - Footnotes 3.

N.B. : All data points above are the slope values of the peak-current vs concentration plots, i.e., Tables 5 and 6, and Figures 17 and 18.

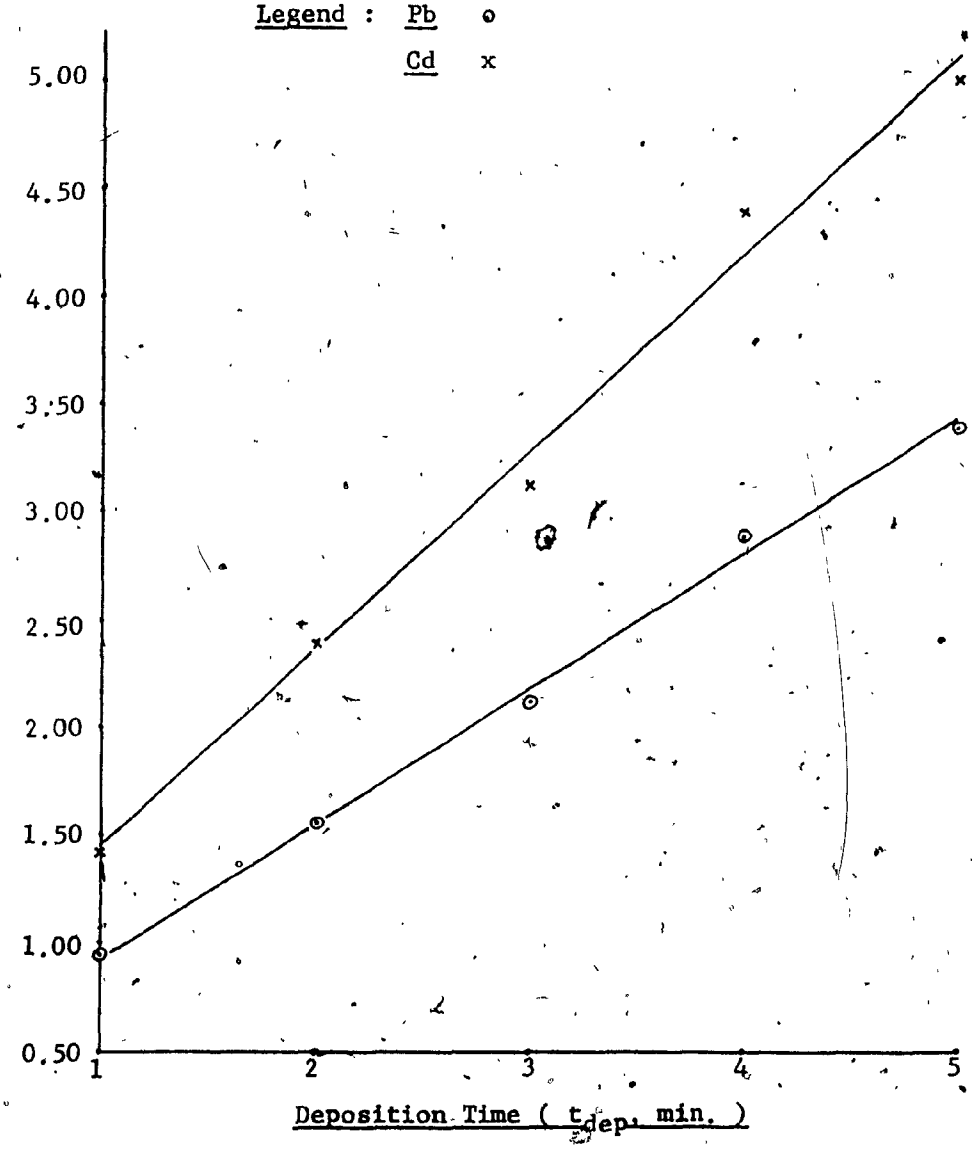

Figure 26 : The unit-concentration responses at the various deposition times.

and 14, respectively. Again an average ratio of approximately 1.5 was obtained in favour of the Cd response.

The reproducibility of the automated DPASP technique can be represented by the overall average relative standard deviation which was calculated from the individual standard deviations listed in Tables 3-6, and was found to be 2.0-3.0% for the analysis of Pb and Cd, in the synthetic samples.

5.2 The Analyses of the Biological Samples

The experimental results obtained from the comparative analysis of Pb and Cd in the biological samples verified the accuracy of DPASP technique, and substantiated the suitability and applicability of the automated electrochemical instrumentation for the analysis of trace heavy metals in samples from diverse sources.

The experimental mean values (± 1 standard deviation), obtained from the analysis of eleven 1-g samples of the N.B.S. material, Bovine Liver No. 1577, are shown in Table 15 and were 0.328 ± 0.045 ppm (ug. per g dry weight) for Pb and 0.267 ± 0.028 ppm for Cd. They yielded the relative deviation of 3.5% and 1.1%, respectively, in comparison with the N.B.S. values of 0.34 ± 0.08 ppm for Pb and 0.27 ± 0.04 ppm for Cd. These latter values were obtained from the determinations involving 6-12 samples by at least two

* See Appendix II - Footnote 3 for explanation.

Table 15 : Experimental results of Pb and Cd in the N.B.S. Material - Bovine Liver (No. 1577).

Analyte	Amount of Analyte Found (ug. per g. dry weight) Exptal. Values	N.B.S. Values*	% Deviation
Pb :			
N =	11	6 ----- 12	
$\bar{X} \pm S$ =	0.328 ± 0.045	0.34 ± 0.08	3.5
$S/\bar{X}$ =	13.7%	23.5%	
Cd :			
N =	11	6 ----- 12	
$\bar{X} \pm S$ =	0.267 ± 0.028	0.27 ± 0.04	1.1
$S/\bar{X}$ =	10.5%	14.8%	

where : N = the number of data values;

$\bar{X} \pm S$ = the mean value ± standard deviation;

$S/\bar{X}$ = the relative standard deviation.

* See Reference 34.

** See Appendix V - A for the treatment of the experimental data.

Table 16 : Experimental results of the fish tissue sample.

Analytical Technique		Amount of Analyte Found (ug/g)	
		Pb	Cd
1. GF-AAS	N =	19*	35
	$\bar{X} \pm S$ =	0.156 ± 0.041	0.055 ± 0.016
	$\bar{X}' \pm S'$ =	0.029 ± 0.008	0.010 ± 0.003
	$S/\bar{X}$ =	26.3%	29.1%
2. Automated DPASP.			
Programme 1 :	N =	38	39
U_{dp} = + 30 mv.;	$\bar{X} \pm S$ =	0.163 ± 0.040	0.052 ± 0.015
t_{dep} = 120 s.	$\bar{X}' \pm S'$ =	0.030 ± 0.008	0.010 ± 0.003
	$S/\bar{X}$ =	24.5%	28.8%
Programme 2 :	N =	10	9
U_{dp} = + 50 mv.;	$\bar{X} \pm S$ =	0.164 ± 0.025	0.054 ± 0.006
t_{dep} = 300 s.	$\bar{X} \pm S'$ =	0.030 ± 0.005	0.010 ± 0.001
	$S/\bar{X}$ =	15.2%	11.1%
Overall Average :	$\bar{X}$ =	0.161	0.054
	$\bar{X}'$ =	0.030	0.010

* More than 15 results were rejected due to their very high spread from the norm of data. These values were undoubtfully the result of contamination, and the loss of material through sample-digestion.

** See Appendix V - B for the treatment of experimental data.

*** $\bar{X}' \pm S'$ = the mean value ± standard deviation - based on the fresh (wet) sample weight.

different trace analytical techniques.

Table 16 shows the experimental results for the analysis of fish muscle tissue samples by the GF-ASS and the automated DPASP techniques. Good agreement was obtained for the values of Cd via the two methods. As for Pb, inference (t-) tests at the 95% confidence level indicated that the deviation between the values was statistically insignificant (Appendix IV - C).

The precision of the electrochemical technique was found generally to be comparable to that of the GF-AAS method, but it had an advantage over the latter method in that the precision could be further improved by increasing the analyte-amalgam concentration in the HMDE, the amplitude of the modulating pulse, or both, as demonstrated in Table 16.

It had been observed that there existed, in DPASP, non-specific interactions whose effects could be utilized to improve the precision of the technique. These interactions might be purely physical (i.e., electronic) interactions existing between some of the instrumental parameters; physicochemical interactions due to the analyte and its surrounding electrolyte, and interfacial phenomena at the electrode surface, that is, electrode-analyte and electrode-supporting electrolyte interfaces. These interactions are generally sensitive and would give rise to different

effects with different combinations of experimental parameters, such as the constitution, ionic strength and concentration of a supporting electrolyte, pH of a sample solution, geometry, chemical and physical make-up of a working electrode, instrumental settings, and so forth. Consequently, various precision levels might be obtained based on differences in interacting effects, even at a constant analyte-concentration.

The reproducibility of the DPASP technique, based on the relative standard deviations of the experimental mean values of the biological samples, varied from 24% for lead, to 29% for cadmium. These precisions compare with those obtained for the GFAAS work, 26% for lead, and 29% for cadmium, quite favourably. They are not as good as those obtained with the DPASP work involving longer deposition times and higher pulse amplitudes, these being 15% for lead, and 11% for cadmium. They are very significantly poorer than the precisions of 4% for lead, and 2% for cadmium obtained in the exploratory work involving synthetic solutions.

While it is possible to give some thought to the possibility that the bulk fish tissue sample may have suffered from a lack of homogeneity due to incomplete batch mixing, etc., it is more likely that the poorer precision obtained for all fish tissue specimens reflects the perturbation possibilities arising out of the much more

complicated matrices of these specimens.

It is worth noting that the DPASP technique can yield improved precisions by the application of longer deposition times and higher pulse amplitudes. This results, of course, from the much higher current peaks obtained, and the much improved signal-to-background ratio obtained.

6.0 CONCLUSION AND SUGGESTIONS FOR FURTHER WORKS

6.1 Conclusions

(a) The automated DPASP technique was found to yield satisfactory results in the determination of lead and cadmium in N.B.S. Bovine Liver No. 1577. The values found were:-

	NBS value (ppb)	DPASP value (ppb)
Lead	0.34 ± 0.08	$0.32^{8} \pm 0.04^{5}$
Cadmium	0.27 ± 0.04	$0.26^{7} \pm 0.02^{8}$

	Precision (%)	Precision (%)	Accuracy (%) on NBS
Lead	± 24	± 14	-3.5
Cadmium	± 15	± 10	-1.1

It was noted that the precision for the automated DPASP method was superior for each element to that obtained for the NBS standard.

(b) The automated DPASP technique was found to yield

satisfactory values in the determination of lead and cadmium in ultratrace amounts in fish (yellow perch) muscle tissue, when compared with the data obtained from application of the GFAAS method. The values were:-

	Lead (with s)(ppb)		Cadmium (with s)(ppb)	
Method	dry tissue	wet tissue	dry tissue	wet tissue
GFAAS	$0.15^{6} \pm 0.04^{1}$	0.029 ± 0.008	$0.05^{5} \pm 0.01^{6}$	0.010 ± 0.003
Precision	± 26%	± 26%	± 29%	± 29%
DPASP 120s dep^{n} + 30mV	$0.16^{3} \pm 0.04^{0}$	0.030 ± 0.008	$0.05^{2} \pm 0.01^{5}$	0.010 ± 0.003
Precision	± 24%	± 24%	± 29%	± 29%
DPASP 300s dep^{n} + 50mV	$0.16^{4} \pm 0.02^{5}$	0.030 ± 0.005	0.054 ± 0.006	0.010 ± 0.001
Precision	± 15%	± 15%	± 11%	± 11%

(c) The precision data for the GFAAS and DPASP methods were comparable for the automated DPASP technique involving a deposition time of 120 seconds, and a pulse amplitude of + 30 mV. They were not felt to be particularly good.

However, a very significant improvement in precision was noted for the automated DPASP technique involving a 300-second deposition time, and a pulse amplitude of + 50mV. The conclusion is that better precision values can be obtained with the application of increased deposition times and higher pulse amplitudes. The increased signal involved

provides for improved signal-to-background and signal uncertainty factors.

(d) Although experimental work was not specifically carried out to determine the influence of supporting electrolyte concentration on both precision and limit of detection factors, it was reasonably apparent that lower supporting electrolyte concentrations than that used (2M each of NH_4OAc and HOAc) would very likely improve both factors. Values of about 0.1M or 0.05M for each supporting electrolyte component were suggested.

It was apparent that the absence of appreciable concentrations of the analytes in the supporting electrolyte was essential, as was minimal concentrations of any interfering substance. This must be achieved by the use of:-

1. Supporting electrolytes previously purified by a pre-electrolysis process. Such purified solutions must be stored in glass bottles with glass stoppers, and should not be kept beyond a 24-hour period.

2. Preparation of the supporting electrolytes from superpure grades of reagents. Again, storage must be in glass bottles with glass stoppers for periods not exceeding 24 hours.

(f) From the points of view of time-of-analysis, capital cost, material cost, limits of detection, and precision, the automated DPASP technique offers distinct

advantages over the automated GFAAS method in the determination of all heavy metals adaptable to the DPASP approach, and in ultratrace amounts in biological tissues and other media.

(g) The limitations relative to the determination of ultratrace heavy metals in fish tissue by the automated DPASP method are concerned more with the metal element involved than with other factors such as nature of the matrix, etc. The technique will become progressively less sensitive as the electrode reaction is more irreversible. For example, under normal aqueous solution conditions, cobalt cannot be determined by the anodic stripping method because of the high degree of irreversibility of the reaction, $Co^{2+} + 2e \rightarrow Co$.

6.2 Suggestions for further works

As suggested in Section 5.1.3, the causes of the parabolic behaviour of the DPASP response at sub-ppb levels of analyte-concentration might be due to two factors :

(a) the scan rates used may be too fast to allow the proper divergent diffusion of analyte-amalgam to the electrode-solution interface so that analyte cations could be stripped out of the HMDE as a linear function of potential changes;

(b) the retardation force from the non-participating supporting electrolyte concentration which lowers the momentum of diffusion of the out-rushing cations into the solution bulk.

It was supposed that, in the first case, a scan rate which is slow enough may allow proper amalgam diffusion in mercury, so that a linear response may be obtained. In the second case, the retardation force may be minimized by the lowering of supporting electrolyte concentration. These suggestions were not tested due to lack of the appropriate data. Hence, it is proposed, as a suggestion for further research in DPASP, that replicate sets of data on the concentration-response curves be secured at:

(1) several scan rates lower than 5 mV/s, and

(2) various concentration levels of the acetate supporting electrolyte, lower than 2M in acetate ion.

It has been found the stripping current of a DPASP response signal can be a function of chemical factors such as pH, composition (36), and concentration of supporting electrolyte (33). For example, lowering the pH of an acetate buffer solution reduces the conductivity of the solution (through protonation of the anion), and decreases the effective stability of metal-acetate complexes, and the combined effect results in enhancement of copper i_p as

the pH decreases. The pH effect is less pronounced in a nitrate base electrolyte, where conductance is increased by the additional protons.

If the effects of the chemical factors were understood, in addition to the role of the various instrumental parameters, there would be a possibility of enhancing further the selectivity and sensitivity of the DPASP technique in quantitative determination of trace heavy metals. The role of these chemical factors has been studied at the thin film mercury electrode, but not so systematic as with the HMDE. It is suggested that, then, a systematic investigation in this area should also be attempted as the next step in the research involving the DPASP technique.

7.0 REFERENCE

1. M.D. Amoos ----- Am. Lab. : 2(8), 33, 1970.
2. T.K. Aidrov and L.G. Aleksondrova ----- Zh. Anal. Khim. : 28, 998, 1973.
3. J. Heyrovsky ----- Chem. Listy : 16, 256, 1922.
4. J. Heyrovsky ----- Trans. Faraday Soc. : 19, 785, 1924.
5. D. Ilkovic ----- Collect. Czech. Chem. Commun. : 6, 498, 1934.
6. Bibliog. A-6 : pp. 132.
7. E. Wahlin ----- Radiometer Polarog. : 1,113, 1952.
8. E. Wahlin and A. Bresle ------ Acta Chem. Scand. : 10, 935, 1956.
9. Bibliog. A-1 : pp. 13.
10. G.C. Barker and I.L. Jenkins ----- Analyst : 77, 685, 1952.
11. R.H. Muller, R.L. Garman, M.E. Droz and J. Petras ----- Anal. Chem. : 10, 339, 1938.
12. Bibliog. A-12 : pp. 105.
13. H. Matsuda ----- Z. Elektrokhem. : 62, 977, 1958.
14. B.B. Damaskin -----"The principles of current methods for the study of electrochem. reactions" pp. 94, McGraw-Hill, 1967.
15. G.C. Barker and A.W. Gardner ----- Z. Anal. Chem. : 173, 79, 1960.
16. Bibliog. B-1 : pp. 19.

17. Bibliog. B-2 : pp. 59.

18. T.M. Florence ----- J. Electroanal. Chem. : 27, 273, 1970.

19. Bibliog. A-6 : pp. 119.

20. H. Malissa ----- Pure Appl. Chem. : 13, 523, 1966.

21. C.K. Mann ----- Anal. Chem. 33, 1484, 1961, 37, 326, 1965.

22. J.H. Christie and J.J. Lingane ----- J. Electroanal. Chem. : 10, 176, 1965.

23. Metrohm ----- 'Operation Manual' - E 608 : VA-Controller.

24. G. Tolg ----- Talanta : 19, 1489, 1972.

25. D.J. Lisk ----- Science : 184, 1137, 1974.

26. T.T. Gorsuch -----"The destruction of org. materials", Pergamon Press, N.Y., 1970.

26a. Bibliog. B-16, C-4, C-6.

27. J. De Luca ----- M.Sc. (Chem.) Thesis, Concordia University, 1979.

28. Metrohm ----- Operation Manual EA 290 : Automated HMDE.

29. W. Lund and D. Onshus ----- Anal. Chim. Acta : 86, 109, 1976.

30. T.R. Copeland, J.H. Christie, R.A. Osteryoung and R.K. Skogerboe ----- Anal. Chem. 45, 2171, 1973.

31. Bibliog. A-11

32. Bibliog. B-2 : pp. 65, B-11.

33. Bibliog. B-9.

34. Natl. Bureau Std. : "Certificate of Anal.", Washington, D.C.

35. C.R.C. Handbook of Chem. & Phys., 59th. Ed., 1978-79.

36. Bibliog. B-12 & B-14.

8.0 : BIBLIOGRAPHY

A. Polarography in General

1. H. Schmidt and M. von Stockelberg : "Modern Polarog. Meth.", Acad. Press, N.Y., 1963.

2. L. Meites : "Polarog. Techniques", Intersci., N.Y., 1955.

3. J. Heyrovsky and J. Kuta : "Principles of Polarog.", Acad. Press, N.Y., 1966.

4. I.M. Kolthoff and J.J. Lingane : "Polarog.", Intersci., N.Y., 1952.

5. P. Zuman, Ed. : "Progress in Polarog.", Intersci., N.Y., 1962.

6. P. Delahay : "New Instrum. Meth. in Electrochem.", Intersci., N.Y., 1954.

7. J.G. Flato ----- Anal. Chem. : 44(11), 75A, 1972.

8. D.E. Burge ----- J. Chem. Ed. : 47, A81, 1970.

9. L. Ramaley and M.S. Krause, Jr. ----- Anal. Chem. : 41, 1362, 1969.

10. P.E. Sturrock and R.J. Carter ----- C.R.C. Critical Rev. in Anal. Chem. : 5, 201, 1975.

11. E.P. Parry and R.A. Osteryoung ----- Anal. Chem. : 37, 1634, 1965.

12. Metrohm : Operation Manual ----- E 506 Polarecord.

B. Stripping Analysis

1. F. Vydra, K. Stulik and E. Julakova : "Electrochem. Stripping Anal.", Halsted Press, N.Y., 1976.

2. E. Barendrecht : "Stripping Voltamm." in "Electroanal. Chem.", Ed. A.L. Bond, V.2, Ch. 2, pp. 53, Marcel

Dekker Inc., N.Y., 1967.

3. T.R. Copeland and R.K. Skogerboe ----- Anal. Chem. : 46, 1257A, 1974.

4. W.D. Ellis ----- J. Chem. Edu. : 50(3), A131, 1973.

5. H.W. Nurnberg ----- Electrochim. Acta : 22, 935, 1977.

6. G.D. Christian ----- J. Electroanal. Chem. :23, 1, 1969.

7. F.P.J. Cahill and G.W. Van Loon ----- Am. Lab. : 8(8), 11, 1976.

8. H. Siegerman and G. O'Dom ----- Am. Lab. : 4(6), 1972.

9. G.E. Batley and T.M. Florence ----- J. Electroanal. Chem. : 55, 23, 1974.

10. W.H. Reinmuth ----- Anal. Chem. :33, 185, 1961; J. Am. Chem. Soc. : 79, 6358, 1957.

11. I. Shain and J. Lewinson ----- Anal. Chem. : 33, 187, 1961.

12. I. Sinko and J. Dolezal ----- J. Electroanal. Chem. : 25, 299, 1970.

13. A. Zirino and S.P. Kounaves ----- Anal. Chem. 49, 56, 1977.

14. E.A. Schonberger and W.F. Pickering ----- Talanta : 27, 11, 1980.

15. I. Sinko and L. Kosta ----- Internatl. J. Environ. Anal. Chem. : 2, 167, 1975.

16. J.W. Jones, R.J. Gajan, K.W. Boyer and J.A. Fiorino ----- J. Assoc. Off. Anal. Chem. : 60, 826, 1977.

C. Atomic Absorption Spectrophotometry

1. G. Ramelow, S. Tugrul, M.A. Ozkan and G. Tuncel ----- Internatl. J. Environ. Anal. Chem. : 5, 125, 1978.

2. E.A. Childs and J.N. Gaffke ----- J. Assoc. Off. Anal. Chem. : 57, 365, 1974.

3. I. Okuno, J.A. Whitehead and R.E. White ----- ibid. : 61, 664, 1978.

4. R.J. Gajan and D. Larry ----- ibid. : 55, 727, 1972.

5. J.F. Alder and D.A. Hickman ----- A.A. Newsletter : 16, 110, 1977.

6. E.E. Menden, D. Brockman, H. Choudhury and H.G. Petering ----- Anal. Chem. : 49, 1644, 1977.

D. Sample Digestion Methods

1. R.J. Gajan, J.H. Gould, J.O. Watts and J.A. Fiorino ----- J. Assoc. Off. Anal. Chem. :56, 876, 1973.

2. T.T. Gorsuch ----- Analyst : 84, 135, 1959.

3. M.M. Schachter and K.W. Boyer ----- Anal. Chem. : 52, 360, 1980.

APPENDIX I : THE PURIFICATION OF SUPPORTING ELECTROLYTE - METHODOLOGY AND INSTRUMENTATION.

The most typical impurities from the point of view of anodic stripping analysis are the heavy metals, which are generally present in all the so-called analytical grade reagents, at the levels that are not suitable for direct use. Purification of base electrolytes made of these chemicals can be carried out most effectively and satisfactory by controlled potential electrolysis at the mercury pool cathode.

The advantages of electrolytic purification over other more efficient methods are: comparatively less time-comsuming, simpler instrumentation, and considerably less equipment cost. The basic instrumentation for controlled potential electrolysis consists of an electrolytic cell with a 3-electrode system, and a potentiostat. The 3-electrode system is composed of a mercury pool cathode, a reference electrode, and a platinum anode. The potentiostat may simply consist of a potentiometer and a dc power supply. The equipment used for this work is shown in Figures 26 and 27, and is listed in Table 17.

The base supporting electrolyte employed for this work was 2M HOAc/2M NH_4OAc. For purification purposes, this electrolyte was prepared at a concentration containing 5M each of the constituents, and the working concentration was then obtained by diluting the purified 5M solution with

deionized-glass-distilled water.

The process was carried out as follows:

1. An appropriate volume, approx. 250-300 ml, for example, was placed into the cathode and anode compartments, until the solution levels became equal.
2. Deaeration of the solutions in both compartments was conducted by passing N_2 for at least 30 min. with constant stirring, at 300-450 rpm.
3. After de-oxygenation, the dc power supply was switched on and adjusted until a voltage of -1.20v was shown on the potentiometer to signal the begining of the electrolysis.
4. The trace heavy metal levels in the electrolyte were monitored at 24-hour intervals during the electro-purification process. An aliquot of 10 ml was withdrawn from the cathodic compartment. After dilution to give 2M concentration, the solution was examined by means of the automated DPASP instrumentation. In the normal run of events, with the starting concentrations of Pb and Cd in the 2M supporting electrolyte at about 8-9 ppb, the following decay trends would be approximated:

Electrolysis time (hrs)	Conc'n in the dil'n (2M) electrolyte (ppb)	
	Pb	Cd
0	8.5	8.0
24	3.0	1.6
48	1.3	0.4
72	0.5	0.2
96	0.3	0.1

Remarks:

1. The purification procedure may be terminated whenever the levels of Pb and Cd have attained values satisfactory relative to the concentrations expected for the sample in hand.
2. In order to avoid contamination of the purified electrolyte, it is advisable to use it within 6 hours after the stoppage of the purification. The following demonstrates the re-contamination of purified 2M electrolyte upon storage in pre-cleaned Nalgene bottles:

Storage time (hrs)	Conc'n in the 2M electrolyte (ppb)	
	Pb	Cd
0	0.3	0.1
24	1.8	1.0
48	5.6	4.3
72	7.0	6.2

TABLE 17

MERCURY CATHODE CELL - PURIFICATION OF SUPPORTING ELECTROLYTES

Item	
1	600 ml beaker. approx. 9 cm diam. by 12.5 cm long
2	Fused in Pt wire to Hg pool. approx. 1 mm diam.
3	Hg pool cathode. approx. 1.5 cm deep by 9 cm diam. approx. 64 sq. cm.
4	Teflon-coated magnetic stirring bar. 9 mm diam. by 40 mm long
5	Anode compartment. 60 ml fritted-disc Pyrex No. 36060 funnel cut to size Approx. 7 cm diam. by 12.5 cm long.
6	Pt gauze cylindrical anode. Approx. 3.2 cm diam. by 3.4 cm long. Surface area, both sides taken as solid, approx. 68 sq. cm.
7	Reference electrode. Ag/AgCl (sat. KCl) with extended frit tube
8	Rubber stopper. Size 14 with appropriate holes
9	Solution requiring electrolytic purification
10	Rubber stopper. Size 9 with appropriate holes.
11	Nitrogen gas inlet tubes. Approx. 1-2 mm bore
12	Nitrogen gas outlet tubes. Approx. 1-2 mm bore
13	Potentiostat. Hewlett/Packard Series STB, Model 6113A 5-digit thumbwheel programmer, 12 V, 2.5 A or 1.2 V, 0.25 A.
14	E300B (old model) Metrohm pH/mV potentiometer or E620 (new model) Metrohm pH/mV potentiometer.
15	Frit at base of anode compartment.

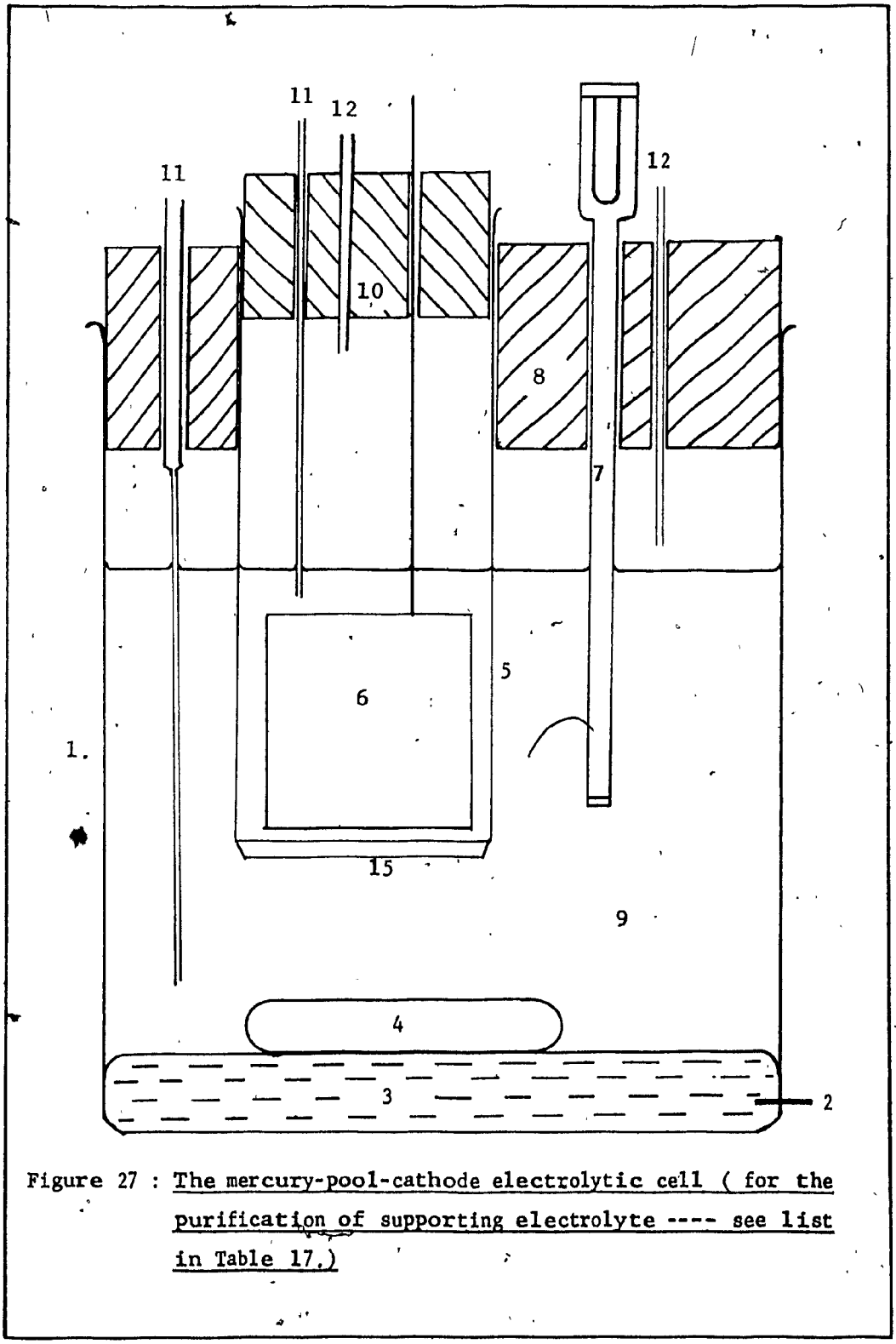

Figure 27 : The mercury-pool-cathode electrolytic cell (for the purification of supporting electrolyte ---- see list in Table 17.)

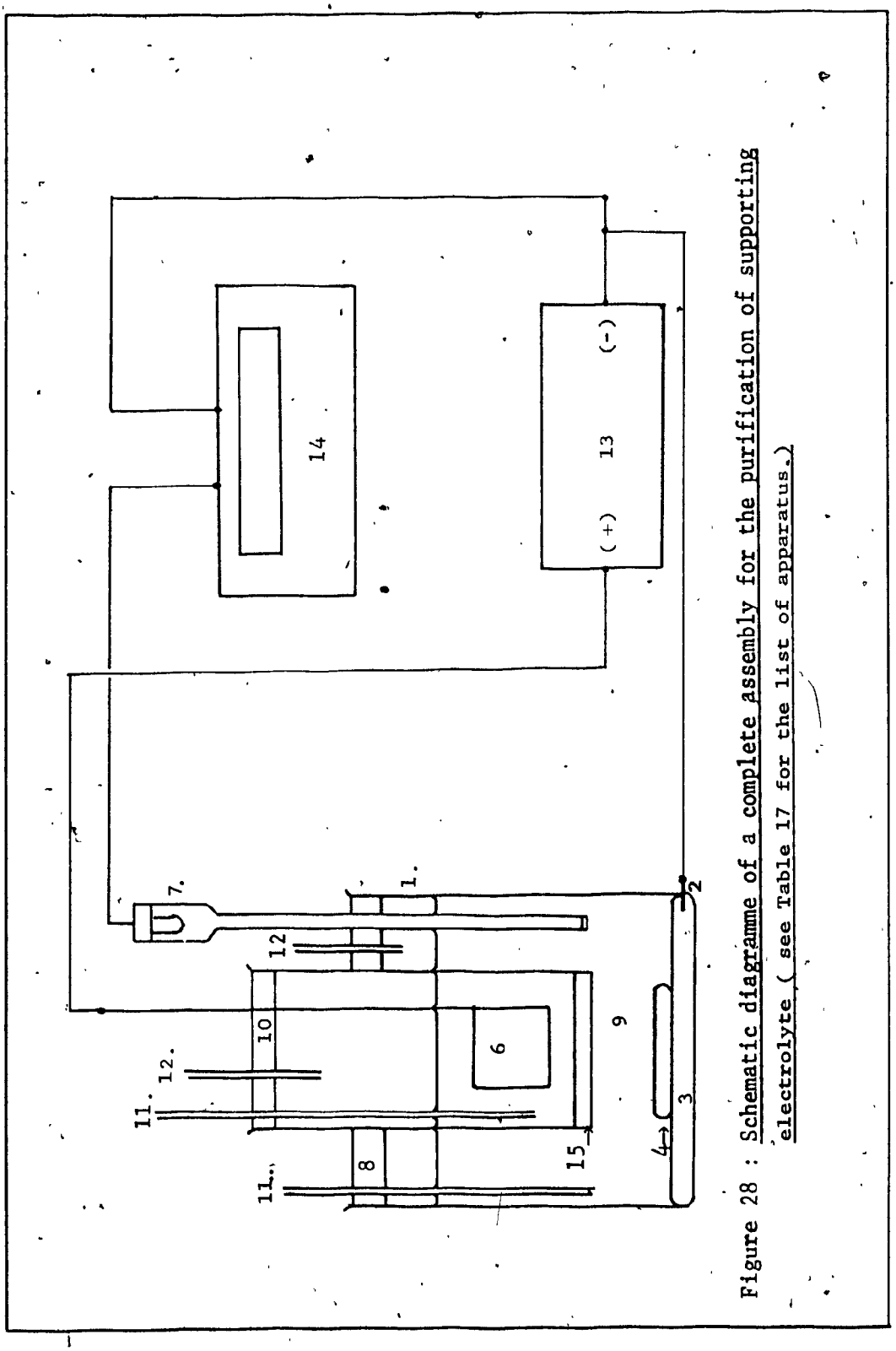

Figure 28 : Schematic diagramme of a complete assembly for the purification of supporting electrolyte (see Table 17 for the list of apparatus.)

APPENDIX II : Footnotes

II - 1. Additions to the Metrohm Automated Stripping Analysis Equipment :

In the latest models of the Metrohm automated stripping analysis equipment, the E 542 Dosifix and two E 535 Dosimats are all replaced by two E 655 microprocessed Dosimats controlled directly from the E 608 VA-Controller. The E 655 has seven (7) programmable functions and is capable of providing the following minimum volume injections with, of course, selected higher volumes :-

Total Burette Volume (ml)	Minimum Volume Injection (ul)	
	Mini. Vol.	Resolution
1	0.1	1
5	0.5	1
10	1	10
20	2	10
50	5	10

II - 2. Description of the Whole Fish Specimen* :

Name : Yellow perch (perca Flavescens) ;
Sample origin : Lake Memphremagog ----- South Basin;
Method of collection : Netting (monofilament gill nets);
Size of specimen : 15 - 25 cm. (head-to-tail);
Amount used : Approx. 20 kg.

*Remark:

The bulk sample of whole fish was collected and provided by the Limnology Research Group (Lake Memphremagog Project) of McGill University, Department of Biology.

II - 3. The polytron was equipped with Teflon bearings when originally ordered, and this was to avoid sample contamination effects which would have occurred with the regular bronze bearing equipped model.

II - 4. Unit Response:

The term, "unit response", may be defined as the DPASP current-response based on a per unit quantity of a variable parameter. It represents the overall average response due to a particular variable, under the conditions in which all other parameters are held constant. Therefore, by definition, the unit-radius response is the average value of current-response due to the size of the HMDE at a radius of 1 mm.; the unit-(deposition-) time is that due to a deposition time of 1 min.; and the unit-concentration response signifies that due to the analyte-concentration of 1 ppb.

The values of unit responses may be considered as normalized average values, which are actually the slope values of the families of calibration curves shown in Tables 3 - 6 and 9 - 12, and Figures 15 - 18 and 21 - 24.

The main purpose of using these values is that one can compare the DPASP responses of two or more analytes, due to the combined effects of analyte-concentrations and one other variable parameter, without regard to the differences in the actual analyte-concentrations.

APPENDIX III : FORMULAE AND CONSTANTS

(A) Formulae of a Sphere.

1. Volume : $V = \frac{4}{3}\pi r^3$ in mm^3;

2. Surf. Area : $A = 4\pi r^2$ in mm^2;

3. Radius : $r = (\frac{3V}{4\pi})^{1/3} = (\frac{A}{4\pi})^{1/2}$, in mm.

(B) Density of Mercury (35).

At 22°C : $D_{Hg} = 13.5413$ g/cm^3 or mg/mm^3;

At 24°C : $D_{Hg} = 13.5364$ g/cm^3 or mg/mm^3;

At the experimental temperature, ca. 23.0° ± 0.2°C, by interpolation : $D_{Hg} = 13.5389 \pm 0.0005$ mg/mm^3.

(C) Volume of a Mercury Drop at 23.0° ± 0.2°C :

$$V. = \frac{\text{Av. Weight of a Mercury Drop}}{D_{Hg}}$$

APPENDIX IV : SPECIFIC PARAMETRIC SETTINGS USED IN THE PRELIMINARY ANALYSES

Parameters 1 :

HMDE	=	varied (as indicated in the Tables listed below.);
t_{dep} (quiescent)	=	30 sec.;
(stirring)	=	180 sec.;
U_{dp}	=	+ 30 mv.;
Scan Rate	=	+ 5 mv/sec;
Damping	=	2 units;
Tables	:	3, 4, 7, 9, 10, and 13.

Parameters 2 :

HMDE	=	5 units (r = 0.360 ± 0.001 mm.)
t_{dep} (quiescent)	=	30 sec.;
(stirring)	=	varied (as indicated in the Tables listed below.);
U_{dp}	=	+ 50 mv.;
Scan Rate	=	+ 5 mv/sec;
Damping	=	1 unit;
Tables	:	5, 6, 8, 11, 12, and 14.

APPENDIX V : TREATMENTS OF EXPERIMENTAL DATA FOR THE BIOLOGICAL SAMPLES.*

V (A) : Determination of Pb and Cd in Bovine Liver (N.B.S. Material No. 1577)

Technique : Automated DPASP

1. Results of Pb (ug. per g. freeze-dried sample)

0.266	0.280	0.284	0.293	0.306	0.332
0.347	0.365	0.370	0.372	0.398	

$N = 11$, $\bar{X} = 0.328$ $S = 0.045$

All values accepted based on $\pm$ 2S, test.

2. Results of Cd (ug. per g. freeze-dried sample)

0.233	0.236	0.253	0.255	0.256	0.260
0.260	0.272	0.279	0.312	0.319	

$N = 11$ $\bar{X} = 0.267$ $S = 0.028$

All values accepted based on $\pm$ 2S, test.

*N.B. : All the individual data points were obtained through the quantitation method of standard additions. Each set of experimental data consisted of triplicate determinations of each of a sample solution, and four (4) "spiked" solutions of the same sample, and resulted a single data point.

V (B) : Determination of Pb and Cd in Fish Muscle Tissue.

V (B-1) : Determination of Pb

(1-a) GF-AAS analysis (ug/g dry weight.)

0.107	0.152	0.117	0.118	0.190
0.110	0.118	0.168	0.176	0.123
0.170	0.107	0.179	0.244*	0.213
0.214	0.228*	0.109	0.185	0.187

N** = 20 $\bar{X}$ = 0.161 S = 0.045

Range (± 1.5S) = 0.094 ---- 0.244

* Doubtful figure : 0.244 0.228

Test : N = 18	Values	Deviation
$\bar{X}$ = 0.152	0.244	0.092 = 2S
S = 0.038	0.228	0.076 = 2S

Conclusion : value 0.244 rejected, and the acceptable result is

N = 19 $\bar{X}$ = 0.156 S = 0.041

N.B. : Dry weight of the fish muscle tissue = 18.64% of its fresh (wet) weight.

Thus : $[Pb^{2+}]$ = 0.156 ± 0.041 ug/g on the dry weight basis;

= 0.029 ± 0.008 ug/g on the wet weight basis.

** More than 15 results were rejected due to their very high spread or deviation from the norm of data. These

values were undoubtfully the results of contamination and the loss of material through sample-digestion.

(1-b) Automated DPASP analysis of Pb.

Programme 1 :

U_{dp} = + 30 mv.;

t_{dep} = 120 s. (stirring) + 30 s (quiescent)

Experimental results : $[Pb^{2+}]$, ug. per g. dry weight

0.220	0.171	0.158	0.157	0.190	0.194
0.160	0.164	0.160	0.114	0.104*	0.124
0.196	0.180	0.100*	0.119	0.123	0.249*
0.167	0.112	0.103*	0.215	0.176	0.230*
0.204	0.103*	0.225	0.222	0.133	0.128
0.230*	0.194	0.148	0.197	0.153	0.161
0.116	0.163	0.164			

N = 39 $\bar{X}$ = 0.165 S = 0.063

Range ($\pm$ 1.5S) = 0.103 ---- 0.228

*Doubtful values	Test	Deviation
0.104	N = 32	0.062 < 2S
0.100	$\bar{X}$ = 0.166	0.066 < 2S
0.103	S = 0.034	0.063 < 2S
0.103	2S = 0.068	0.063 < 2S
0.230		0.064 < 2S
0.230		0.064 > 2S
0.249		0.083 > 2S

Conclusion : value 0.249 rejected, and the acceptable result is

$$N = 38 \quad \bar{X} = 0.163 \quad S = 0.040$$

Thus : $[Pb^{2+}] = 0.163 \pm 0.040$ ug/g on the dry weight basis;

$= 0.030 \pm 0.008$ ug/g on the wet weight basis.

(1-b) Automated DPASP analysis of Pb.

Programme 2 :

U_{dp} = + 50 mv.;

t_{dep} = 300 s. (stirring) + 30 s. (quiescent).

Experimental results : $[Pb^{2+}]$, ug. per g. dry weight

0.164	0.132	0.192	0.164	0.199
0.181	0.144	0.169	0.172	0.122

$N = 10 \quad \bar{X} = 0.164 \quad S = 0.025$

Conclusion : all values accepted based on 2S.

Thus : $[Pb^{2+}] = 0.164 \pm 0.025$ ug/g on the dry weight basis;

$= 0.030 \pm 0.005$ ug/g on the wet weight basis.

V (B-2) : Determination of Cd.

(2-a) : GF-AAS analysis (ug/g dry weight)

0.030	0.050	0.025*	0.075	0.059	0.036
0.084*	0.085*	0.052	0.026*	0.076	0.083
0.062	0.052	0.066	0.029	0.075	0.049
0.054	0.062	0.051	0.076	0.095*	0.047
0.037	0.054	0.033	0.048	0.042	0.057
0.057	0.015*	0.069	0.043	0.072	0.034
0.072	0.060				

$N = 38$ $\bar{X} = 0.055$ $S = 0.019$

Range ($\pm$ 1.5S) = 0.026^5 ----- 0.083^5

*Doubtful values	Test	Deviation
0.026	N = 32	0.029 < 2S
0.084	$\bar{X}$ = 0.055	0.029 < 2S
0.085	S = 0.015	0.030 = 2S
0.015	2S = 0.030	0.040 > 2S
0.025		0.030 = 2S
0.095		0.040 > 2S

Conclusion : values 0.085, 0.025, 0.015, and 0.095 are rejected, and the acceptable result is

$N = 34$ $\bar{X} = 0.055$ $S = 0.016$

Thus : $[Cd^{2+}] = 0.055 \pm 0.016$ ug/g on the dry weight basis;

$= 0.010 \pm 0.003$ ug/g on the wet weight basis.

(2-b) : Automated DPASP analysis of Cd.

Programme 1 :

U_{dp} = + 30 mv.;

t_{dep} = 120 s. (stirring) + 30 s (quiescent)

Experimental results : $[Cd^{2+}]$, ug. per g. dry weight

0.067	0.068	0.072	0.036	0.082	0.034
0.084	0.040	0.036	0.037	0.037	0.069
0.076	0.034	0.040	0.050	0.045	0.058
0.034	0.038	0.058	0.037	0.056	0.055
0.057	0.088*	0.054	0.034	0.047	0.044
0.049	0.068	0.064	0.044	0.034	0.059
0.062	0.048	0.068	0.047	0.089*	0.098*
0.112*	0.090*				

N = 44 $\bar{X}$ = 0.057 S = 0.020

Range ($\pm$ 1.5S) = 0.027 ---- 0.087

*Doubtful values	Test	Deviation
0.088	N = 39	0.036 > 2S
0.089	$\bar{X}$ = 0.052	0.037 > 2S
0.098	S = 0.015	0.046 > 2S
0.112	2S = 0.030	0.060 > 2S
0.090		0.038 > 2S

Conclusion : values 0.088, 0.089, 0.098, 0.112, and 0.090 are rejected, and the acceptable result is

N = 39 $\bar{X}$ = 0.052 S = 0.015

Thus : $[Cd^{2+}]$ = 0.052 ± 0.015 ug/g on the dry weight basis;
= 0.010 ± 0.003 ug/g on the wet weight basis.

(2-b) : Automated DPASP analysis of Cd.

Programme 2 :

U_{dp} = + 50 mv.;

t_{dep} = 300 s. (stirring) + 30 s (quiescent)

Experimental results : $[Cd^{2+}]$, ug. per g. dry weight

0.055	0.058	0.088*	0.047	0.055
0.046	0.058	0.067	0.054	0.051

N = 10 $\bar{X}$ = 0.058 S = 0.012

Doubtful Value	Test	Deviation
0.088	N = 9	0.034 > 2S (=0.012)
	$\bar{X}$ = 0.054	
	S = 0.006	

Conclusion : value 0.088 rejected.

Thus : $[Cd^{2+}]$ = 0.054 ± 0.006 ug/g on the dry weight basis;
= 0.010 ± 0.001 ug/g on the wet weight basis.

V (C) : Statistical (Inference, t-) Test on the Values of Pb Obtained by the Two Methods

Experimental Results : $[Pb^{2+}]$, ug/g dry weight

	Technique		
	GF-AAS (Y)	Automated DPASP (X)	
		Programme	
		1.	2.
N	19	38	10
$\bar{X}$	0.156	0.163	0.164
S	0.041	0.040	0.025
S^2	0.0017	0.0016	0.0006

t-Test :

$$t^2 = \frac{(\bar{X} - \bar{Y})^2}{\frac{(N_x - 1)\cdot S_x^2 + (N_y - 1)\cdot S_y^2}{N_x + N_y - 2} \cdot \left(\frac{1}{N_x} + \frac{1}{N_y}\right)}$$

Case 1:

$$t^2 = \frac{(0.163 - 0.156)^2}{\frac{(37 \times 0.0016) + (18 \times 0.0017)}{27} \cdot \frac{19 + 9}{9 \times 19}}$$

$$t = 0.617 \quad (\beta = N_x + N_y - 2 = 55)$$

Case 2:

$$t = 0.541$$

For Case 1 : $t^*\ (\alpha = 0.05,\ \beta = 60) = 2.000 >> t\ (\beta = 19 + 38 - 2) = 0.617$

For Case 2 : $t^*\ (\alpha = 0.05,\ \beta = 27) = 2.052 >> t\ (\beta = 19 + 10 - 2) = 0.541$

Conclusion : Based on the t-tests (2-tailed) at the 95% confidence level, it is concluded that there was no significant deviation between the values of Pb obtained by the two different techniques.

APPENDIX VI : Sample Calculation for an N.B.S. Material (Bovine Liver - No. 1577)

A. Instrumental Settings

1. E506 Polarecord

U_{start} : -0.80 v. (vs. Ag/AgCl - sat'd KCl)

ΔU : +1.50 v.

t_{drop} : 1.2 s.

mm/t_{drop} : 1

Scan rate : +5 mv/s

Sensitivity : 1×10^{-10} A/mm (= 0.1 nA/mm)

U_{dp} : +30 mv.

2. E608 VA-Controller

Deaeration : 10 min. (N_2)

HMDE : 5 units (r= 0.360 ± 0.001 mm)

Deposition : (stirring) 90 s ---- for sample

120 s ---- for blank

(quiescent) 30 s

Determination: 92 s

Pause : 30 s

ΔU_{dep} : -0.30 v.

ΔU_{pause} : +0.10 v.

* $U_{dep} = U_{start} + \Delta U_{dep} = -1.10$ v.(vs Ag/Agcl - KCl)

3. E542 Dosifix

Volume of spike/addition = 0.025 ml (= 25 µl)

B. Experimental Parameters

1. Volume of test solution = 25.00 ± 0.02 ml.

2. Concentration of standard "spiking" solution:

$[Pb^{2+}] = 4.94$ ppm

$[Cd^{2+}] = 4.90$ ppm

N.B.: Experimental results are calculated and presented in Table 18 and Figures 29 and 30.

Table 18 : The determination of Pb and Cd in a sample blank and an N.B.S. Bovine Liver sample (1577)

Amt. added $[Pb^{2+}]$, ppb	Av. Peak Current ± Std. Dev'n. (ip, nA)		Amt. added $[Cd^{2+}]$, ppb	Av. Peak Current ± Std. Dev'n. (ip, nA)	
	Blank	Sample		Blank	Sample
0	0.58 ± 0.08	8.08 ± 0.25	0	0.60 ± 0.00	12.20 ± 0.33
4.94	2.17 ± 0.06	10.90 ± 0.20	4.90^2	2.95 ± 0.07	18.20 ± 0.73
9.88	4.30 ± 0.10	13.81 ± 0.07	9.80^4	6.63 ± 0.11	22.54 ± 0.71
14.82	6.76 ± 0.15	17.58 ± 0.11	14.70^6	10.25 ± 0.15	26.42 ± 0.39
Corr. Coefficient	0.9976	0.9974		0.9974	0.9946
Slope (nA/ppb)	0.4289	0.6358		0.6875	0.9588
X (Y = 0), ppb	0.70	12.40		0.15^4	13.34
Total in 25 ml solution	0.0170 ug	0.3100 ug		0.0039 ug	0.3335 ug
Actual amt. in sample		0.308 ug			0.330 ug
Amt. of sample used		1.0562 g.			1.0562 g
Amt. metal content		0.29^2 ppm (ug/g dry wt.)			0.31^2 ppm

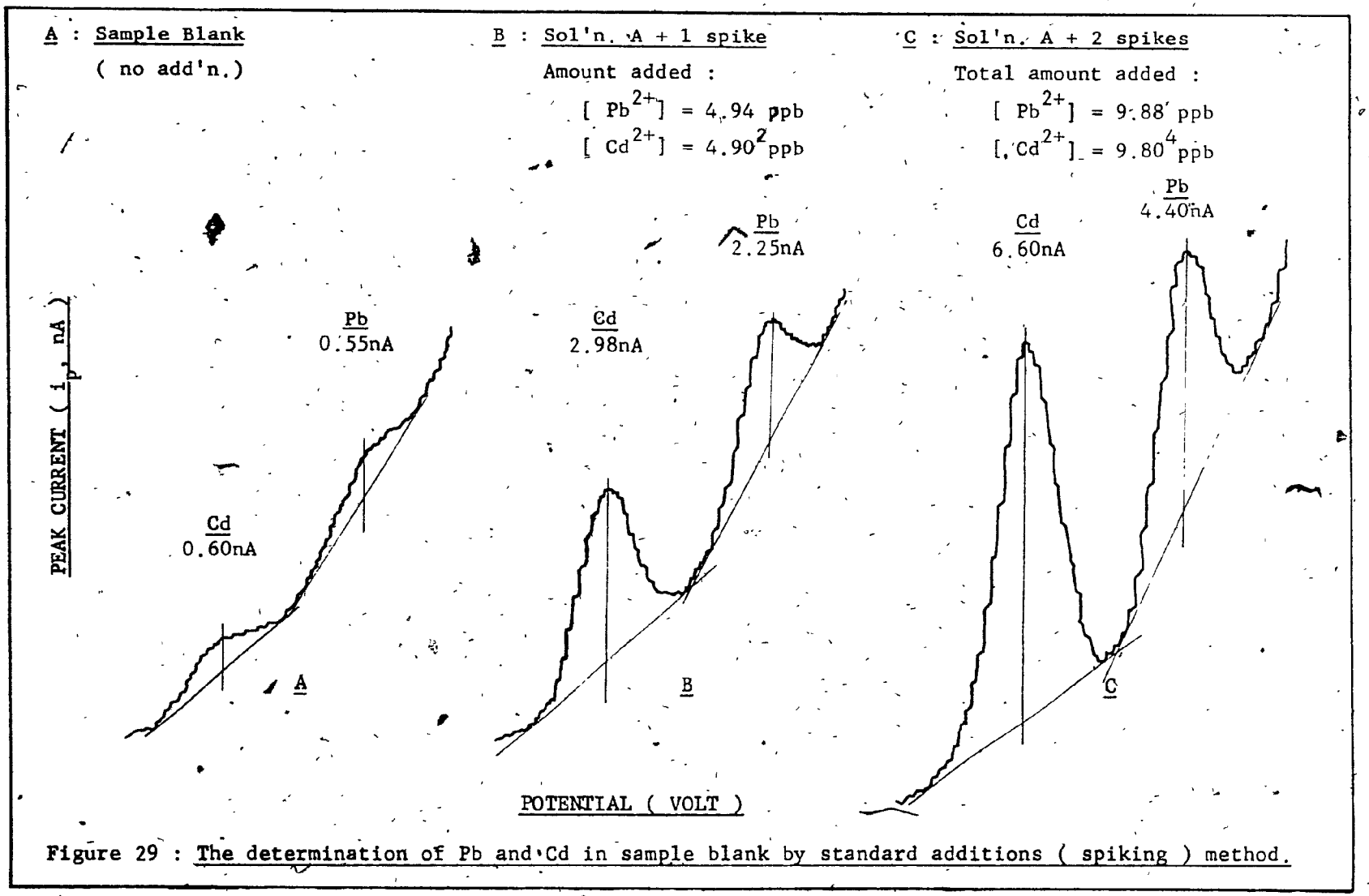

Figure 29 : The determination of Pb and Cd in sample blank by standard additions (spiking) method.

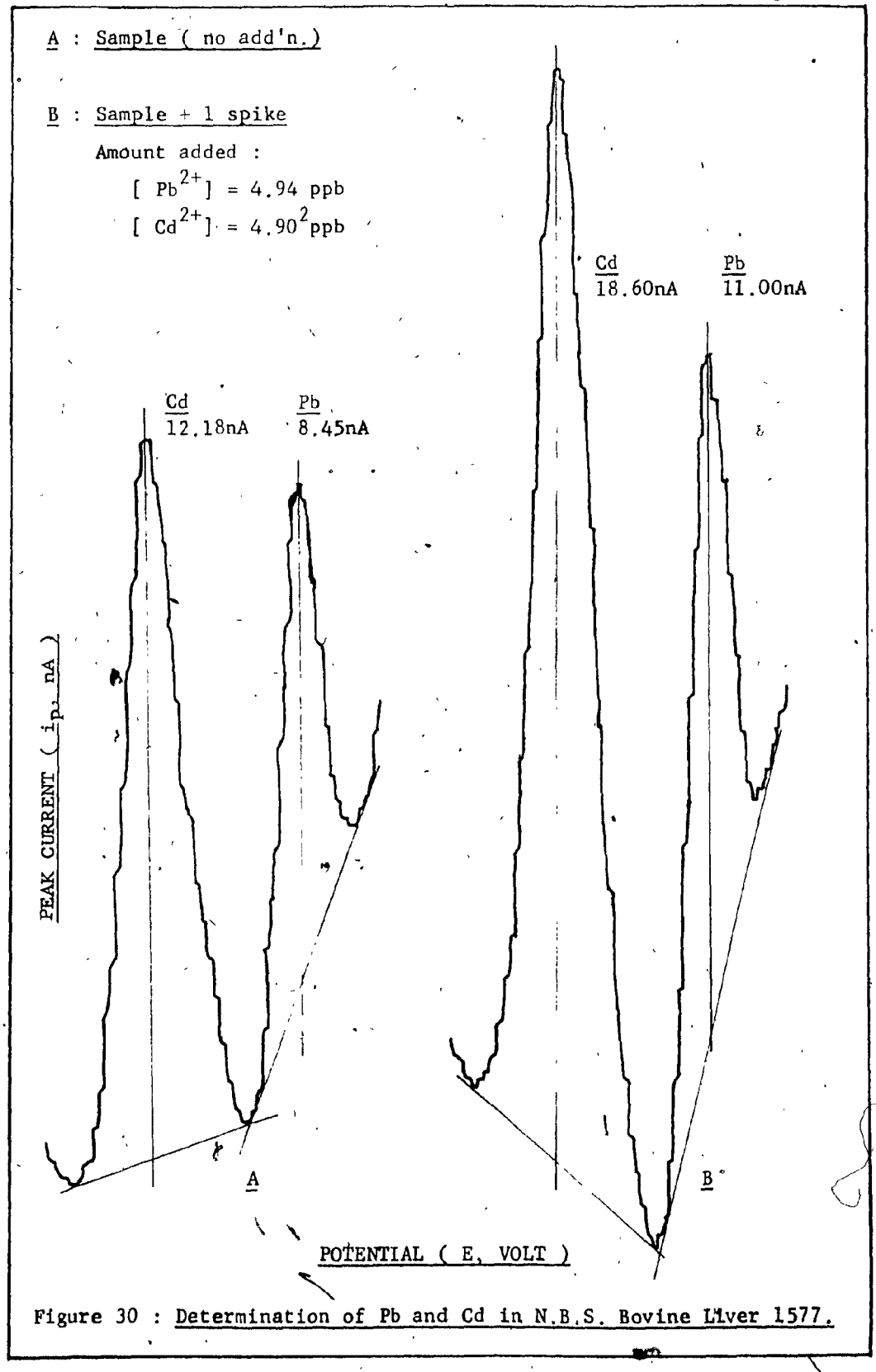

Figure 30 : Determination of Pb and Cd in N.B.S. Bovine Liver 1577.